

An International Journal

# Nature and Science

ISSN 1545-0740

Volume 4 - Number 3 (Cumulated No. 10), August 10, 2006



Marsland Company, Michigan, The United States

# Nature and Science

The *Nature and Science* is an international journal with a purpose to enhance our natural and scientific knowledge dissemination in the world under the free publication principle. Any valuable papers that describe natural phenomena and existence or any reports that convey scientific research and pursuit are welcome, including both natural and social sciences. Papers submitted could be reviews, objective descriptions, research reports, opinions/debates, news, letters, and other types of writings that are nature and science related.

**Editor-in-Chief:** Hongbao Ma

**Associate Editors-in-Chief:** Qiang Fu, Yongsheng Ma, Margaret Young

**Editors:** George Chen, Shen Chong, Mark Hansen, Mary Herbert, Wayne Jiang, Xuemei Liang, Mark Lindley, Mike Ma, Da Ouyang, Xiaofeng Ren, Shufang Shi, Tracy X Qiao, George Warren, Qing Xia, Yonggang Xie, Shulai Xu, Lijian Yang, Yan Young, Tina Zhang, Ruanbao Zhou, Yi Zhu

**Web Design:** Jenny Young

## Introductions to Authors

### 1. General Information

**(1) Goals:** As an international journal published both in print and on internet, *Nature and Science* is dedicated to the dissemination of fundamental knowledge in all areas of nature and science. The main purpose of *Nature and Science* is to enhance our knowledge spreading in the world under the free publication principle. It publishes full-length papers (original contributions), reviews, rapid communications, and any debates and opinions in all the fields of nature and science.

**(2) What to Do:** *Nature and Science* provides a place for discussion of scientific news, research, theory, philosophy, profession and technology - that will drive scientific progress. Research reports and regular manuscripts that contain new and significant information of general interest are welcome.

**(3) Who:** All people are welcome to submit manuscripts in any fields of nature and science.

**(4) Distributions:** Web version of the journal is freely opened to the world, without any payment or registration. The journal will be distributed to the selected libraries and institutions for free. For the subscription of other readers please contact with: [editor@americanscience.org](mailto:editor@americanscience.org) or [americansciencej@gmail.com](mailto:americansciencej@gmail.com) or [editor@sciencepub.net](mailto:editor@sciencepub.net)

**(5) Advertisements:** The price will be calculated as US\$400/page, i.e. US\$200/a half page, US\$100/a quarter page, etc. Any size of the advertisement is welcome.

### 2. Manuscripts Submission

**(1) Submission Methods:** Electronic submission through email is encouraged and hard copies plus an IBM formatted computer diskette would also be accepted.

**(2) Software:** The Microsoft Word file will be preferred.

**(3) Font:** Normal, Times New Roman, 10 pt, single space.

**(5) Manuscript:** Don't use "Footnote" or "Header and Footer".

**(6) Cover Page:** Put detail information of authors and a short title in the cover page.

**(7) Title:** Use Title Case in the title and subtitles, e.g. "Debt and Agency Costs".

**(8) Figures and Tables:** Use full word of figure and table, e.g. "Figure 1. Annual Income of Different Groups", "Table 1. Annual Increase of Investment".

**(9) References:** Cite references by "last name, year", e.g. "(Smith, 2003)". References should include all the authors' last names and initials, title, journal, year, volume, issue, and pages etc.

### Reference Examples:

**Journal Article:** Hacker J, Hentschel U, Dobrindt U. Prokaryotic chromosomes and disease. *Science* 2003;301(34):790-3.

**Book:** Berkowitz BA, Katzung BG. Basic and clinical evaluation of new drugs. In: Katzung BG, ed. Basic and clinical pharmacology. Appleton & Lance Publisher. Norwalk, Connecticut, USA. 1995:60-9.

**(10) Submission Address:** [editor@sciencepub.net](mailto:editor@sciencepub.net), Marsland Company, P.O. Box 21126, Lansing, Michigan 48909, The United States, 517-980-4106.

**(11) Reviewers:** Authors are encouraged to suggest 2-8 competent reviewers with their name and email.

### 2. Manuscript Preparation

Each manuscript is suggested to include the following components but authors can do their own ways:

**(1) Title page:** including the complete article title; each author's full name; institution(s) with which each author is affiliated, with city, state/province, zip code, and country; and the name, complete mailing address, telephone number, facsimile number (if available), and e-mail address for all correspondence.

**(2) Abstract:** including Background, Materials and Methods, Results, and Discussions.

**(3) Keywords.**

**(4) Introduction.**

**(5) Materials and Methods.**

**(6) Results.**

**(7) Discussions.**

**(8) References.**

**(9) Acknowledgments.**

### Journal Address:

Marsland Company  
P.O. Box 21126  
Lansing, Michigan 48909  
The United States  
Telephone:(517) 303-3990  
E-mail: [editor@sciencepub.net](mailto:editor@sciencepub.net);  
[naturesciencej@gmail.com](mailto:naturesciencej@gmail.com)  
Websites: <http://www.sciencepub.org>

# Nature and Science

ISSN: 1545-0740

Cover Page ([Word](#)), Introduction ([Word](#)), Contents ([Word](#)), Call for Papers ([Word](#)), All in one file

## Contents

1-1. <a href="#">Estimation of Microbiologically Influenced Corrosion of Aluminium Alloy in Natural Aqueous Environment</a> ( <a href="#">pdf</a> )	
Balaji Ganesh A, Radhakrishnan T K	1
2-5. <a href="#">Ichthyophthiriasis: Various Fish Susceptibility or Presence of More than one Strain of the Parasite?</a> ( <a href="#">pdf</a> )	
Ehab E. Elsayed, Nisreen Ezz El Dien, Mahmoud A. Mahmoud	5
3-14. <a href="#">Study of Transmission Electron Microscopy (TEM) and Scanning Electron Microscopy (SEM)</a> ( <a href="#">pdf</a> )	
Hongbao Ma, Kuan-Jiunn Shieh, Tracy X. Qiao	14
4-23. <a href="#">An Improved Neural Networks Prediction Model and Its Application in Supply Chain Management</a> ( <a href="#">pdf</a> )	
Xiaoni Dong, Guangrui Wen	
5-28. <a href="#">Research of Novel Three-phase Inverter and its Modulation Technique</a> ( <a href="#">pdf</a> )	
Wang Shuwen, Ji Yanchao, Fang Junlong	28
6-37. <a href="#">Microbiological and Nutritional Qualities of Dairy Products: Nono and Wara</a> ( <a href="#">pdf</a> )	
Roseline E. Uzeh, Regina E. Ohenhen, Ayodeji K. Rojumbokan	37
7-41. <a href="#">The Study of a Novel Microstrip Antenna Being Used for the Estimation of Sample Material Dielectric Coefficient under Electromagnetic Wave at 2.4 GHz</a> ( <a href="#">pdf</a> )	
Yu-Min Li, Chia-ching Chu, Yuan-Tung Cheng, Hsien-Chiao Teng, Shen Cherng	41
8-45. <a href="#">Extra Dimensions, Brane Worlds, and the Vanishing of Axion Contributions to Inflation?</a> ( <a href="#">pdf</a> )	
W. Beckwith	45
9-51. <a href="#">Hydrocarbon Degrading Potentials of Bacteria Isolated from a Nigerian Bitumen (Tarsand) Deposit</a> ( <a href="#">pdf</a> )	
Bola O. Oboh, Matthew O. Ilori, Joseph O. Akinyemi, Sunday A. Adebusoye	51
10-58. <a href="#">Physiological and Biochemical Studies of <math>\beta</math>-Carotene on Atherosclerosis and Thrombosis</a> ( <a href="#">pdf</a> )	
Kuan-Jiunn Shieh, Mei-Ying Chuang	58
11-65. <a href="#">Utilisation of Alicyclic Compounds by Soil Bacteria</a> ( <a href="#">pdf</a> )	
Olukayode O. Amund, Matthew, O. Ilori, Sunday A. Adebusoye, and K. I. Musa	65
12-69. <a href="#">An In Silico Investigation into the Discovery of Novel Cis-acting Elements within the Intronic Regions of Human PAX7</a> ( <a href="#">pdf</a> )	
Maika G. Mitchell, Melanie Ziman	69
13-86. <a href="#">Noble Prize List from 1901</a> ( <a href="#">pdf</a> )	
Hongbao Ma	86
14-95. <a href="#">Conference Information: New Target and Delivery Systems in Cancer Diagnosis and Treatment – Sidney 2007</a> ( <a href="#">pdf</a> )	
	95

# *Nature and Science*

## Call for Papers

The international academic journal, “*Nature and Science*” (ISSN: 1545-0740), is registered in the United States, and invites you to publish your papers.

Any valuable papers that describe natural phenomena and existence and reports that convey scientific research and pursuit are welcome, including both natural and social sciences. Papers submitted could be reviews, objective descriptions, research reports, opinions/debates, news, letters, and other types of writings that are nature and science related.

Here is a new avenue to publish your outstanding reports and ideas. Please also help spread this to your colleagues and friends and invite them to contribute papers to the journal. Let's make efforts to disseminate our research results and our opinions in the worldwide for the benefit of the whole human community.

Papers in all fields are welcome.

Please send your manuscript to [editor@sciencepub.net](mailto:editor@sciencepub.net); [naturesciencej@gmail.com](mailto:naturesciencej@gmail.com)

For more information, please visit: <http://www.sciencepub.org>

Marsland Company  
P.O. Box 21126  
Lansing, Michigan 48909  
The United States  
Telephone: (517) 303-3990  
Email: [editor@sciencepub.net](mailto:editor@sciencepub.net); [naturesciencej@gmail.com](mailto:naturesciencej@gmail.com)  
Website: <http://www.sciencepub.org>

# Estimation of Microbiologically Influenced Corrosion of Aluminium Alloy in Natural Aqueous Environment

Balaji Ganesh A, Radhakrishnan T K

Department of Chemical Engineering, National Institute of Technology, Tiruchirappalli 620015, Tamil Nadu, India.  
[abganesh\\_nitt@yahoo.com](mailto:abganesh_nitt@yahoo.com), [radha@nitt.edu](mailto:radha@nitt.edu)

**Abstract:** This paper describes microbiologically influenced corrosion (MIC) behaviour of aluminium alloy (AA2024-T3) in natural aqueous environment. An optical microscopy is used to confirm the micro colony formation of rod and cocci bacterial species. The viable cell counts after one month are averaged  $1730 \times 10^7$  CFU/ml and the species *Pseudomonas* found dominant. The changes in chemical constituents of test solution including pH, dissolved oxygen and conductivity are also studied. Polarization study is also carried out to determine the shift in free corrosion potential of metallic structure due to biofilm formation. Corrosion rate is determined by finding the intersection point of  $E_{\text{corr}}$  and  $I_{\text{corr}}$  in the polarization curve. [Nature and Science. 2006;4(3):1-4].

**Keywords:** aluminum alloy (AA2024-T3); Microbiologically Influenced Corrosion (MIC); polarization study

## 1. Introduction

Aluminium is considered a reactive alloy (NACE, 1984). The good corrosion resistance of aluminium is due to the formation of a self-protecting, thin, invisible aluminium oxide film that forms immediately on the metal surface. The protective film is susceptible to corrosion by attack from halide ions such as chlorides. This susceptibility to localized corrosion appears to make aluminium alloys vulnerable to MIC. More reports are for AA2024-T3 alloy is used in aircraft or in underground fuel storage tanks, Little (1991), Wagner (1992), ASM (1985), Rosales (1980), Videla (1986). Contaminants in the fuel such as surfactants, water and water-soluble salts may contribute to bacterial growth. The two mechanisms for MIC of aluminium alloys have been documented: the production of water-soluble acids by bacteria and fungi, and the formation of differential aeration cells, Little (1991).

Microbial colonization of metal surfaces causes severe change in the ions concentration, pH, conductivity, and redox potential, altering the passive or active behaviour of the metallic substratum and its corrosion products, as well as the electrochemical variables. Micro organisms influence corrosion by changing the electrochemical conditions at the metal-solution interface. These changes may have different effects, ranging from the induction of localized corrosion to corrosion inhibition through a change in the rate of general corrosion (Beech 2004). A proper identity of bacteria by which corrosion may be exploited on metal surface and role of microbial contaminants in the specific environment as a useful tool to prevent frequent MIC effects (Videla 2005). In the last two decades, significant progress regarding

electrochemical interpretation of MIC has been achieved as a consequence of better understanding of MIC, Dexter (1991), Dickinson (1998), Shobhana (2005), Uhlig's (2000), Stoecker (2001). The usefulness of electrochemical techniques to assess MIC can be improved by documenting the presence of complex deposits of corrosion products, microbial metabolites, and EPS.

This paper describes assessment methods to elucidate microbial corrosion behaviour of aluminium alloy (AA2024-T3) in natural aqueous environment. The quantification includes determination of biomass, cell density and shift in free corrosion potential of metallic structure. Biomass is evaluated as a spectrophotometric analysis of carbohydrate and protein content. The bacterial colonies are expressed as colony-forming units per ml (CFU/ml). The bacterial species are identified up to genus level by employing morphological and biochemical characterization. The microbial corrosion effects on test material are also assessed by polarization study against a saturated calomel reference electrode (SCE).

## 2. Experimental

This work is carried out with aluminium alloy (AA2024-T3) test coupon having weight composition of 4.4 Cu, 0.6 Mn, 1.5 Mg and the rest of 93.5 Al. The specimen is polished using SiC emery papers up to 600 grades and degreased with acetone, washed with distilled water and dried. Biofilms are consented to grow on metal surfaces under laboratory conditions using 1% of glucose as nutrient to natural lake water. The contamination of water is avoided by adding 25 ml of fresh natural lake water after the same quantity of water is pipetted out from the

system for every five days. The chemical constituents of water sample, such as, water temperature, pH, conductivity and dissolved oxygen concentration are measured through out the experiment. All the experiments are carried out at constant atmospheric conditions. An UV-VIS spectrophotometer is used for carbohydrate and protein content analysis (M/s Shimadzu, Japan). Micro colony confirmation is done by an optical microscopy with CCD camera (M/s Shimadzu, Japan). Enumeration of viable cell can be counted by plate count technique using digital colony counter (M/s ELICO, India). The polarization studies are carried out using Potentiostat/Galvanostat (M/s Princeton, Model No. 362). All the chemicals used in this experiment, are purchased from M/s Fluka.

### 2.1. Biomass measurement

Biofilm samples for mass analysis are obtained from the outer surface of each metal at the end of experiments. Biomass data represents the average of ten measurements from the same sample. The biofilm samples from the respective metal are subjected for the analysis of carbohydrates and protein. The analysis of carbohydrates involves the treatment of samples with sulphuric acid to cause the hydrolysis of glycosidic linkages and to dehydrate the monosaccharide in order to allow the reaction with anthrone to yield blue-green coloured complex which is measured calorimetrically at 630 nm (Sadasivam, 1992). Bradford protein assay is based on the observation that the absorbance maximum for an acidic solution of Coomassie Brilliant Blue G-250 shifts from 465 nm to 595 nm when binding to protein occurs (Bradford, 1976). The metal biofilm samples are also subjected to determine the presence of sulphate reducing bacteria. The detection of sulphate reducing bacteria in biofilm samples can be performed using the method developed by the American Petroleum Institute (API, 1982).

### 2.3. Identification of bacteria

The biofilm samples are carefully scraped with a non-metallic spatula and are serially diluted. Then the samples are plated on nutrient agar medium to enumerate the heterotrophic bacteria (Murugesan, 1995). The bacterial colonies are expressed as colony-forming units per ml (CFU/ml). The most numerous similar colonies from all plates are identified through their morphological and biochemical characteristics (Staley, 1989).

### 2.4. Electrochemical study

The biofilm growth on metal surface can influence a change in free corrosion potential and also corrosion current. Corrosion potential and corrosion current of biofilm adhered aluminium alloy

is measured against a saturated calomel reference electrode (SCE). The working electrodes constitute test material of 1 cm<sup>2</sup> of test area. All the experiments are carried out at constant temperature with natural lake water as an electrolyte. The slope of the polarization curve can be used to characterize the degree to which any stage of anodic or cathodic processes is inhibited. The coordinates of this point define the free corrosion potential of the system, as well as total corrosion current ( $I_{\text{corr}} = I_{\text{anodic}} = I_{\text{cathodic}}$ ). The intersecting point of  $E_{\text{corr}}$  and  $I_{\text{corr}}$  in the polarization curve can be used to determine the corrosion rates through the Faradays law equation (1) (Pound, 1979).

$$\text{Corrosion Rate (CR)} = (I_{\text{corr}} * M) / zAF\rho \quad (1)$$

where CR is the corrosion rate (mm/yr),  $I_{\text{corr}}$  is the corrosion current (A), M is the molar mass of metal (g/mole), A is area of electrode (mm<sup>2</sup>), z is number of electrons transferred per metal atom, F is the Faraday's constant and  $\rho$  is the density of metal (g/mm<sup>3</sup>).

## 3. Results and discussion

### 3.1. Bacteria identification

The biofilm structures of all the three metal samples are confirmed on examination under a computer enhanced optical microscopy with CCD camera. The CCD image of dominant bacterial species *Pseudomonas* is shown in Figure 1.

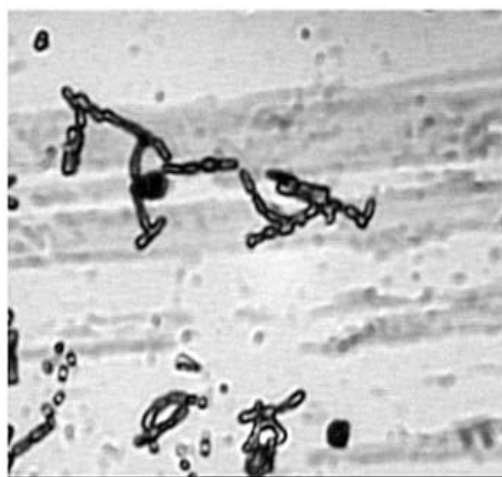


Figure 1. CCD camera image of dominant species *Pseudomonas*

A mixture of micro colony formation, including rod shaped bacteria and cocci are identified through microscopic analysis. The viable cell counts after one month are averaged  $1730 \times 10^7$  CFU/ml. The biofilm sample is subjected to find out the presence of

Table 1. Analysis of chemical constituents of water

Test Coupon	Chemical Constituent					
	pH		TDS ( $\mu$ S)		Dissolved Oxygen (mg/L)	
	Initial	Final (Average)	Initial	Final (Average)	Initial	Final (Average)
AA2024-T3	8.6	8.1	840	910	1287.08	701.89

sulphate reducing bacteria. Based on the results of sulphate reducing bacteria determination, it is confirmed that the biofilm sample is not constituted with sulphate reducing bacteria. The changes in chemical constituents of water, such as pH, conductivity and dissolved oxygen after one month are averaged (Table 1).

### 3.2. Corrosion assessment by polarization experiment

The test coupon exposed to natural lake water is subjected to polarization experiments. The potentiodynamic polarization curve of aluminium alloy immersed in natural lake water is shown in Figure 2.

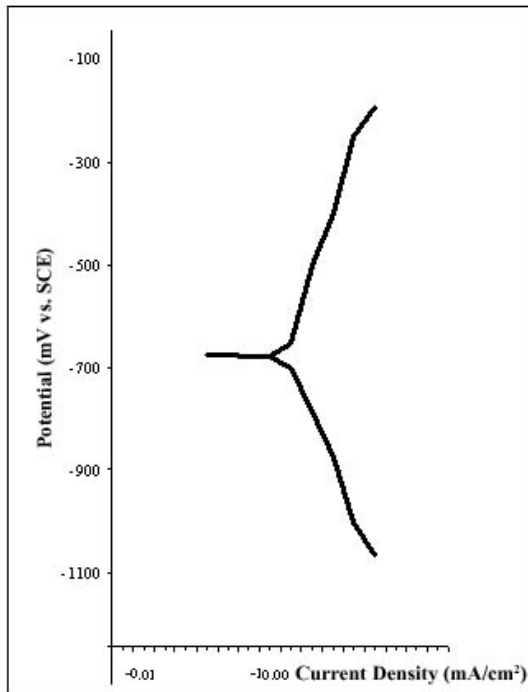


Figure 2. Polarization curve

The  $E_{corr}$  value achieved is typical for this experimental procedure with the aluminium alloy having a potential of -675 mV relative to SCE. The corrosion current density is the measure of corrosion activity. From the polarization curves, the corrosion current density ( $I_{corr}$ ) is determined by Tafel extrapolation method. Passive behaviour is not prevalent for test sample after one month period, but exhibited Tafel behaviour, indicating the surface is under polarization control. The obtained anodic current density is probably a result of the decreasing surface aluminium oxide film on the sample surface. The intersecting point of open circuit potential and corrosion current can be used to determine the microbial corrosion rate of aluminium alloy (AA2024-T3). The corrosion rate of aluminium alloy after one month immersed in natural lake water is estimated 0.01 mm/year. The table 2 summarizes the obtained results for this experimental procedure. It should be noted that the experiment is carried out with constant laboratory conditions in 1% glucose nutrient to natural lake water.

Table 2. Assessment of microbial corrosion behaviour of aluminium alloy

Test Coupon	Biomass (mg/ml)		Cell Count (CFU/ml)	Dominant Species	$E_{corr}$ (mV vs. Ag/AgCl)	$I_{corr}$ ( $\text{mA}/\text{cm}^2$ ) $\times 10^{-3}$	Corrosion Rate (mm/year)
	Carbohydrate	Protein					
AA2024-T3	0.3935	0.1914	$1730 \times 10^7$	<i>Pseudomonas</i>	-675	4.2	0.01

#### 4. Conclusion

Microbial corrosion behaviour of aluminium alloy (AA2024-T3) is evaluated through simple assessment techniques. Microscope with CCD camera is used to confirm the presence of micro organism on the surface of aluminium sample. Bacterial viable cell counts are averaged  $1730 \times 10^7$  CFU/ml after one month period and the species *Pseudomonas* found dominant in biofilm metal sample. Biomass is estimated as a spectrophotometric analysis of carbohydrate and protein content. The chemical constituents of natural lake water are continuously evaluated during the test period. The measurement of corrosion potential and corrosion current is successfully used to estimate the microbial corrosion of aluminium alloy through graphical method. The estimated corrosion rate offers the conclusion that the aluminium alloy (AA2024-T3) is the ideal alloy for long term condensation.

#### Correspondence to:

Balaji Ganesh A, Radhakrishnan T K  
Department of Chemical Engineering  
National Institute of Technology  
Tiruchirappalli- 620015, Tamil Nadu, India.  
[abganesh\\_nitt@yahoo.com](mailto:abganesh_nitt@yahoo.com), [radha@nitt.edu](mailto:radha@nitt.edu)

#### References

1. A Practical Manual on Microbiologically Influenced Corrosion, Vol 2; J.G. Stoecker II, Ed., National Association of Corrosion Engineers International, 2001.
2. API Recommended practice for biological analysis of subsurface injection waters, American Petroleum Institute, Washington, D.C., 1982.
3. ASM Metals Handbook, 1985, Desk Edition, ASM International, Metals Park, OH, p 6-70.
4. Beech IB, Sunner JA. Biocorrosion: towards understanding interactions between biofilms and metals, Curr. Opin. Biotechnol. 2004; 15(3), 181-186
5. Bradford MM. A rapid and sensitive for the quantization of microgram quantities of protein utilizing the principle of protein-dye binding, Analytical Biochemistry, 1976; 72, 248-254.
6. Dexter SC, Duquette DJ, Siebert OW, Videla HA. Use and limitations of electrochemical techniques for investigating microbiological corrosion, Corrosion, 1991; 47,308-318.
7. Dickinson WH, Lewandowski Z. Electrochemical concepts and techniques in the study of stainless steel ennoblement, Biodegradation, 1998; 9(1), 11-21.
8. Little B, Wagner P, Mansfeld, F. Microbiologically influenced corrosion of metals and alloys, International Materials Review, 1991;36(6) 253.
9. Murugesan AG, Rajakumari C. Environmental Science and Biotechnology, Vol 1, MJP publishers, 1995.
10. NACE, 1984, Corrosion Basics, An Introduction, National Association of Corrosion Engineers, Houston, TX, p 75.
11. Pound BG, Abdurrahman MH, Glucina MP, Sharp RM, Wright GA. The Measurement of Corrosion Rates of carbon Steel in Geothermal Media by the Polarization Resistance Technique, Proceedings of the 2nd New Zealand Geothermal Workshop, 1979; 97-100.
12. Rosales BM, De Schiapparelli ER, 1980, Materials Performance 19(8) 41.
13. Sadasivam S, Manickam A, Biochemical methods for Agricultural sciences, Wiley Eastern Limited, New Delhi, 1992
14. Shobhana Chongdar, Gunasekaran G, Pradeep Kumar. Corrosion inhibition of mild steel by aerobic biofilm, Electrochimica Acta, 2005; 50 (24) ,4655-4665.
15. Staley JT, Bryant MP, Pfenning N, Bergey's Manual of Systematic Bacteriology, Vol 3, Williams & Wilkins, 1989.
16. Uhlig's Corrosion Handbook, 2nd ed.; R.W. Revie, Ed.; John Wiley & Sons, Inc. 2000.
17. Videla HA. The action of *Cladosporium resinae* growth on the electrochemical behavior of aluminum, in Biologically influenced corrosion, Dexter, S.C., ed., National Association of Corrosion Engineers, Houston, TX. 1996.
18. Videla HA, Herrera LK, Microbiologically influenced corrosion: looking to the future, International microbiology, 2005; 8,169-180.
19. Wagner P., Little B.J., and Boronstein S.W. The influence of metallurgy on microbiologically influenced corrosion, Proc. Marine Technology Society, Washington, DC, 1992, p 1044.



## Ichthyophthiriasis: Various Fish Susceptibility or Presence of More than one Strain of the Parasite?

Ehab. E. Elsayed<sup>1</sup>, Nisreen. Ezz El Dien<sup>2</sup>, Mahmoud. A. Mahmoud<sup>3</sup>

<sup>1</sup>Department of Pathobiology and Diagnostic Investigation, Michigan State University, East Lansing, Michigan 48824, USA. 517-353-9323, [elsayed@msu.edu](mailto:elsayed@msu.edu)

<sup>2</sup>Department of Parasitology, Faculty of Veterinary Medicine, Cairo University, Cairo, Egypt.

<sup>3</sup>Department of Pathology, Faculty of Veterinary Medicine, Cairo University  
Cairo, Egypt.

**Abstract:** White spot disease is one of the devastating protozoal infections affecting freshwater fish. Commonly known as “Ich”, the Ichthyophthiriasis can infect almost all freshwater fish causing devastating losses in susceptible fish. In the present study, an outbreak of Ichthyophthiriasis erupted in one of the holding tanks of two ornamental fish species, Siamese shark (*Pangasius sutchi*) and goldfish (*Carassius auratus* var. *bicausatus*). Initial observation of the outbreak showed that only *Pangasius sutchi* was affected by typical white spots associated with mortalities. However, *Carassius auratus*, a known susceptible species for *Ichthyophthirius multifiliis* (Ich) in the same aquarium showed only mild erythema that disappeared during the course of infection with no mortalities. To confirm the previous observation, an experimental design was performed in which infection with *Ichthyophthirius* was induced in *Pangasius sutchi* species alone. Cohabitation was performed between the Ich-induced *Pangasius sutchi* and *Carassius auratus*. Three days after the induction, *Pangasius sutchi* started showing the typical clinical signs. Mortalities associated with severe infection were recorded in *Pangasius sutchi* by 7<sup>th</sup> day after infection. Associated *Carassius auratus* showed only mild erythema that disappeared by the end of experiment. Histopathological examination of skin from both species in natural and experimental infection was performed to evaluate the severity of infection on the tissue level. Substantial numbers of typical large size trophonts surrounded by layers of fibrous tissue, melanophores and hemorrhages were detected in dermal and epidermal layers. Underlying myodegeneration was also associated the skin lesions in *Pangasius sutchi*. In contrary, pathological changes in the skin of *Carassius auratus* were mild and few numbers of immature trophonts were noticed in the epidermal layers. Possible reasons for such infection discrepancies between the two susceptible species are discussed. [Nature and Science. 2006;4(3):5-13].

**Keyword:** *Ichthyophthirius multifiliis*, *Pangasius sutchi*, *Carassius auratus*, infection, protozoa, ciliates

### Introduction

Commonly known as “Ich”, the white spot disease (Ichthyophthiriasis), can infect almost all freshwater fish (Ventura and Paperna, 1985) and at least one species of amphibian (Gleeson, 1999). The disease is recognized as one of the most pathogenic diseases of fish caused by eukaryote parasites resulting in significant economic losses in the affected cultured fish species (Matthews, 1994). Ich is caused by a hymenostomatid ciliate, *Ichthyophthirius multifiliis* Fouquet, 1876 (*I. Multifiliis*). The parasite is commonly distributed, occurring in tropical, subtropical and temperate regions, and extending north to the Arctic Circle (Matthews, 1994). It causes severe epizootics among different fish species in aquaria, hatcheries, and ponds, as well as in wild fish populations (Ezz El-Dien

*et al.*, 1998; Thilakaratne, *et al.*, 2003; Kim *et al.*, 2002). Naturally occurring outbreaks of Ichthyophthiriasis in wild fish populations can yield devastating effects. For example, natural outbreak of the Ich was blamed for the deaths of 18 millions *Orestias agassi* in Lake Titicaca, Peru (Wurtsbaugh and Tapia, 1988). In intensive aquaculture systems, Ich epizootics are more common (Valtonen and Keränen, 1981) due to the confinement of fish under stressful condition and the exponential increase in parasite numbers (Clark *et al.*, 1995).

The life cycle of *Ichthyophthirius multifiliis* is a direct one and requires no intermediate host (Ewing and Kocan, 1992). Invasion of the infective theront gives rise to the trophont that grows inside the host epithelium to the size of 1 mm in diameter (Lom and Dykova, 1992). The trophont becomes easily visible owing to the

opacity of the cytoplasm in the fish skin (Matthews, 1994) and the formation of somatic cyst by the fish body around the parasite (Price and Bone, 1985). These white spots are easily countable. However, a single white spot does not necessarily represent a single trophont, since aggregations of trophonts can occur in one large white spot as a result of multiple entries at single site (Matthews, 1994). Nevertheless, scoring of individual white spots with appropriate controls provides a direct, quantifiable measure of infection levels on fish (Ventura and Paperna, 1985). The trophonts mature inside the host and develop into tomites, each of which is able to produce up to 3000 tomites which released as theronts. After being released, the free-swimming theronts can infect a new host or re-infect the same host, thus compromising its health status (Lome and Dykova, 1992). Severe damage of the skin epithelium occurs due to the break of the parasites through host skin during infection and their release. This damage might lead to concession of osmoregulatory process and ion regulation and might serve as a portal of entry for secondary invaders, leading eventually to death of fish (Ewing & Kocan, 1987, Ewing *et al.*, 1994 and Tumbol *et al.*, 2001).

Increasing reports are continually published indicating that different fish species and populations have significance difference in their resistance to Ich. These differences in susceptibility were attributed primarily to environmental factors and/or genetic make up of the host (Hines *et al.*, 1974; Clayton and Price, 1992; Clayton and Price, 1994; Price and Clayton, 1999; Gleeson *et al.*, 2000). Another line of reports assumed the presence of more than one strain of *I. Multifiliis* were assumed. This assumption was based primarily on the wide distribution of the parasite, subtle variation in cell morphology and serotypic variations among isolates based on immobilization antigens (Nigrelli *et al.*, 1976, Dickerson *et al.*, 1993 and Leff *et al.*, 1994). Yet, no clinical or field evidences were reported to support this assumption.

Results from the current study report the Ichthyophthiriasis in Siamese shark (*Pangasius sutchi*) for the first time. Initial observations of clinical signs discrepancies of Ichthyophthiriasis in two aquarium fish species under similar conditions were also reported. Investigational approaches might provide a potential clinical clue for the presence of more than one *Ichthyophthirius multifiliis* strain.

## Materials and Methods

### Natural outbreak

A total of 17 fish; 10 Siamese Shark (*Pangasius sutchi*) and 7 Goldfish (*Carrasius auratus* var. bicausatus) were introduced to one aquarium at the

department of fish disease and management, College of Veterinary Medicine, Cairo University in July of 2001. Two days later, the *Pangasius sutchi* (*P. sutchi*) fish started showing itching behaviors, hemorrhagic patches, fin rot and white spots all over the fish body. Seven of the *Pangasius sutchi* died 10 days after eruption of the clinical signs. The *Carrasius auratus* (*C. auratus*) in the same aquarium showed only mild hemorrhages on the side of fish body by the third day and these signs were completely disappeared by the seventh day. No mortalities or white spots were noticed on goldfish during the course of the outbreak.

### Experimental Infection

To confirm the previously mentioned observations, an experiment was designed as in Table 1. A total number of 36 apparently healthy *P. sutchi* (total length  $7 \pm 2$  cm) and 30 fingerlings goldfish (total length  $3 \pm 1$  cm) were used in the experiment. The *P. sutchi* were bought from a commercial dealer while the goldfish were generously donated to the lab by a local ornamental fish breeder with a health history indicating that the fingerlings and their parents had never been previously exposed to ich. The fish were allowed to acclimatize for a period of 4 weeks in glass aquaria and supplied with clean dechlorinated water, aeration and fed on Tetra food fish flakes 2% of the their body weight at water temperature 25°C. After the acclimatization period, the fish (Siamese shark and goldfish) were divided into 4 designated aquaria A, B, C, D and E as shown in (Table 1). The dimension of each aquarium was 60X40X30 cm (Length X Height X Width). At the beginning of experiment, the *P. sutchi* (6 fish) in aquarium (A) were used as the source of infection after induction of Ich. By sudden change in water temperature (5-7°C temperature differences) 3-4 times on 1 hr intervals. Previous work in our lab with ornamental fish indicated that the sudden and repeated water changes of the water temperature induce infection by Ich in the exposed fish within 3-4 days. After induction, the *P. sutchi* fish were split equally between aquarium B and D (3 fish each aquarium). The fish in the 4 aquaria were monitored for a period of two weeks, clinical signs were recorded, and dead fish were removed on a daily basis and kept in 10% formalin. Representative samples (2 fishes) of fish showing clinical signs were also sacrificed and preserved in 10% formalin for histopathological examination.

### Histopathological Examination

Tissue specimens from affected fish (Skin, muscles and gills) were collected after clinical and gross examination and immediately fixed in neutral buffered

formalin 10% for 1 week; dehydration was done using ascending grades of ethanol (70, 80, 90, and 100% for 1 hour each). The specimens were then cleared in 2 changes of xylene. After blocking using soft paraffin, serial sections of 4µm thickness were done. The sections were stained using routine hematoxylin and eosin stain (Ezz El-Dien, et al., 1998).

### Parasitological Examination

Macroscopic examination of the affected fish was done carefully for detection of visible lesions. Fresh as well as Geimsa stained smears from body surface, fins and gills were microscopically examined according to Pritchard and Kruse (1982). The detected protozoan parasite was photomicrographed and measured using ocular micrometer.

### Results

Upon the initial natural outbreaks, typical white spots characteristic of Ich. appeared on *P. sutchi*, while *C. auratus* showed only non specific signs of mild skin irritation. At the beginning of the outbreak “two days after arrival” the *P. sutchi* were restless, swimming erratically and itching against fixed objects. Small white spots appeared on the sides of the fish body, fins and head (Figure 1). In some cases, the small white spots coalesce together forming larger white spots. Hemorrhagic patches appeared on the bases of the fins, fish sides and mouth. Fin rot appeared sometimes on some of the affected fish. Six days later, the fish stopped feeding, appeared lethargic and swam near to the water surface. Seven of the *P. sutchi* died 10 days after arrival. Skin scrapping revealed the presence of different developmental stages of the *I. multifiliis*. The most predominant stage was the mature trophont with the C-shaped macronucleus (Figure 2). During the initial natural outbreaks, the goldfish showed only focal areas of hemorrhages (petichiation), especially at the root of the scales (Figure 3). Sometimes the hemorrhagic spots were enlarged and tinged with mucous. Fish swam erratically during the first 3 days, and then returned to their normal behavioral. Skin scrapping from the goldfish during the clinical signs showed small immature stage of the *I. multifiliis* trophont. It was surprising that no mortalities were

recorded in the goldfish during the initial natural outbreak.

To confirm the previously mentioned observations, the Ich was induced experimentally and allowed to join other non induced fish in aquaria B and D. Control groups (groups C, D and E – Table 1) were not exposed to any handling and were maintained at the same environmental conditions. The fish in the treated and control groups were monitored daily for abnormal signs. Three days later, the Siamese shark started showing erratic swimming behavior, itching, hemorrhagic patches on the sides of the body with few small white spots. The body of the fish was completely covered with white spots by the fifth day. A total of 5 and 7 fish died in tank (B) and (D) respectively by the end of the experiment. Goldfish showed only mild congestion at fin basis and small patches of hemorrhages on their sides and gill covers that disappeared by the fifth day of exposure. No mortalities were recorded in the goldfish during experimental infection exposure. Microscopic examination of the skin scrapping of the affected Siamese shark and goldfish revealed the same picture found in the natural outbreak.

Histological sections of the skin of *P. sutchi* revealed large trophonts of the *I. multifiliis* that were prominently lodged in the epidermal layers. The parasite appeared with large C-shaped macronucleus. Most trophonts observed were adjacent to the basement membrane of the epithelial layer and the surrounding tissue did not show any evidence of damage (Figure 4). In many sections, there were no signs of damage to the epidermal cells surrounding the trophont. In other sections, however, the cells between the parasite and the basement membrane were hydropic, vacuolated and/or necrotic with pyknotic nuclei. In other cases, the macronucleus was not demonstrated in the section either due to the level of the sectioning or the stage of maturation of the trophont. Large aggregations of melanophores were clear around the trophonts and a large number of club cells activation (Figure 5). Epidermal cells around the parasite appeared atrophied. Myodegeneration of the underlying musculature was clearly observed where the muscle fibers were hyalinized with prominent destruction of the nuclei. In goldfish, the detected trophonts in the epidermis were very small in all examined sections. The tissue reaction was less common where the melanophores activation was neglected. Free red blood cells were noticed either between the epidermal cells or in the dermal layers (Figure 6).

Table 1. Design for the experimental infection with *I. Multifiliis*:

Aquarium	Gold fish #	Siamese Shark #	Experimental Group
A	0	6 fish were used for induction then joined later to B& C aquarium	
B	10	10	Treatment group
C	10	10	Control group
D	-	10	Control group
E	10	-	Control group

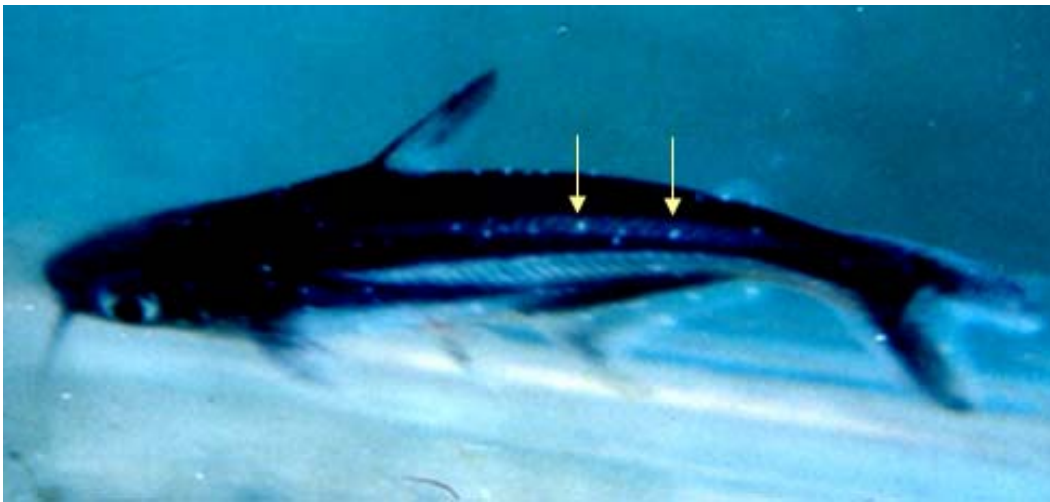


Figure 1. Siamese shark fish infected with Ich. Note the multiple white spots on fish side (arrows)



Figure 2. Wet mount of the Siamese shark skin during infection with Ich. Note the C-shape nucleus of the *I. multifiliis* (bar= 75  $\mu$ m).

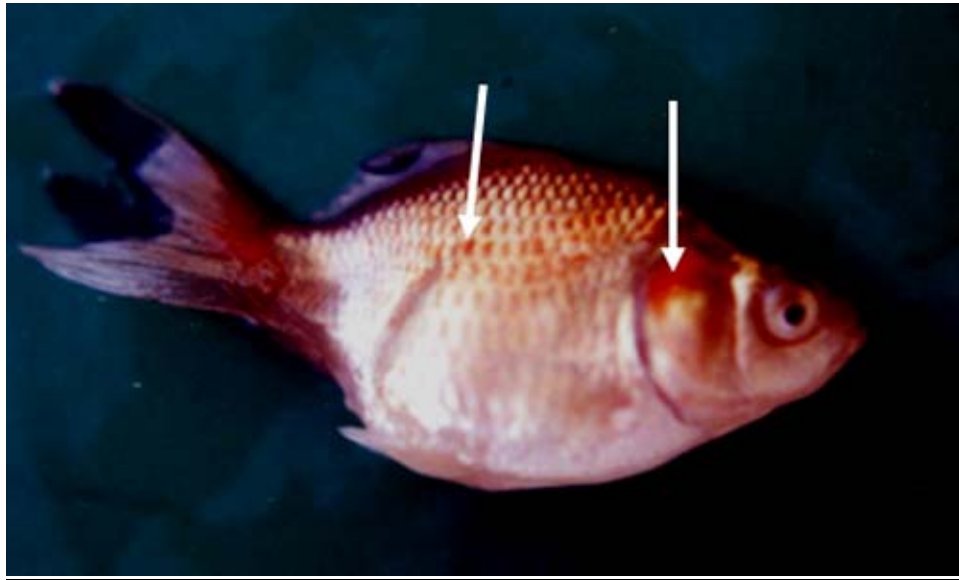


Figure 3. Goldfish showing focal hemorrhages at the base of scales and gill cover (arrows)

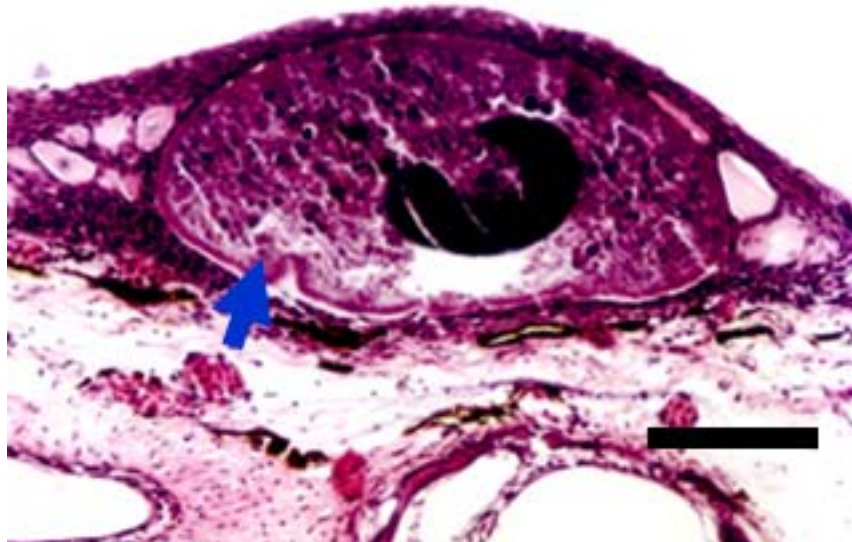


Figure 4. Mature trophont of *Ichthyophthirius multifiliis* in the epidermal layer of Siamese shark (arrow)  
(bar = 100  $\mu$ m)

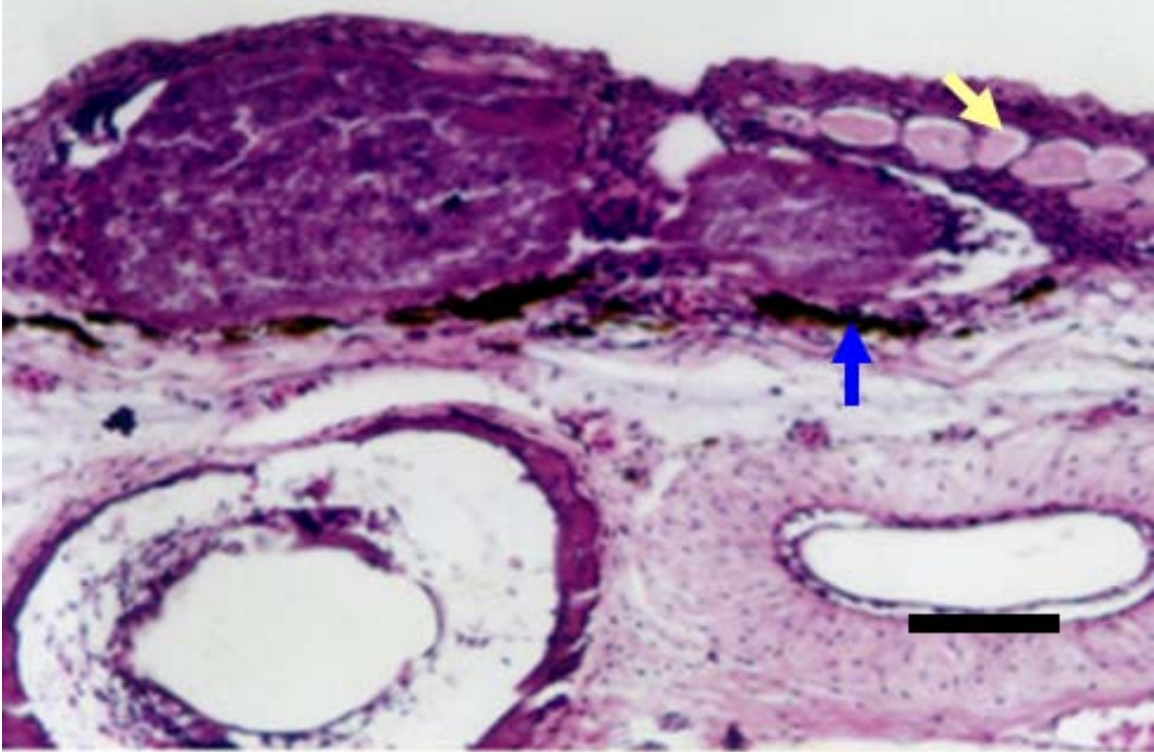


Figure 5. Melanophores accumulation (blue arrow) around the *Ichthyophthirius multifiliis* trophont. Note the activated club cells at the surface of epidermis (yellow arrow) (bar = 100  $\mu$ m)

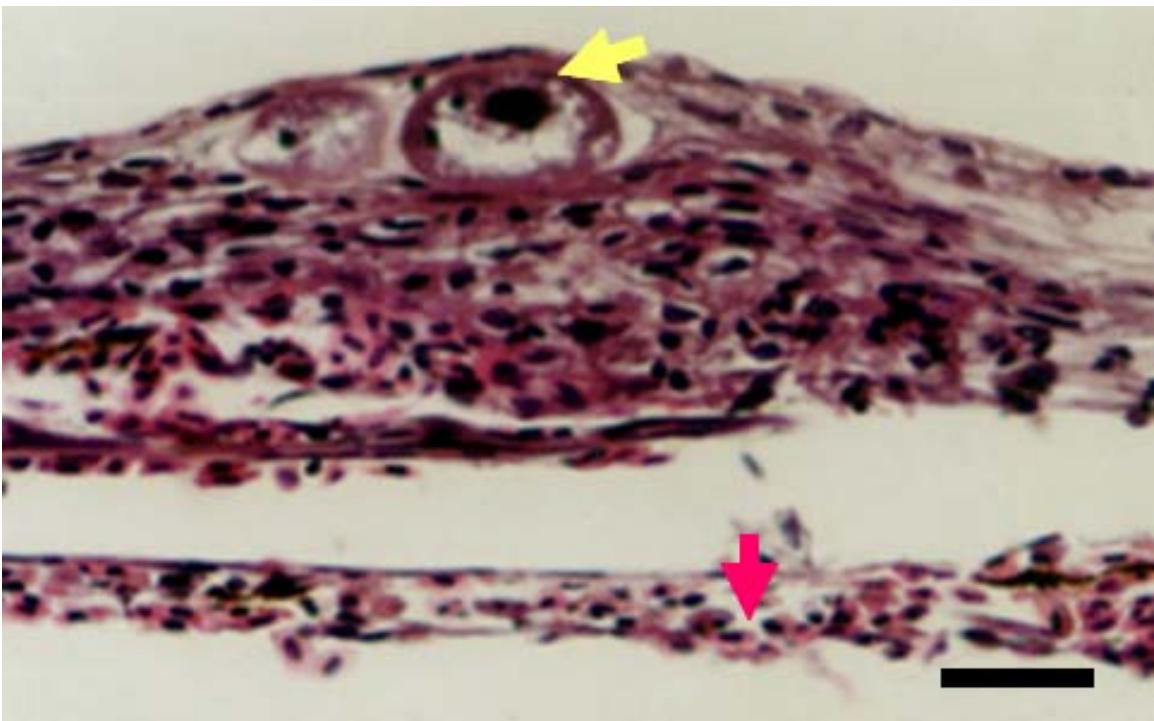


Figure 6. Small immature trophont of *Ichthyophthirius multifiliis* (yellow arrow) in the skin of goldfish. Note the blood cells resulted from the hemorrhages in the dermal layer (red arrow) (bar = 25  $\mu$ m)

## Discussion

Initial observation of the natural outbreaks indicated that the Siamese sharks showed typical Ichthyophthiriasis signs, while the goldfish showed mild signs of skin irritation. Current stud reports the first record of white spot disease in Siamese shark (*P. suctchi*). However the presence of the atypical mild clinical signs in the goldfish, a known susceptible fish species, was a surprising finding. To confirm these clinical signs, an experiment was designed to mimic the natural outbreak in the Siamese shark. The Ich was induced in *P. suctchi* which were introduced later to aquaria contained both *P. suctchi* and *C. auratus*. The experiment was repeated three times to confirm the clinical signs and ensure consistency of the obtained data. Clinical signs obtained in each time of the experiment were consistent with what was recorded in the natural outbreak.

Discrepancies in the clinical signs between the two exposed fish species were puzzling and could be attributed to fish susceptibility. Earlier reports on ichthyophthiriasis in fish indicated that different fish species show significant differences in their ability to resist disease (Hines et al., 1974). As early as 1947, authors observed that Rainbow trout were more susceptible to infection by *Ichthyophthirius multifiliis* than brown trout (Butcher, 1947). Also, Clayton and Price (1992) demonstrated that susceptibility to Ich varies between different strains of platy, an aquarium fish. However, this assumption contradicted with previous data regarding goldfish. Natural repeated outbreaks of Ich associated with typical clinical signs in goldfish indicated the high susceptibility of this species to *Ichthyophthirius multifiliis* (Ezz Eldin, et al., 1998). A similar report was also published in this regard (Ling et al., 1993). Moreover, goldfish in a controlled experimental infection with Ich usually develop typical clinical signs upon contact with theronts (Ling et al., 1993).

In the current experiment, goldfish developed only atypical mild clinical signs upon contact with the infected Siamese shark fish. This might raise a concern about the variation of exposure of the two species to the infective agent, theront, in the water, infection dose and the method of infection used in the experimental infection. To exclude these assumptions, goldfish and Siamese shark were exposed to the infection through the induced fish at the same time to ensure the exposure of both species to the same infection dose. Moreover the fish during the first 2 days of adding the goldfish were held in a low water column (not exceeding 20 cm) to ensure high concentration of the infective agents.

Previous reports for experimental infection with Ichthyophthiriasis usually used active culture of

*Ichthyophthirius multifiliis* maintained in the lab for long time (Xu & Klesius 2003 and Sigh & Buchmann, 2000). This active culture usually used the same fish species of origin in the passage or adapted in different species. In either case, the parasite might loss its pathogenicity over long term of passage or become more pathogenic for the new host over long time of passage. In the current study, we used the natural method of inducing infection rather than laboratory culture to investigate the initial observation. Using this method of infection induction mimic the natural infection process and are considered standard to investigate natural infection using controlled experiment. However, a question might rise about the source of theronts in the current study upon sudden temperature change induction. Where is the infective stage come from especially under controlled environmental conditions? Could it be a normal flora of fish skin that flares up upon exposure to stress factors and transform to pathogenic form? Could it be a part of the aquatic system inhabited by any aquatic animal? A trail of questions needed to be thoroughly addressed to clarify the Ich epidemiology completely.

The likelihood of maternal immunity could be raised as another assumption for the mild infection in the goldfish during the natural outbreak. It is well documented that maternal antibodies passed from mothers to their offspring directly via eggs (Mor & Avtalion, 1988 and Sin et al., 1994) or indirectly in mouth-brooding fish via mucus of buccal cavity (Sin et al., 1994). To investigate this possibility, a naïve goldfish from a brood stock that had never been exposed to Ichthyophthiriasis was used in the experimental study. Results excluded the responsibility of maternal immunity for the atypical mild signs in the goldfish during the natural and experimental infection. Meanwhile, the Siamese shark expressed the typical clinical signs for ichthyophthiriasis, associated with mortalities reached to 70% and 50 % in natural infection and experimental infection respectively. This could be an indication of the susceptibility of the fish and/or the host specificity of the parasite. In evaluating discrepancies associated with susceptibility to a disease, there is often a dilemma of having to use a norm such as mortality. There are probable rationales as to why one group of fish differs from another in resistance to a disease (Chevassus & Dorson, 1990). This is rather inadequate since the measurement of resistance (mortality) is rather distant from the authentic infection process. In ichthyophthiriasis, this is not so much a predicament since both exposure to infection and resulting infection levels on the fish can easily be quantified. The presence of white spots along with associated hemorrhages and behavioral changes is

considered the ultimate indication for the presence and susceptibility of any fish species to the infection with ichthyophthiriasis.

Histopathological examination of Siamese shark skin indicated the typical pathological changes induced by *I. multifiliis* infection mentioned in previous reports (Ezz El-dien, et al., 1998). On the other hand, goldfish skin showed only mild inflammatory reaction and trophonts in the epidermis were very small and never reached maturity. This was an indication of the success of the infection process in goldfish, yet it didn't reach the final stages for some reasons. Also, there was no formation of somatic cysts by the fish body around the parasite that typically encountered in typical Ichthyophthiriasis (Price & Bone, 1985). Combine this pathological picture with the previous reports of goldfish susceptibility might indicate that the reason could be related to non specificity of the parasite strain rather than host resistance. Because of the non specificity of this parasite, the host tissue reacted in a way which forced the parasite to leave the body without completing its life cycle. This is consistent with previous studies which suggest that rather than killing the infective stage of the parasite, the host body forces the parasite to exit prematurely in response to immune response (Wahli & Matthews 1999).

Current study assumed the presence of more than one strain of *I. multifiliis* which differ in their pathogenicity to different fish species. Previous record suggested the presence of more than one species of *I. multifiliis* that possess similar morphological criteria (Yunchis 1997). These findings could be describing the atypical mild signs found in the goldfish upon concurrent infection with Siamese shark. However, molecular investigation is needed to prove such assumption. Future research will be focusing on differentiating the *I. multifiliis* isolates from both goldfish and Siamese shark using molecular tools.

#### Correspondence to:

Ehab Elsayed, DVM, PhD  
Natural Resources Building- Room 4  
Michigan State University  
East Lansing, MI 48824, USA  
Phone#517-353-9323  
E-mail: [elsayed@msu.edu](mailto:elsayed@msu.edu)

#### References

- Butcher AD (1947). Ichthyophthiriasis in Australian trout hatchery. *Progressive Fish Culturist* **9**, 21-26.
- Chevassus B & Dorson M (1990). Genetic resistance to disease in fishes. *Genetics in Aquaculture III*, pp. 83-107, *Aquaculture* **85**, 1-4.
- Clark TG, Lin T L & Dickerson H W (1995). Surface immobilization antigens of *Ichthyophthirius multifiliis*: Their role in protective immunity. *Annual Review of Fish Diseases* **5**, 113-131.
- Clayton GM & Price DJ (1992). Interspecific and intraspecific variation in resistance to ichthyophthiriasis among poeciliid and goodeid fishes. *Journal of Fish Biology* **40**, 445-453.
- Clayton GM & Price DJ (1994). Heterosis in resistance to *Ichthyophthirius multifiliis* infections in poeciliid fish. *Journal of Fish Biology* **44**, 59-66.
- Dickerson H W, Clark TG & Leff AA (1993). Serotypic variation among isolates of *Ichthyophthirius multifiliis* based on immobilization. *Journal of Eukaryotic Microbiology* **40**, 816-820.
- Ewing MS & Kocan KM (1987). *Ichthyophthirius multifiliis* (Ciliophora) exit from gill epithelium. *Journal of Protozoology* **34**, 309-312.
- Ewing MS & Kocan KM (1992). Invasion and development strategies of *Ichthyophthirius multifiliis*, a parasitic ciliate of fish. *Parasitology Today* **8**, 204-208.
- Ewing MS, Black MC, Blazer VS & Kocan KM (1994). Plasma chloride and gill epithelial response of channel catfish to infection with *Ichthyophthirius multifiliis*. *Journal of Aquatic Animal Health* **6**, 187-196.
- Ezz El-Dien N M, Aly SM & Elsayed EE (1998). Outbreak of *Ichthyophthirius multifiliis* in ornamental goldfish (*Carassius auratus*) in Egypt. *Egyptian Journal of Comparative Pathology and Clinical Pathology* **2**, 235-244.
- Gleeson DJ (1999). Experimental infection of striped marshfrog tadpoles (*Limnodynastes peronii*) by *Ichthyophthirius multifiliis*. *Journal of Parasitology* **85**, 568-570.
- Gleeson DJ, McCallum HI & Owens IP (2000). Differences in initial and acquired resistance to *Ichthyophthirius multifiliis* between populations of rainbowfish. *Journal of Fish Biology* **57**, 466-475.
- Hines RS, Wohlfarth GW, Moav R & Hulata G (1974). Genetic differences in susceptibility to two disease among strains of the common carp. *Aquaculture* **3**, 187-197.
- Kim Jeong-Ho, Hayward CJ, Joh Seong-Joh & Heo Gang-Joon (2002). Parasitic infections in live freshwater tropical fishes imported to Korea. *Diseases of Aquatic Organisms* **52**, 169-173.
- Leff AA, Yoshinaga T & Dickerson HW (1994). Cross immunity in Channel catfish, *Ictalurus punctatus* (Rafinesque), against two immobilization serotypes of *Ichthyophthirius multifiliis* (Fouquet). *Journal of Fish Diseases* **17**, 429-432.
- Ling KH, Sin YM & Lam TJ (1993). Protection of goldfish against some common ectoparasitic protozoans using *Ichthyophthirius multifiliis* and *Tetrahymena pyriformis* for vaccination. *Aquaculture* **116**, 303-314.
- Lom J & Dykova I (1992). Protozoan parasites of fishes. *Developments in Aquaculture and Fisheries Science*, pp. 253-259. Elsevier, Amsterdam.
- Matthews RA (1994). *Ichthyophthirius multifiliis* Fouquet, 1876: Infection and protective response within the fish host. In (Pike AW & Lewis JW Eds.), pp.17-42. *Parasitic Disease of Fish*. Samara Publishing, Tresaith, UK.
- Mor A & Avtalion RR (1988). Evidence of immunity from mother to eggs in tilapias. *Bamidgh* **40**, 22-28.
- Nigrelli RF, Pokomy KS & Ruggieri GD (1976). Notes on *Ichthyophthirius multifiliis*, a ciliate parasitic on freshwater fishes, with some remarks on possible physiological races and species. *Transaction of The American Microscopic Society* **251**, 607-613.
- Price DJ & Bone LM (1985). Maternal effects and resistance to infection by *Ichthyophthirius multifiliis* in *Xiphophorus maculatus*. In (Manning MJ & Tatner MF, Eds.), pp. 233-244. *Fish Immunology*. Academic Press Inc. London.
- Price DJ & Clayton GM (1999). Genotype-environment interactions in the susceptibility of the common carp, *Cyprinus carpio*, to *Ichthyophthirius multifiliis* infections. *Aquaculture* **173**, 149-160.



23. Pritchard MH & Kruse GW (1982). The collection and preservation of animal parasites, University of Nebraska Press.
24. Sigh J & Buchmann K (2000). Association between epidermal thionin-positive cells and skin parasitic infections in brown trout, *Salmo trutta*. *Diseases of Aquatic Organisms* **41**, 135-139.
25. Sigh J & Buchmann K (2000). Associations between epidermal thionin-positive cells and skin parasitic infections in brown trout *Salmo trutta*. *Diseases of Aquatic Organisms* **41**, 135-139.
26. Sin YM, Ling K H & Lam TJ (1994). Passive transfer of protective immunity against ichthyophthiriasis from vaccinated mother to fry in tilapias. *Aquaculture* **120**, 229-237.
27. Thilakarathne ID, Rajapaksha G, Hewakopara A, Rajapakse RP & Faizal AC (2003). Parasitic infections in freshwater ornamental fish in Sri Lanka. *Diseases of Aquatic Organisms* **54**, 157-162.
28. Tumbol RA, Powell MD & Nowak BF (2001). Ionic effects of infection of *Ichthyophthirius multifiliis* in goldfish. *Journal of Aquatic Animal Health* **13**, 20-26.
29. Valtonen ET & Keränen AL (1981). Ichthyophthiriasis of Atlantic salmon, *Salmo salar* L. at the Montta hatchery in northern Finland in 1978-1979. *Journal of Fish Diseases* **4**, 405-411.
30. Ventura MT & Paperna I (1985). Histopathology of *Ichthyophthirius multifiliis* infections in fishes. *Journal of Fish Biology* **27**, 185-203.
31. Wahli T & Matthews RA (1999). Ichthyophthiriasis in carp *Cyprinus carpio*: infectivity of trophonts prematurely exiting both the immune and non-immune host. *Diseases of Aquatic Organisms* **36**, 201-207.
32. Wurtsbaugh WA & Tapia RA (1988). Mass mortality in lake Titicaca (Peru-Bolivia) associated with the protozoan parasite *Ichthyophthirius multifiliis*. *Transaction of the American Fisheries Society* **117**, 213-217.
33. Xu DH & Klesius PH (2003). Protective effect of cutaneous antibody produced by channel catfish, *Ictalurus punctatus* (Rafinesque), immune to *Ichthyophthirius multifiliis* Fouquet on cohabited non-immune catfish. *Journal of Fish Diseases* **26**, 287-291.
34. Yunchis ON (1997). New species of *Ichthyophthirius* Fouquet, 1876. 8th International Conference of the European Association of Fish Pathologists: Diseases of Fish and Shellfish, 14-19 Sep, Edinburgh, UK.

# Study of Transmission Electron Microscopy (TEM) and Scanning Electron Microscopy (SEM)

Hongbao Ma \*, Kuan-Jiunn Shieh \*\*, Tracy X. Qiao \*\*\*

\* Department of Medicine, Michigan State University, East Lansing, Michigan 48824, USA  
Telephone: 517-303-3990; Email: [hongbao@msu.edu](mailto:hongbao@msu.edu)

\*\* Department of Chemistry, Chinese Military Academy, Fengshan, Kaohsiung, Taiwan 830, ROC.  
Telephone: 011-886-7742-9442; Email: [chemistry0220@gmail.com](mailto:chemistry0220@gmail.com)

\*\*\* University of Michigan, Ann Arbor, Michigan 48105, USA  
Telephone: 734-623-9719; Email: [xiaotan@umich.edu](mailto:xiaotan@umich.edu)

**Abstract:** Scanning electron microscopy (SEM) and transmission electron microscopy (TEM) are widely used in material science, metallurgy science and life science researches. TEM is an imaging technique where a beam of electrons is focused onto a specimen causing an enlarged version to appear on a fluorescent screen or layer of photographic film. SEM is a technique of electron microscope to produce high resolution images of a sample surface. This article describes the basic principle of TEM and SEM, and their applications. [Nature and Science. 2006;4(3):14-22].

**Keywords:** electron; microscopy; scattering; transmission

## 1. Introduction

Transmission electron microscopy (TEM) is an imaging technique where a beam of electrons is focused onto a specimen causing an enlarged version to appear on a fluorescent screen or layer of photographic film. The first practical TEM was built by Albert Prebus and James Hillier at the University of Toronto in 1938 using concepts developed earlier by Max Knoll and Ernst Ruska (Wikipedia, 2006). Scanning electron microscope (SEM) is a technique of electron microscope to produce high resolution images of a sample surface. Due to the manner in SEM the image is created, its images have a characteristic three-dimensional appearance and are useful show the surface structure of the target sample.

TEM and SEM are widely used in material science, metallurgy science and life science researches. An electron passing through a solid could be scattered for once (single scattering), several times (plural scattering), or very many times (multiple scattering). Each scattering event might be elastic or inelastic. The scattered electron is most likely to be forward scattered but there is a small chance that it will be backscattered. The probability of scattering is either as an "interaction cross-section" or a mean free path.

Single scattering is an electron undergoes only one scattering event as it passes through a specimen. Plural

scattering is an electron undergoes more than one scattering event but less than 20 as it passes through a specimen. Multiple scattering is an electron undergoes more than 20 scattering events as it passes through a specimen. Elastic scattering is the scattering of an electron if a negligible amount of energy is lost by the primary electron in the process. The direction of the electron may change, but the energy not. Inelastic scattering is a process by which the primary electron loses a significant amount of energy.

When the solid specimen is thicker than about twice the mean free path, plural scattering happens. This can be modelled using the Monte Carlo technique. The important features are the fraction of electron scattering forward and backwards and the volume of the specimen in which most of the interactions happen.

## 2. TEM Basic

The following is a brief description for the TEM techniques (Williams, 2000).

Many physical techniques rely on the interaction between high energy electrons and the atoms in a solid. There are many possible interactions and some of the more useful (in that they give rise to measurable effects) are simulated on the next page. In the simulations that follow, high energy electrons, typically 20 keV or higher, are allowed to interact, one by one, with a single

atom of aluminium. This atom is assumed to be part of a solid metallic specimen and it contributes 3 electrons to a valence band or conduction band. In TEM a thin specimen is illuminated with electrons, the primary electrons. This section details some of the interactions between those electrons and the specimen.

After an inner shell excitation an atom has an energy above its ground state. It can relax and lose some of this energy in several ways. This simulation models the interaction of high energy electrons with atoms of aluminium. The incoming primary (red) electron can be elastically scattered, losing very little energy, or it can undergo an inelastic scattering process.

The interactions modelled include the excitation of inner shell electrons, the creation of plasmons and interactions with single valence electrons.

In the simulation, each incoming primary electron is shown separately after you click on the "Next electron" button. Subsequent relaxation of inner shell excited atoms may occur by the emission of an X-ray or an Auger electron.

Every electron microscope, of whatever type, must have a source of high energy primary electrons - an electron gun. The function of the gun is to produce a fine beam of electrons of precisely controlled energy (i.e. velocity) all coming from a small source region.

A thermionic electron gun is operated as follows: Select the accelerating potential (kV). Increase the current passing through the filament until the knee of the emission curve is reached (saturation), giving the best compromise between the beam current emitted (as high as possible) and the filament lifetime (as long as possible). Adjust the bias to give the desired combination of source size and beam current.

Here are two parameters which control the electron gun: (1) Filament current. The filament current controls the temperature of the filament and hence the number of electrons emitted or 'beam current'. Generally we want a large number of electrons emitted from a small region of the filament. This is done by saturating the filament - increasing the filament current until the beam current no longer rises. (2) Bias. The bias potential controls the size of the region of filament which emits electrons and hence it affects both the source size and the beam current. If the bias is too high no region of the filament will emit and the beam is said to be pinched off. The main reason to alter bias is to change the brightness of the beam.

Diffraction at an aperture (leading to Airy rings) limits the resolution of many optical systems. Use the simulation to show that the size of the central disc of illumination varies inversely with the size of the aperture (W).

where

( $\theta$  is the angular deflection of the beam at the aperture.)

16% of the intensity (electrons in the TEM) falls outside the central disc. Adjust the brightness in the simulation to see how low the intensity of the rings is compared to that of the central disc. The Rayleigh criterion for resolution indicates how close together two points can be brought together before they can no longer be distinguished as separate. Resolution (or strictly resolving power) is defined as the closest spacing of two points which can be resolved by the microscope to be separate entities. This simulation shows two sets of Airy rings showing the variation in light intensity across the rings.

The actual beam diameter results from the diameter of the original beam leaving the electron gun,  $d_g$  broadened by the effect of spherical aberration in the lenses  $d_s$  and diffraction at the aperture,  $d_d$ . These depend on the current,  $i$ , convergence angle,  $\alpha$ , brightness,  $\beta$ , spherical aberration coefficient,  $C_s$ , and wavelength,  $\lambda$ , via

$$d_g = \frac{2}{\pi} \sqrt{\frac{i}{\beta}} \frac{1}{\alpha}$$

$$d_s = 0.5 C_s \alpha^3$$

$$d_d = 1.22 \frac{\lambda}{\alpha}$$

The total beam diameter is found by adding these three effects in quadrature i.e.

$$d_t = \sqrt{d_s^2 + d_g^2 + d_d^2}$$

For best resolution in many applications we need to use the smallest beam diameter.

Electron lenses are the magnetic equivalent of the glass lenses in an optical microscope and to a large extent, we can draw comparisons between the two. For

example the behaviour of all the lenses in a TEM can be approximated to the action of a convex (converging) glass lens on monochromatic light. The lens is basically used to do two things: (1) either take all the rays emanating from a point in an object and recreate a point in an image, (2) or focus parallel rays to a point in the focal plane of the lens.

A strong magnetic field is generated by passing a current through a set of windings. This field acts as a convex lens, bringing off axis rays back to focus. Click on 'Draw rays' to compare the action of an electromagnetic lens with an optical lens.

The image is rotated, to a degree that depends on the strength of the lens. Focal length can be altered by changing the strength of the current.

All electromagnetic lenses act like 'thin' convex lenses - their thickness can be ignored for most purposes. The most important property of a thin lens is its focal length  $f$ . Parallel rays entering the lens are brought to focus at the distance  $f$  shown in the diagram.

Try moving the object (red bar) along the optical axis noting size position, and orientation of the image. Simple geometry shows that the magnification  $M$ , of the lens:

$u$ ,  $v$  and  $f$  are related by the thin lens equation:

In microscopy, lenses are often used to demagnify (make smaller) the diameter of the beam. In this case it is more appropriate to draw the ray diagram as shown here.

The double condenser system or illumination system consists of two or more lenses and an aperture. It is used in both SEM and TEM. Its function is to control spot size and beam convergence.

Two or more lenses can act together (as shown here) and their ray diagrams can be constructed using the thin lens approximation for each of them.

The diagram opposite shows the ray diagram for the double condenser system. The black dots represent the focal point of each lens.

The condenser aperture controls the fraction of the beam which is allowed to hit the specimen. It therefore helps to control the intensity of illumination, and in the SEM, the depth of field. The objective lens forms an inverted initial image, which is subsequently magnified. In the back focal plane of the objective lens a

diffraction pattern is formed. The objective aperture can be inserted here. The effect of inserting the aperture is shown on the next page.

The depth of field,  $D_{ob}$  is the range of distance along the optical axis in which the specimen can move without the image appearing to lose sharpness. This obviously depends on the resolution of the microscope.

$$D_{ob} = \frac{d_{ob}}{\beta_{ob}}$$

The depth of focus,  $D_{im}$  is the extent of the region around the image plane in which the image will appear to be sharp. This depends on magnification,  $M_T$ .

$$D_{im} = \frac{d_{ob}}{\beta_{ob}} M_T^2$$

The use of two sets of deflection coils enable us to translate (scan) the beam across the specimen without apparently changing the angle of incidence or to tilt the beam without changing its position on the specimen.

An important microscope alignment involves the centering of the condenser aperture about the optical axis. If the aperture is off-centre the beam is displaced away from the axis as the condenser lens is focused.

Astigmatism in the condenser lenses distorts the beam to an elliptical shape either side of focus and prevents the beam being fully focused. It is corrected by applying two orthogonal correction fields in the  $x$  and  $y$  directions.

When we form images in TEM, we either form an image using the central spot, or we use some or all of the scattered electrons. The way we choose which electrons form the image is to insert an aperture into the back focal plane of the objective lens, thus blocking out most of the diffraction pattern except that which is visible through the aperture. We use the external drives to move the aperture so that either the direct electrons or some scattered electrons go through it. If the direct beam is selected we call the resultant image a bright-field image, and if we select scattered electrons of any form, we call it a dark-field image.

A Bright Field (BF) detector is placed in a conjugate plane to the back focal plane to intercept the direct beam while a concentric Annular Dark Field (ADF) detector intercepts the diffracted electrons. The signals from either detector are amplified and modulate the STEM CRT. The specimen (Au islands on a C film) gives complementary ADF and BF images as can be seen by clicking the button opposite.

The image of a hole in an amorphous carbon film illuminated with a parallel beam showing that with the

objective lens underfocused (0-2) a bright Fresnel fringe is visible inside the hole; with the objective lens overfocused (4-6) a dark fringe is visible inside the hole; at exact focus (3) there is no fringe; the appearance of the image varies as the x and y correction (-, OK or +) is altered.

Electromagnetic lenses cause image rotation and therefore in many microscopes the image will rotate as the magnification is changed.

As the crystalline specimen is tilted slightly, the fundamental spot pattern remains but Kikuchi lines move across the pattern.

The imaging and characterization of dislocations is commonly carried out by thin foil TEM using diffraction contrast imaging. However, the thin foil approach is limited by difficult sample preparation, thin foil artifacts, relatively small viewable areas, and constraints on carrying out in situ studies. Electron channeling imaging of electron channeling contrast imaging (ECCI) offers an alternative approach for imaging crystalline defects, including dislocations. Because ECCI is carried out with field emission gun scanning electron microscope (FEG-SEM) using bulk specimens, many of the limitations of TEM thin foil analysis are overcome (Crimp, 2006).

According to Schaublin's description, nanometric crystal defects play an important role as they influence, generally in a detrimental way, physical properties. For instance, radiation-induced damage in metals strongly degrades mechanical properties, rendering the material stronger but brittle (Schaublin, 2006).

### 3. SEM Basic

In a typical SEM electrons are thermionically emitted from a tungsten or lanthanum hexaboride ( $\text{LaB}_6$ ) cathode and are accelerated towards an anode. Alternatively electrons can be emitted via field emission. Tungsten has the highest melting point and lowest vapour pressure of metals and this is important for electron emission. The electron beam with the energy of 100 - 50000 eV is focused by one or two condenser lenses into a beam with a very fine focal spot sized 1 - 5 nm. The electron beam passes through scanning coils in the objective lens that deflect the beam in a raster fashion over a rectangular area of the sample surface. As the primary electrons strike the surface they are inelastically scattered by atoms in the sample. With the scattering the primary electron beam effectively spreads and fills a teardrop-shaped volume that extends less than 100 - 5000 nm into the surface. Interactions in this region lead to the subsequent emission of electrons which are then detected to produce an image. X-rays, which are also produced by the interaction of electrons with the sample, may also be detected in an SEM

equipped for energy dispersive X-ray spectroscopy or wavelength dispersive X-ray spectroscopy.

The most common imaging mode monitors low energy secondary electrons that is less than 50 eV. Due to the low energy, these electrons originate within several nm from the surface. The electrons are detected by a scintillator-photomultiplier device and the resulting signal is rendered into a two-dimensional intensity distribution that can be viewed and saved as a Digital image and treated by a computer. The brightness of the signal depends on the number of secondary electrons reaching the detector. If the beam enters the sample perpendicular to the surface, the activated region is uniform about the axis of the beam and a certain number of electrons escape from samples. As the angle of incidence increases, the escape distance of one side of the beam will decrease and more secondary electrons will be emitted. The steep surfaces and edges tend to be brighter than flat surfaces, which results in images with a well-defined, three-dimensional appearance.

For SEM technique, backscattered electrons can also be detected. With backscattered we can detect contrast between areas with different chemical compositions. There are fewer backscattered electrons emitted from a sample than secondary electrons. The number of backscattered electrons leaving the sample surface upward might be significantly lower than those that follow trajectories toward the sides.

The spatial resolution of the SEM depends on the size of the electron spot which in turn depends on the magnetic electron-optical system which produces the scanning beam. The resolution is also limited by the size of the interaction volume, or the extent of material which interacts with the electron beam. The spot size and the interaction volume are both very large compared to the distances between atoms, so the resolution of the SEM is not high enough to image down to the atomic scale, as is possible in TEM. SEM has compensating advantages, though, including the ability to image a comparatively large area of the specimen; the ability to image bulk materials and the variety of analytical modes available for measuring the composition and nature of the specimen. The Scanning Electron Microscope is revealing new levels of detail and complexity in the amazing world of micro-organisms and miniature structures.

For SEM, Conventional light microscopes use a series of glass lenses to bend light waves and create a magnified image. SEM creates the magnified images by using electrons instead of light waves, and it shows very detailed 3-dimensional images at much higher magnifications than is possible with a light microscope. The images created without light waves are rendered black and white. Samples have to be prepared

carefully to withstand the vacuum inside the microscope. Biological specimens are dried in a special manner that prevents them from shriveling. Because the SEM illuminates them with electrons, the samples also have to be made to conduct electricity. When start the measurement, the sample is placed inside the microscope's vacuum column through an air-tight door. After the air is pumped out of the column, an electron gun emits a beam of high energy electrons. This beam travels downward through a series of magnetic lenses designed to focus the electrons to a very fine spot. Near the bottom, a set of scanning coils moves the focused beam back and forth across the specimen, row by row. As the electron beam hits each spot on the sample, secondary electrons are knocked loose from its surface. A detector counts these electrons and sends the signals to an amplifier. The final image is built up from the number of electrons emitted from each spot on the sample. The resolution normally is 1 - 20 nm, and Resolutions of SEM can be less than 1 nm with a better instrument. It is easier to treat SEM images that to treat images of TEM. In our researches, we used SEM more than we used TEM in our researches.

#### 4. JEOL Transmission Electron Microscopes and JEOL Scanning Electron Microscopes

JEOL has produced TEMs since 1949, and currently markets state-of-the-art instruments in the 100 keV to 1 MeV ranges designed to support all TEM applications. Also, JEOL has played a leading role in

the development and evolution of scanning electron microscopy since the early 1960s. Over the past four decades, the SEM has become an indispensable tool in both advanced research and routine analysis for science and industry. JEOL has installed more than 8000 SEMs worldwide. The instrument we used in our experiments is the JEOL scanning electron microscope of Model JSM-6400V (Ma, et al, 2006).

Since 1949, the JEOL legacy has been one of outstanding innovation in developing instruments used to advance scientific research and technology. JEOL has more than 50 years of expertise in the fields of electron microscopy and mass spectrometry, and more than 20 years in e-beam lithography and defect analysis.

JEOL USA, Inc., a wholly-owned subsidiary of JEOL Ltd. Japan, was incorporated in the United States in 1962. The primary business of JEOL USA is sales of new instruments and peripherals and support of a vast installed base of instruments throughout the United States, Canada, Mexico, and South America (JEOL, 2006). The following gives JEOL TEM and SEM main products as the references for readers (Tables 1-7).

#### (1) Current JEOL TEM products

The Table 1, Table 2 and Table 3 are describing the JEOL TEM instruments currently available (Tables 1, 2, 3).

Table 1. 100 / 120 kV TEM

	Resolution	Accelerating Voltage	Magnification
JEM-1011	0.2 nm Lattice	40 to 100 kV	x50 to 1,000,000
JEM-1230	0.2 nm Lattice	40 to 120 kV	x50 to 600,000

Table 2. 200 kV TEM/FEG TEM

	Resolution	Accelerating Voltage	Magnification
JEM-2100F	0.14 nm Lattice	80 to 200 kV	x50 to 1,500,000
JEM-2100LaB <sub>6</sub>	0.14 nm Lattice	80 to 200 kV	x50 to 1,500,000
JEM-2200FS	Point-image 0.19 nm/0.23 nm/0.25 nm /0.28 nm (200 kV)	80 to 200 kV	x100 to 1,500,000
JEM-2500SE	STEM, 0.2 nm Lattice TEM, 0.14 nm Lattice	80 to 200 kV	x100 to 20,000,000

Table 3. IVEM 300 kV TEM/FEG TEM

	Resolution	Accelerating Voltage	Magnification
JEM-3100F	0.14 nm Lattice	100 to 300 kV	x60 to 1,500,000
JEM-3010	0.14 nm Lattice	100 to 300 kV	x50 to 1,500,000
JEM-3200FS	0.17 nm Lattice	100 to 300 kV	x50 to 1,500,000
JEM-3200FSC	0.204 nm Lattice	100 to 300 kV	x50 to 1,500,000

**(2) Current JEOL SEM products**

The Table 4, Table 5, Table 6 and Table 7 are describing the JEOL SEM instruments currently available (Tables 4, 5, 6, 7).

Table 4. Conventional Tungsten High Vacuum SEMs

	Resolution	Accelerating Voltage	Magnification	Stage
JSM-6390	3.0 nm	0.3 to 30 kV	x5 to 300,000	GS Type: X=20 mm, Y=10 mm LGS Type: X=80 mm, Y=40 mm
JSM-6490	3.0 nm	0.3 to 30 kV	x5 to 300,000	X=125 mm, Y=100 mm

Table 5. Conventional Tungsten Low Vacuum SEMs

	Resolution	Accelerating Voltage	Magnification	Stage
JSM-6390LV	HV 3.0 nm LV 4.0 nm	0.5 to 30 kV	x5 to 300,000	GS Type: X=20 mm, Y=10 mm LGS Type: X=80 mm, Y=40 mm
JSM-6490LV	HV 3.0 nm LV 4.0 nm	0.3 to 30 kV	x5 to 300,000	X=125 mm, Y=100 mm

Table 6. Conventional Thermal Field Emission SEMs

	Gun Type	Resolution	Accelerating Voltage	Magnification	Stage
JSM-7000F	in-lens thermal	1.2 nm (30 kV) 3.0 nm (1 kV) 3.0 nm (15 kV)	0.5 to 30 kV	x10 to 650,000	Type I: X=50 mm, Y=70 mm Type II: X=110 mm, Y=80 mm Type III: X=140 mm, Y=80 mm

Table 7. Semi-in-Lens Cold Cathode Field Emission SEMs

	Resolution	Accelerating Voltage	Magnification	Stage
JSM-6700F	1.0 nm 2.2 nm (1 kV)	0.5 to 30 kV	x25 to 650,000	Type I: X=70 mm, Y=50 mm Type II: X=110 mm, Y=80 mm Type III: X=140 mm, Y=80 mm
JSM-7401F	1.0 nm (15 kV) 1.5 nm (1 kV) 0.8 nm (30 kV STEM)	0.1 to 30 kV	x25 to 1,000,000	Type I: X=70 mm, Y=50 mm Type II: X=110 mm, Y=80 mm
JSM-7500F	1.0 nm (15 kV) 1.4 nm (1 kV) 0.6 nm (30 kV)	0.1 to 30 kV	x25 to 1,000,000	Type III: X=140 mm, Y=80 mm
JSM-7700F	0.6 nm (5 kV) 1.0 nm (1 kV) 1.0 nm (15 kV) 0.7 nm (1 kV)	0.1 to 30 kV	x25 to 2,000,000	X=2.5 mm, Y=25 mm

**5. TEM and SEM Research Examples**

As examples, the following is what we have done in our rabbit atherosclerosis and thrombosis studies that see can see the handles and result comparisons of light microscopy, TEM and SEM (Ma, 2006):

**(1) Light Microscopy**

Rabbit arterial tissue specimen were embedded in paraffin, cut and mounted on glass slides. The sections were then stained with hematoxylin and

eosin and Masson's trichrome stains. Gross examination showed that white thrombi with attached fibrin rich thrombi could be seen on the intimal surface of the aorta in more than half the triggered rabbits, and light microscopy showed that platelet rich thrombi were noted overlying sites of eroded plaque surfaces, and other areas appeared to have had plaque disruption the thrombus site. The light microscopy result give a clear overview for the sample and it is useful for the anatomic view

(Figure 1, Figure 2). White thrombi were noted to be firmly adherent to the arterial wall. These were cylindrical in shape and had rounded edges. This demonstrated areas of plaque disruption with super imposed platelet-rich thrombi. Also, commonly noted were areas of large lipid cores and thin caps. These lesions have great resemblance to the vulnerable human plaques. There was no visible difference in plaque morphology between the two atherosclerotic groups.

**(2) Electron Microscopy (TEM and SEM)**

The tissue samples were fixed overnight in 4% glutaraldehyde (Fisher Scientific, Pittsburgh, PA, USA) with 0.1 M phosphate buffer (pH 7.4). Rabbit arterial segments (5 mm long) were subjected to critical point drying in liquid CO<sub>2</sub>, mounted on stubs and gold-coated in a sputter coater. The intimal surface was examined using a JEOL scanning electron microscope (JEOL Ltd, Model JSM-6400V, Tokyo, Japan). Tissue sections were obtained and processed routinely for ultrastructural examination. Thin sections were stained with uranyl acetate and lead citrate and then examined with a transmission electron microscope (BEI preamplifier, Au Evirotech Company, Germany). SEM showed that fissures of various lengths could be seen at the site where thrombus was present (Figure 3) and. TEM showed that white thrombi were composed of a dense platelet rich matrix (Figure 4).

**A. Scanning Electron Microscopy:** After triggering, the intimal surface of rabbit aorta and ilio-femoral arteries in atherosclerotic group had focal clusters of red blood cells and adherent platelets (Figure 3). The plaques had an irregular surface and ulceration with blood cells and fibrin.

**B. Transmission Electron Microscopy:** When compared with control rabbit, atherosclerotic rabbit arterial wall had increased elastin, degenerated organelles, lipid droplets, and bundles of microfibrils. The cytoskeletal and sub-cellular appearance of smooth muscle cells were altered with the atherosclerotic diet. The lipid distribution was mainly in the extracellular spaces with cholesterol crystal formation (Figure 4).



Figure 1. Gross examination: White thrombi with attached fibrin rich thrombi can be seen on the intimal surface of the aorta in more than half the triggered rabbits.

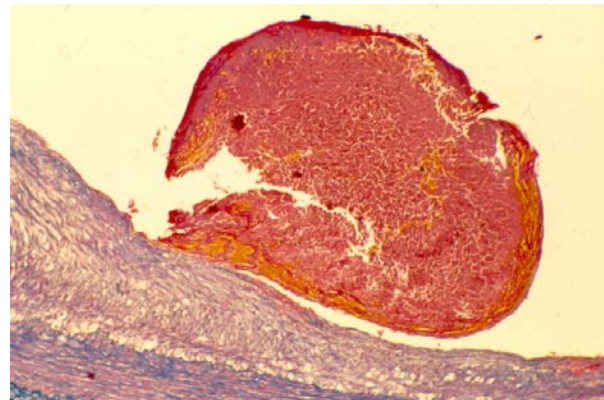


Figure 2. Light microscopy: Platelet rich thrombi were noted overlying sites of eroded plaque surfaces. Other areas appeared to have had plaque disruption the thrombus site.

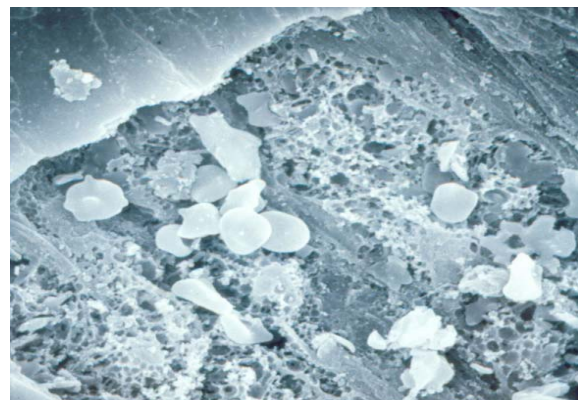


Figure 3. Scanning electron microscopy: Fissures of various lengths could be seen at the site where thrombus was present.



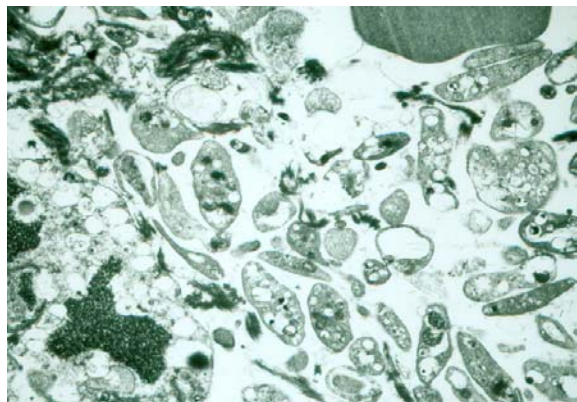


Figure 4. Transmission electron microscopy: White thrombi were composed of a dense platelet rich matrix.

## 6. Applications

Because electron microscopes use a beam of highly energetic electrons to examine objects on a very fine scale. The examination can provide the unique information. That includes, topography – the surface features of an object of the looks. Its texture, direct relation between these features and materials properties; morphology – the shape and size of the particles making up the object that related between these structures and material properties which character specially in the biological fields; composition the elements and compounds that the object is composed of and the relative amounts of them and to determine relationship between composition and materials properties; finally crystallographic information – the atoms arrangement of the object.

Along with SEM, TEM has been widely applied in life science studies. We have successfully used TEM and SEM in the atherosclerosis, thrombosis and platelet function studies (Prieto, et al, 2002; Abela, et al, 2003; Ma, et al, 2006)

The basic procedures for TEM and SEM are well established, for biological and medical science that involves with sample collection, fixation and dehydration, embedding, ultrathin sectioning, staining of ultra thin section, magnification and resolution calibration while observation and recording the image, and last analysis the graphs. For SEM, beside preparation of particulate specimens which including freeze-fraction for biological sample, mounting and coating samples are commonly used.

Recently, Yucel et al used analyzed rats via TEM. Corneal autofluorescence measurements were also performed in all experimental groups. Their results showed: Electron microscopic evaluation revealed that aminoguanidine treatment in diabetic rats prevented the formation of intracellular spaces between neighbouring cells in the superficial corneal epithelium.

Hyperglycemia-induced degeneration of intracellular organelles and formation of cytoplasmic vacuoles in the corneal stroma was also prevented with the treatment of AG. Corneal autofluorescence detected in the diabetic group (5.98 +/- 2.17 Fi/mg protein) was found to be significantly greater than the control (3.92 +/- 0.56 Fi/mg protein) and the AG-treated diabetic group (4.18 +/- 0.59 Fi/mg protein) ( $p < 0.05$ ). Interpretation: The presented data provide evidence that AG is preventive against corneal alterations in experimental diabetes (Yucel, 2006).

With TEM technique, Prieto et al found that thrombostatin and aspirin treated rabbit atherosclerotic arteries had less platelet adhesion on the arterial surface when compared to balloon injured controls (Prieto et al, 2002).

In Koufakis et al experiments, conjunctival tissue specimens from seven normal subjects and eight patients with SS were obtained by bulbar conjunctival biopsy and examined by transmission electron microscopy. Their results demonstrated: The average number of microvilli per 8.3 microm epithelial length was significantly lower in the SS group than that in the control. The microvillus height and height-width ratio in the conjunctival epithelium in the SS group were significantly lower than those in normal individuals. They concluded that ultrastructural morphology of the apical conjunctival epithelium is altered in patients with SS and the findings suggest that an intact OSG may play a key role in the maintenance of a healthy ocular surface, possibly by preventing abrasive influences on the apical epithelial cells (Koufakis et al, 2006).

Energy filtering TEM (EFTEM) with modern spectrometers and software offers new possibilities for element analysis and image generation in plant cells. In the present review, applications of EFTEM in plant physiology, such as identification of light elements and ion transport, analyses of natural cell incrustations, determination of element exchange between fungi and rootlets during mycorrhiza development, heavy metal storage and detoxification, and employment in plant physiological experiments are summarized. In addition, it is demonstrated that EFTEM can be successfully used in more practical approaches, for example, in phytoremediation, food and wood industry, and agriculture (Lutz-Meindl, 2006).

### Correspondence to:

Hongbao Ma  
Michigan State University  
East Lansing, MI 48824, USA  
Telephone: 517-303-3990  
Email: [hongbao@msu.edu](mailto:hongbao@msu.edu)

Received: June 10, 2006.

## References

1. Abela GS, Huang R, Ma H, Prieto AR, Lei M, Schmaier AH, Schwartz KA, Davis JM. Laser-light scattering, a new method for continuous monitoring of platelet activation in circulating fluid. *Journal of Laboratory and Clinical Medicine* 2003;141(1):50-7.
2. Crimp MA. Scanning electron microscopy imaging of dislocations in bulk materials, using electron channeling contrast. *Microsc Res Tech* 2006;69(5):374-81.
3. Koufakis DI, Karabatsas CH, Sakkas LI, Alvanou A, Manthos AK, Chatzoulis DZ. Conjunctival surface changes in patients with Sjogren's syndrome: a transmission electron microscopy study. *Invest Ophthalmol Vis Sci* 2006;47(2):541-4.
4. Lutz-Meindl U. Use of energy filtering transmission electron microscopy for image generation and element analysis in plant organisms. *Micron*. 2006.
5. Ma H, Aziz KS, Huang R, Abela GS. Arterial wall cholesterol content is directly related to serum cholesterol and is a predictor of the development and severity of arterial thrombosis in atherosclerotic arteries. *Journal of Thrombosis and Thrombolysis* 2006;22(1):5-11.
6. Prieto AR, Ma H, Huang R, Khan G, Schwartz KA, Hage-Korban EE, Schmaier AH, Davis JM, Hasan AA, Abela GS. Thrombostatin, a bradykinin metabolite, reduces platelet activation in a model of arterial wall injury. *Cardiovasc Res* 2002;53(4):984-92.
7. Schaublin R. Nanometric crystal defects in transmission electron microscopy. *Microsc Res Tech* 2006;69(5):305-16.
8. Wikipedia, the free encyclopedia. Transmission electron microscopy. 2006  
[http://en.wikipedia.org/wiki/Transmission\\_electron\\_microscope](http://en.wikipedia.org/wiki/Transmission_electron_microscope).
9. Williams DB, Carter CB. Transmission Electron Microscopy (TEM). Humphreys and Beanland, 3rd Edition. The University of Liverpool Liverpool, L69 3GH, U.K. 2000.
10. Yucel I, Yucel G, Akar Y, Demir N, Gurbuz N, Aslan M. Transmission electron microscopy and autofluorescence findings in the cornea of diabetic rats treated with aminoguanidine. *Can J Ophthalmol* 2006;41(1):60-6.
11. JEOL. TEM and SEM. <http://www.jeolusa.com>. 2006.

# An Improved Neural Networks Prediction Model and Its Application in Supply Chain

Xiaoni Dong<sup>1</sup>, Guangrui Wen<sup>2</sup>

<sup>1</sup>Department of Industrial Engineering, Xi'an Siyuan University,  
Xi'an Shaanxi 710038, China, [birdy\\_dong@163.com](mailto:birdy_dong@163.com)

<sup>2</sup>College of Mechanical Engineering, Xi'an Jiaotong University,  
Xi'an Shaanxi 710049, China, [grwen@mail.xjtu.edu.cn](mailto:grwen@mail.xjtu.edu.cn)

**Abstract:** Accurate prediction of demand is the key to reduce the cost of inventory for an enterprise in Supply Chain. Based on recurrent neural networks, a new prediction model of demand in supply chain is proposed. The learning algorithm of the prediction is also imposed to obtain better prediction of time series in future. In order to validate the prediction performance of recurrent neural networks, a simulated time series data and a practical sales data have been used. By comparing the prediction result of Multi-Layer feedback neural networks and recurrent neural networks, it can be shown that the recurrent neural networks prediction model can help in improving the prediction accuracy. [Nature and Science. 2006;4(3):23-27].

**Keywords:** supply chain; inventory management; recurrent neural networks; multi-step prediction

## 1. Introduction

A company may hold inventories of raw materials, parts, work in process, or finished products for a variety of reasons, such as the following [1]: To create buffers against the uncertainties of supply and demand; To take advantage of lower purchasing and transportation costs associated with high volumes; To take advantage of economics of scale associated with manufacturing products in batches; To build up reserves for seasonal demands or promotional sales; To accommodate product flowing from one location to another (work in process or in transit); To exploit speculative opportunities for buying and selling commodities and other products.

Recently, attention has focused on developing better forecasting models that reduce or eliminate inventories, which reflects the cost of inventory management in supply chain. ANN, as a new tool, has already been used in forecasting field due to their ability to learn complicated functions.

In 1995, Chao-Chee Ku [2] proposed dynamical recurrent neural networks (DRNN) that overcome the static modeling problem of multi-layers feed-forward neural networks in modeling. Y. X. He [3] combined data mining & knowledge discovery and neural networks technology to solve inventory problem. C. T. Xuan [4] summarized applications of neural networks in supply chain management (SCM) including optimization, prediction, decision-making support, modeling & simulation and management. This paper is a first attempt to use recurrent neural networks as forecasting technology to reduce the uncertainty of inventory management.

## 2. Prediction Model Based on Feed-forward Neural Networks

The neural networks models most widely used in time series applications are based in feed-forward neural networks with backpropagation learning algorithm [5]. This model usually constructs multi-layer feed-forward neural network, and then evaluate function  $F$  by time series. These models consist of a common nonlinear auto-regressing model appearing in Equation (1), which is also called NAR Model. In this case, the value at  $k+1$  of this time series is often represented by  $d+1$  entries time series values, thus:

$$x(k+1) = F(x(k), \dots, x(k-d)) \quad (1)$$

Where  $k$  represents the time variable,  $F$  is a nonlinear function that defines this time series.

The common prediction method based on neural network, namely the single-step neural network prediction method, set up non-linear prediction model of the neural network. The following predicting equation represents the prediction model:

$$x(k+1) = \sum_i^d f_i(x)x(k-i) + \varepsilon \quad i = 0, \dots, d \quad (2)$$

in which  $f_i(x)$  is the non-linear function of input variable,  $d+1$  is the number of input nodes in predicting network.

During the Neural network predicting, the following equation can be got from the predicting model:

$$\tilde{x}(k+1) = \sum_i^d f_i(x)x(k-i) \quad (3)$$

According to the predicting model, figure 1 shows the structure of the Multi-step predicting. Use the predicting value into the predicting model; the multi-step value of the future can be got step by step. In this kind of multi-

step predicting process, when the single-step predicting result is got, there has being a predicting error which can be expressed as:

$$\varepsilon_{k+1} = \frac{1}{2} [x(k+1) - \tilde{x}(k+1)]^2 \quad (4)$$

During the course of inference, using  $\tilde{x}(k+1)$  and the following predicting value as the input of the network leads to the input error. And as the increasing of the predicting value, the accumulating error increases rapidly, which cannot ensure the accuracy of multi-step predicting. Figure 1 shows the traditional neural networks recursion multi-step prediction model.

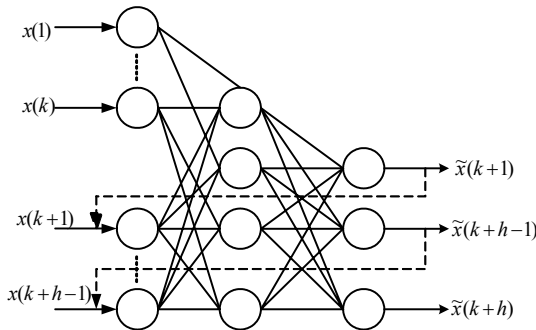


Figure 1. Traditional Neural Networks Prediction Model

### 3. Prediction Model Based on Recurrent Neural Networks and Its Learning Algorithm

In this section, a prediction method based on recurrent neural networks is introduced. The recurrent neural networks used to build up the prediction model consist of adding feedback connections from the output neuron to the input layer, which memorize previous prediction values<sup>[6]</sup>. In this case, parameters of the multi-step prediction model are determined to minimize the error along interval  $[k+1, k+h+1]$ , where  $h$  is the length of multi-step prediction. Thus, the model is trained for long-term prediction.

#### 3.1 Description of Recurrent Prediction Model

In order to overcome limitation of traditional feed-forward prediction model and make full use of the input vectors to the model, a new prediction model based on recurrent networks is built up<sup>[7-8]</sup>. The recurrent network is constructed by starting from a multilayer feed-forward neural network and by adding feedback connections from the output neuron to the input layer as shown in Figure 2.

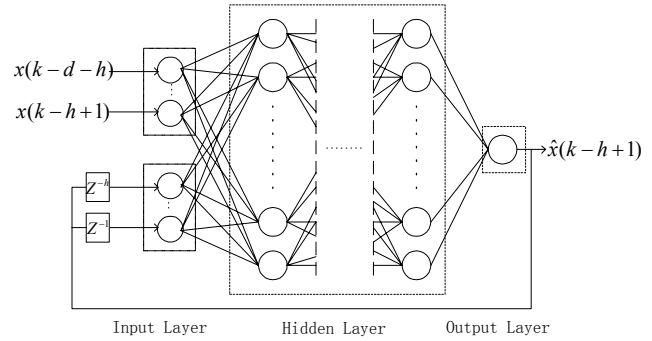


Figure 2. Recurrent network architecture

Neural network is divided into three parts: input layer, hidden layer and output layer. Where  $\hat{x}$  represents the network output, and  $Z^{-i}$  is an operator that delays by  $i$  terms the network output sequence. The input layer is composed of two groups of neurons. The first group acts as the external inputs to the network gathering the original or measured time series data. The second group is formed by the context neurons, which memorize previous output of the network. Introducing the vector  $C(k)$  ( $C(k) = (C_1(k), \dots, C_h(k))$ ) to indicate the activation of context neurons, each component is calculated as:

$$C_i(k) = Z^{-i}(\hat{x}(k+h+1)) = \hat{x}(k+h+1-i) \quad i = 1, \dots, h \quad (5)$$

#### 3.2 Learning Algorithm[9]

Assuming that the prediction length is fixed to  $h$ , and that at instant  $k$  the goal is to predict the time series values at instants  $k+1, k+2, \dots, k+h+1$ , the number of input units decreases from  $d+1$  to  $d+1-h$ , and the number of context neurons increases from 0 to  $h$ , respectively. Thus, the sequences received by the external inputs and the context neurons, at every instant  $k$ , are given by the following sequence:

1. The number of context neurons is initialized from zero, which will be included in the external inputs accordingly.
2. The future instants  $k+i$  for  $i = 2, \dots, h+1$  are not real, but simulated. Now the input units receive the vector  $x(k+i), \dots, x(k-d-i)$ , and the  $(i-1)^{th}$  context neurons memorize the previous  $i-1$  outputs of the network, i.e.:

$$C_1(k) = \hat{x}(k+i-1) \dots C_{i-1}(k) = \hat{x}(k+1) \quad (6)$$

3. The external inputs and the context neurons are resettled.

Below are the complete training procedures of a multi-step recurrent prediction model. At each instant  $k$ , starting with  $k = d$  :

**Step1.** The number of context neurons is initialized to zero.  $d+1$  external input neurons are one set receiving the measured values of the time series,  $x(k), \dots, x(k-d)$ . The output of network is given by following equation:

$$\hat{x}(k+1) = \hat{F}(x(k), \dots, x(k-d), W_2) \quad (7)$$

**Step 2.** The number of context neurons is increased in one unit and the number of external units is decreased also in one unit. The context neuron memorizes the output of the network previously calculated,  $\hat{x}(k+1)$ . Thus the prediction at the simulated instant  $k+2$  is given by:

$$\hat{x}(k+2) = \hat{F}(\hat{x}(k+1), x(k), \dots, x(k-d+1), W_2) \quad (8)$$

**Step 3.** Step 2 is repeated until  $h$  context neurons will be achieved. The output of the recurrent model at simulated instants  $k+3, \dots, k+h+1$  are given by the following equations, respectively:

$$\hat{x}(k+3) = \hat{F}(\hat{x}(k+2), \hat{x}(k+1), x(k), \dots, x(k-d+2), W_2) \quad (9)$$

$$\hat{x}(k+h+1) = \hat{F}(\hat{x}(k+h), \dots, \hat{x}(k+1), x(k), \dots, x(k-d+h), W_2) \quad (10)$$

**Step 4.** The parameter set of the model,  $W_2$ , is updated by following the negative gradient direction of the error function given by:

$$e(k+1) = \frac{1}{2} \sum_{i=1}^h (x(k+i+1) - \hat{x}(k+i+1))^2 \quad (11)$$

In order to avoid the long computational effort required by dynamic back-propagation rules when the prediction length is high, the updates of the parameters are realized using traditional backpropagation learning rule.

**Step 5.** At this moment the time variable  $k$  is increased in one unit and the procedure is returned to Step 1.

The procedure is repeated for the complete training set until it reaches the convergence.

#### 4. Simulation Experiment

The simulated time series is given by following equation:

$$x(k+1) = \lambda x(k)(1-x(k)) \quad (12)$$

Where  $\lambda = 3.97$  and  $x(0) = 0.5$ .

The equation describes a strong chaotic time series. As to enterprise, customer's demand is of uncertainty due to the influence in such measures as the rival, the change of customer's favor, production cycle and the price reducing, etc., the supply chain system is a complicated non-linear system. So, such unordered time array can well use simulate such a system, at the same time, can test the performance of the prediction model.

We initialize parameter  $k$  from  $k=0$  to  $k=100$ . Table 1 and 2 show the prediction errors of two models over the training data and predicting data respectively. Figure 3 and Figure 4 display the single step prediction curves of two models respectively and Fig.5 and Fig.6 display the multi-step prediction curves of two models respectively. It is evident that multi-step recurrent prediction model's prediction accuracy is much higher than that of traditional model.

**Table 1.** Logistic time series: prediction errors over the training data

length h	Traditional model (3-10-1)	Recurrent model (7-15-1)
0	0.0015	0.0015
7	0.0850	0.0135

**Table 2.** Logistic time series: prediction errors over the predicting data

length h	Traditional model (3-10-1)	Recurrent model (7-15-1)
0	0.002	0.002
7	0.105	0.026

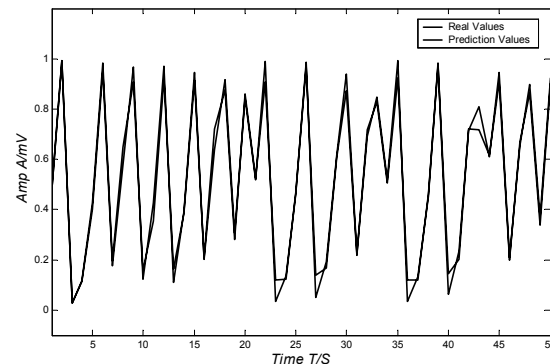


Figure 3. Traditional MFNN prediction at  $h=0$

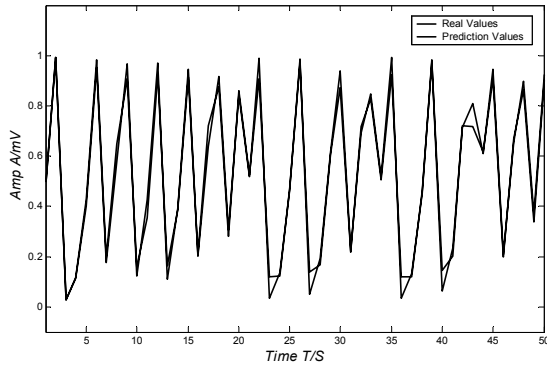


Figure 4. MSRN prediction at h=0

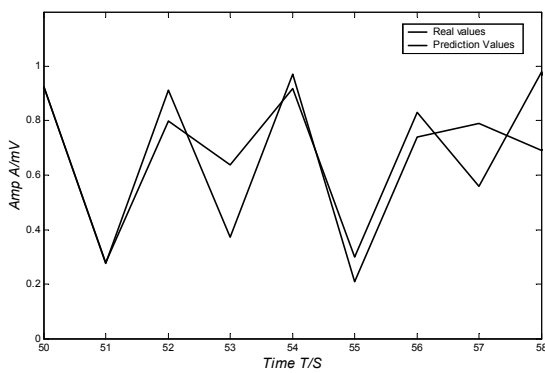


Figure 5. Traditional M-FNN model prediction at h=7

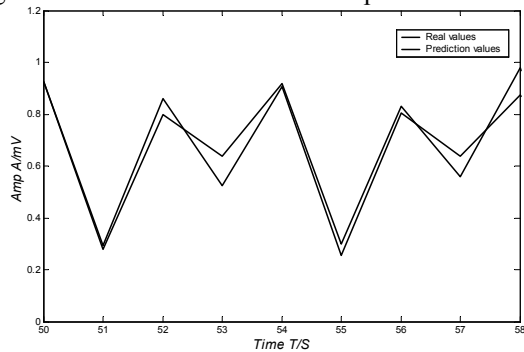


Figure 6. MSRN prediction at h=7

### 5. Application

This paper regards selling data of paper for one week of one papermaking enterprise as the target that is studied by the neural network<sup>[10]</sup>. According to the experience and investigation from its marketing department, the factors affecting sales of paper include season, paper category, unit price, middleman in various regions, growth rate of macroeconomy in that year, etc..

We just consider two major influence factors, season and paper category, for building the forecasting model. Firstly, 52 data of week sales volume for No.1

warehouse in 2002 can be obtained by statistics method. Secondly, three layers recurrent neural networks model is adopted. The input layer includes four nodes, for considering the influence of different seasons. The output layer includes one node, and the hidden layer has ten nodes. First 46 data as training samples and last 6 data as testing samples are used to construct forecasting model of sales. Thirdly, in order to improve the rate of networks convergence in training processes, normalization technique is applied to 46 training data, and the batch training method (BTM) is adopted.

Table 3 lists the forecasting errors. Most errors are controlled below 0.1, and the trend of sales accords with actual situation. The results of training and forecasting are shown in Figure 7.

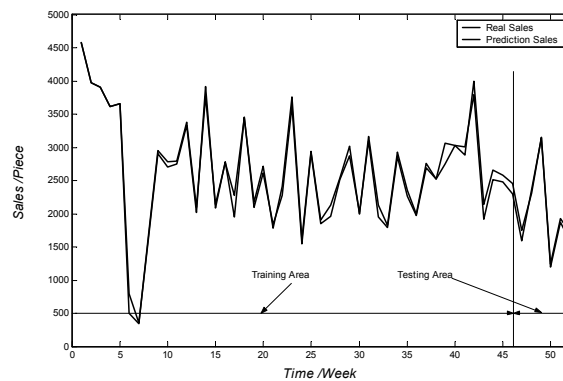


Figure 7. Training and forecasting of paper sales

In Figure 7, the data from 47<sup>th</sup> to 52<sup>th</sup> points in dash line denote the results of forecasting, and the solid line presents the real sales volume.

Table 3. Errors between Prediction Sales and Real Sales

Week	Forecasting data	Real data	error
47	1593	1743	0.0858
48	2361	2310	0.0220
49	3137	3151	0.0044
50	1201	1243	0.0337
51	1873	1924	0.0267
52	1581	1710	0.0757

### 6. Conclusions

This paper presents a new forecasting model for inventory management, which is based on multi-step recurrent neural networks. The recurrent neural networks have advantages of higher precision and robustness over the traditional feed-forward neural networks in multi-step prediction. The forecasting results in some paper mill certified the new method. The model will be favor of the inventory decision-making for decreasing the inventory to minimum.

**Correspondence to:**

Xiaoni Dong  
Department of Industrial Engineering  
Xi'an Siyuan University  
Xian, Shaanxi 710038, China  
E-mail: [birdy\\_dong@163.com](mailto:birdy_dong@163.com)

**References**

1. Jeremy F. Shapiro, *Modeling the Supply Chain*, Wadsworth Group, a division of Thomson Learning, America, 2001.
2. Ku C.C., Lee K.Y., "Diagonal recurrent neural networks for dynamic Systems control", *IEEE Trans.Neuralnetworks*, Vol 6, No. 1, pp. 144-155, 1995.
3. Yanxiang He, Feng Li, Zhikai Song and Ge Zhang, "Neural Networks Technology for Inventory Management", *Computer Engineering and Application*, No.15, pp. 182-184, 2002.
4. Chaoting Xuan, Peiqing Huang and Dong Lu, Applications of Neural Network Technology in Supply Chain Management, *Industrial Engineering and Management*, No.3, pp. 41-44, 2000.
5. Svozil, Daniel, etc., Introduction to multi-layer feed-forward neural networks, *Chemometrics and Intelligent Laboratory Systems*, Vol 39, pp . 43-62, 1997.
6. M.G. Ines and I. Pedro, Multi-step learning rule for recurrent neural models: an application to time series forecasting, *Neural Processing Letters*, pp. 115-133, 2001.
7. I. Galvan and J. Zaldivar, Application of recurrent neural networks in batch reactors. Part I: NARMA modeling of the dynamic behavior of the heat transfer fluid temperature, *Chemical Engineering and Processing*, pp .505-518, 1997.
8. G.R. Wen and L.S. Qu, "Equipment Behavior Predictability Evaluation Based on Redundancy". *Journal of Xi'an Jiaotong University*, Vol 37, No.7, pp. 699-703, Jul. 2003.
9. G.R. Wen and L.S Qu, Multi-step forecasting method based on recurrent neural networks, *Journal of Xi'an Jiaotong University*, Vol 36, No.7, pp. 722-726, Jul. 2002.
10. Shengshu Jiang , Chunjie Yang and Ping Li, Research on application of BP-ANN forecast in process supply chain, *Opreations Research and Management Science*, Vol 12, No.5, pp. 57-61, Oct. 2003.

# Research of Novel Three-phase Inverter and its Modulation Technique

Wang Shuwen<sup>1, 2</sup>, Ji Yanchao<sup>1</sup>, Fang Junlong<sup>1</sup>

1. Harbin Institute of Technology, Harbin, Heilongjiang 150001, China. Email: [wswtr@163.com](mailto:wswtr@163.com)

2. Northeast agricultural University, Harbin, Heilongjiang 150001, China

**Abstract:** This paper proposes a novel three-phase uncontrollable rectifier inverter without or with a quite small dc-link capacitor. Because a modulation wave reconstruction-SPWM (MWR-SPWM) technique is adopted which can greatly eliminate the harmonics of output voltage, the DC filter capacitor is greatly decreased or even removed. In addition, the size of the input ac filter and the output ac filter is reduced. The principle of operation and harmonics elimination of the novel inverter topology are elaborated. A through analysis on its performance is presented. This inverter has many advantages such as simpler structure, higher reliability, more effective harmonics elimination. The performance of this inverter using MWR-SPWM technique is compared with traditional inverter by simulation and experiment, and the results show that the theoretical analysis is correct. [Nature and Science. 2006;4(3):28-36].

**Keywords:** inverter; MWR-SPWM; harmonics elimination

## I. INTRODUCTION

Inverter are widely used in many industrial applications such as variable-frequency velocity modulation<sup>[1][2][3]</sup>, UPS, VAR compensator etc. In order to supply high quality power for loads, it is significant for this inverter to eliminate harmonics in output voltage effectively. Pulse width modulation (PWM) technique that has satisfied performance in harmonics elimination, voltage regulation, responding speed is widely used in all kinds of inverters.<sup>[4][5]</sup>

Conventionally, all PWM-controlled inverters are based on ideal dc voltage, in practice a bulky dc filter capacitor is installed after the three-phase uncontrollable rectifier to obtain low-ripple dc voltage, as shown in Figure 1. However, the dc filter capacitor has several disadvantages from the viewpoints of size, weight, cost, and reliability<sup>[6]</sup>. Moreover, the properties of the dc filter capacitor deteriorate gradually due to continuous

out-gassing. Hence, dc filter capacitor is the major factor limiting the lifetime of inverter systems<sup>[7]</sup>.

In order to solve the above-mentioned problems, we propose a novel three-phase inverter based on modulation wave reconstruction - SPWM (MWR-SPWM) technique, as shown in Figure 2. Due to MWR-SPWM technique is adopted, the dc filter capacitor is decreased largely or even removed and the harmonics in output voltage is eliminated effectively. The main use of capacitor isn't filtering harmonics but buffering energy. When the power factor of load is high enough, the capacitor can be omitted. Meanwhile the size of input ac filter and the output ac filter are proportionately reduced.

## II. PRINCIPLE OF OPERATION

The novel inverter topology mainly consists of a three-phase diode bridge and an inverter. The output of



the three-phase diode bridge rectifier  $V_{dc}$  is a type of six-pulse dc voltage as shown in Figure 3, which contains inherent harmonics of the  $6n f_0$  ( $f_0$  is the system frequency) besides dc component. Using conventional SPWM technique the output voltage of inverter  $V_{out}$  contains harmonics of  $f_{6k} \pm f_{sin}$  ( $f_{6k} = 6kf_0$ ,  $f_{sin}$  is the modulation wave frequency) besides fundamental component in low frequency band. How can we obtain the desired fundamental component and eliminate the unwanted low-order harmonics in  $V_{out}$  by a simple approach?

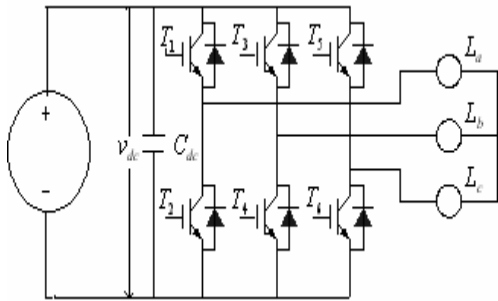


Figure 1. A conventional inverter

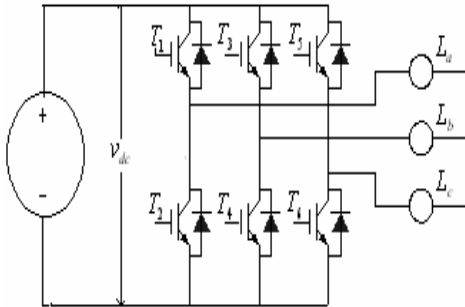


Figure 2. The proposed inverter

We can achieve this purpose by using modulation wave reconstruction-SPWM technique. Meanwhile the value and frequency regulation of the output voltage can be conventionally achieved by regulating modulation wave. In the next section, the detailed analysis is given.

### III. MODULATION WAVE RECONSTRUCTION - SPWM TECHNIQUE

#### 1. Analysis of Output Voltage Using Conventional SPWM Technique

In this section, the proposed inverter is analyzed under steady-state condition.

In Figure 2,  $v_{dc}$  is the output dc voltage of the three-phase diode bridge rectifier, we choose its midpoint as zero potential reference. In order to make the analysis comprehensive, the expression of  $v_{dc}$  can be represented by the following Fourier series in (1).

$$v_{dc} = V_D + \sum_{i=1}^{\infty} U_i \cos \phi_i \cos w_i t + \sum_{i=1}^{\infty} U_i \sin \phi_i \sin w_i t \quad (1)$$

Firstly, we chose standard three-phase sinusoidal wave as modulation wave, take phase a for example, it's expressed as follows.

$$u_{s1} = U_B \sin(\omega t + \theta) \quad (2)$$

Figure 3 shows the relationship among triangular-wave voltage  $u_{tr}$ , modulation wave voltage  $u_{s1}$  and voltage of a phase  $u_a$ . Switching status is determined by the compared result between  $u_{s1}$  and  $u_{tr}$  as follows: the switch turns on when  $u_{s1} > u_{tr}$ , but turns off when  $u_{s1} < u_{tr}$ . The frequency of triangular-wave  $f_{tr}$  is M times to the frequency of sinusoidal modulation wave  $f_{sin}$ . The sinusoidal wave is "chopped" 2 M times in per sinusoidal cycle. We get 2 M angles, define them as  $\alpha_i$  ( $i = 1, 2, \dots, 2 M$ ).

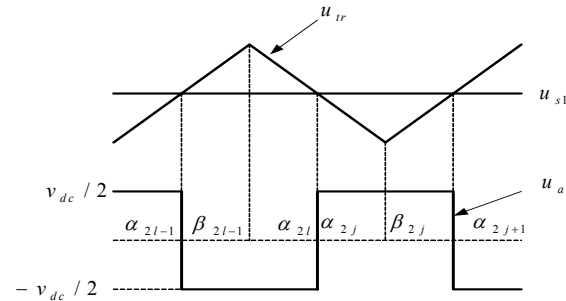


Figure 3. The relationship of  $u_{tr}$ ,  $u_{s1}$ ,  $u_a$ ,

When (1) is modulated under (2), the Fourier series coefficients of output voltage  $u_a$  are respectively expressed as  $a_n^{(1,1)}$ ,  $b_n^{(1,1)}$ ,  $a_n^{(2,1)}$ ,  $b_n^{(2,1)}$ ,  $a_n^{(3,1)}$ ,  $b_n^{(3,1)}$ . The output voltage  $u_a$  fluctuates between  $v_{dc}/2$  and  $-v_{dc}/2$ , and its Fourier series can be expressed as (3), given at the bottom of this page.

Since the frequency of the triangular wave is sufficiently high, we can believe that  $u_{s1}$  and  $v_{dc}$  is constant during one triangular-wave cycle.

Therefore

$$\frac{\alpha_{2j+1} + \alpha_{2j}}{2} \approx \beta_{2j} \quad (4)$$

$$\frac{\alpha_{2l} + \alpha_{2l-1}}{2} \approx \beta_{2l-1} \quad (5)$$

$$\frac{\alpha_{2j+1} - \alpha_{2j}}{2} \approx \frac{U_B \sin(\beta_{2j} + \theta) - V_{trl}}{V_{trm} - V_{trl}} \cdot \frac{\omega T_{tr}}{2} \quad (6)$$

$$\frac{\alpha_{2l} - \alpha_{2l-1}}{2} \approx \frac{V_{trm} - U_B \sin(\beta_{2l-1} + \theta)}{V_{trm} - V_{trl}} \cdot \frac{\omega T_{tr}}{2} \quad (7)$$

$$\sin\left(n \frac{\alpha_{2j+1} - \alpha_{2j}}{2}\right) \approx n \frac{\alpha_{2j+1} - \alpha_{2j}}{2} \quad (8)$$

$$\sin\left(n \frac{\alpha_{2l} - \alpha_{2l-1}}{2}\right) \approx n \frac{\alpha_{2l} - \alpha_{2l-1}}{2} \quad (9)$$

$a_n^{(1,1)}$  is expressed as (10), given at the bottom of this page. Substituting (4)--(9) into (10), we can obtain (11).

Because  $\omega T_{tr}$  is so small, we can convert the form of the first step in (11) into an integral one, which simplifies the result.  $b_n^{(1,1)}$  can be derived by using the same method.

$$u_a = \frac{1}{2} \left( a_0^{(1,1)} + a_0^{(2,1)} + a_0^{(3,1)} \right) + \sum_{n=1}^{\infty} \left[ \left( a_n^{(1,1)} + a_n^{(2,1)} + a_n^{(3,1)} \right) \cos n\omega t + \left( b_n^{(1,1)} + b_n^{(2,1)} + b_n^{(3,1)} \right) \sin n\omega t \right] \quad (3)$$

$$a_n^{(1,1)} = \frac{1}{2} \left[ \sum_{j=1}^M \frac{1}{\pi} \int_{\alpha_{2j}}^{\alpha_{2j+1}} U_D \cos n\alpha d\alpha + \sum_{l=1}^M \frac{1}{\pi} \int_{\alpha_{2l-1}}^{\alpha_{2l}} (-U_D) \cos n\alpha d\alpha \right] \quad (n=0, 1, 2, \dots) \quad (10)$$

$$= \frac{1}{2} \left[ \sum_{j=1}^M \frac{2U_D}{n\pi} \cos\left(n \frac{\alpha_{2j+1} + \alpha_{2j}}{2}\right) \sin\left(n \frac{\alpha_{2j+1} - \alpha_{2j}}{2}\right) + \sum_{l=1}^M \frac{-2U_D}{n\pi} \cos\left(n \frac{\alpha_{2l} + \alpha_{2l-1}}{2}\right) \sin\left(n \frac{\alpha_{2l} - \alpha_{2l-1}}{2}\right) \right]$$

$$\begin{aligned}
 a_n^{(1,1)} &\approx \frac{1}{2} \left[ \sum_{j=1}^M \frac{2U_D}{\pi} \cos n\beta_{2j} \frac{U_B \sin(\beta_{2j} + \theta) - V_{trl}}{V_{trm} - V_{trl}} \cdot \frac{\omega T_{tr}}{2} \right. \\
 &\quad \left. + \sum_{l=1}^M -\frac{2U_D}{\pi} \cos n\beta_{2l-1} \frac{V_{trm} - U_B \sin(\beta_{2l-1} + \theta)}{V_{trm} - V_{trl}} \cdot \frac{\omega T_{tr}}{2} \right] \\
 &= \frac{U_D}{2\pi(V_{trm} - V_{trl})} \int_{-\pi}^{\pi} -U_B \sin((n-1)\beta - \theta) d\beta \quad (n = 0, 1, 2, \dots) \quad (11)
 \end{aligned}$$

$$\begin{aligned}
 b_n^{(1,1)} &= \frac{1}{2} \left[ \sum_{j=1}^M \frac{1}{\pi} \int_{\alpha_{2j}}^{\alpha_{2j+1}} U_D \sin n\alpha d\alpha \right. \\
 &\quad \left. + \sum_{l=1}^M \frac{1}{\pi} \int_{\alpha_{2l-1}}^{\alpha_{2l}} (-U_D) \sin n\alpha d\alpha \right] = \frac{U_D}{2\pi(V_{trm} - V_{trl})} \int_{-\pi}^{\pi} U_B \cos((n-1)\beta - \theta) d\beta \quad (12)
 \end{aligned}$$

$a_n^{(2,1)}$  can be expressed as (13). Substituting (4)—(9) into (13), we can obtain (14).

$$\begin{aligned}
 a_n^{(2,1)} &= \frac{1}{2} \left[ \sum_{j=1}^M \frac{1}{\pi} \int_{\alpha_{2j}}^{\alpha_{2j+1}} \sum_{k=1}^{\infty} U_k \cos \phi_k \cos(\omega_k \pm n) \frac{\alpha_{2j+1} + \alpha_{2j}}{2} \cos n\alpha d\alpha \right. \\
 &\quad \left. + \sum_{l=1}^M \frac{1}{\pi} \int_{\alpha_{2l-1}}^{\alpha_{2l}} \sum_{k=1}^{\infty} -U_k \cos \phi_k \cos(\omega_k \pm n) \frac{\alpha_{2j+1} + \alpha_{2j}}{2} \cos n\alpha d\alpha \right] \\
 &= \frac{1}{2\pi} \left\{ \sum_{j=1}^M \left[ \sum_{k=1}^{\infty} \frac{1}{\frac{\omega_k}{\omega} \pm n} U_k \cos \phi_k \cos\left(\frac{\omega_k}{\omega} \pm n\right) \frac{\alpha_{2l+1} + \alpha_{2l}}{2} \cdot \sin\left(\frac{\omega_k}{\omega} \pm n\right) \frac{\alpha_{2l+1} - \alpha_{2l}}{2} \right] \right. \\
 &\quad \left. - \sum_{l=1}^M \left[ \sum_{k=1}^{\infty} \frac{1}{\frac{\omega_k}{\omega} \pm n} U_k \cos \phi_k \cos\left(\frac{\omega_k}{\omega} \pm n\right) \frac{\alpha_{2l+1} + \alpha_{2l}}{2} \cdot \sin\left(\frac{\omega_k}{\omega} \pm n\right) \frac{\alpha_{2l+1} - \alpha_{2l}}{2} \right] \right\} \quad (13)
 \end{aligned}$$

$$\begin{aligned}
 a_n^{(2,1)} &\approx \frac{1}{2\pi} \left\{ \sum_{j=1}^M \sum_{k=1}^{\infty} \left[ \left( \cos\left(\frac{\omega_k}{\omega} + n\right) \beta_{2j} \frac{U_B \sin(\beta_{2j} + \theta) - V_{trl}}{V_{irm} - V_{trl}} \right) \right. \right. \\
 &\quad \left. \left. + \cos\left(\frac{\omega_k}{\omega} - n\right) \beta_{2j} \frac{U_B \sin(\beta_{2j} + \theta) - V_{trl}}{V_{irm} - V_{trl}} \right) \cdot \frac{\omega T_{tr}}{2} \cdot U_k \cos \phi_k \right] \\
 &\quad - \sum_{l=1}^M \sum_{k=1}^{\infty} \left[ \left( \cos\left(\frac{\omega_k}{\omega} + n\right) \beta_{2l-1} \frac{V_{irm} - U_B \sin(\beta_{2l-1} + \theta)}{V_{irm} - V_{trl}} \right) \right. \\
 &\quad \left. + \cos\left(\frac{\omega_k}{\omega} - n\right) \beta_{2l-1} \frac{V_{irm} - U_B \sin(\beta_{2l-1} + \theta)}{V_{irm} - V_{trl}} \right) \cdot \frac{\omega T_{tr}}{2} U_k \cos \phi_k \right] \\
 &= \frac{\omega T_{tr}}{2\pi(V_{irm} - V_{trl})} \left\{ \sum_{j=1}^M \sum_{k=1}^{\infty} \left[ \left( \frac{U_B}{2} \begin{pmatrix} \sin\left(\left(6k \frac{\omega_k}{\omega} + 1 \pm n\right) \beta_{2j} + \theta\right) \\ -\sin\left(\left(6k \frac{\omega_k}{\omega} - 1 \pm n\right) \beta_{2j} - \theta\right) \end{pmatrix} \right) \right. \right. \\
 &\quad \left. \left. - \cos\left(\frac{\omega_k}{\omega} \pm n\right) \beta_{2j} V_{trl} \right) \cdot U_k \cos \phi_k \right] \right. \\
 &\quad \left. - \sum_{l=1}^M \sum_{k=1}^{\infty} \left[ \left( -\frac{U_B}{2} \begin{pmatrix} \sin\left(\left(\frac{\omega_k}{\omega} + 1 \pm n\right) \beta_{2l-1} + \theta\right) \\ -\sin\left(\left(\frac{\omega_k}{\omega} - 1 \pm n\right) \beta_{2l-1} - \theta\right) \end{pmatrix} \right) \right. \right. \\
 &\quad \left. \left. + \cos\left(\frac{\omega_k}{\omega} \pm n\right) \beta_{2l-1} V_{irm} \right) \cdot U_k \cos \phi_k \right] \right\} \quad (14)
 \end{aligned}$$

Because the frequency of triangular-wave is sufficiently high, we can believe that

$\sin\left(\left(\frac{\omega_k}{\omega} + 1 \pm n\right) \alpha + \theta\right)$  is constant during one

triangular-wave cycle. Therefore, we can obtain (15) and (16), which are shown at the bottom of this page.

$$\sum_{j=1}^M \sin\left(\left(\frac{\omega_k}{\omega} + 1 \pm n\right) \beta_{2j} + \theta\right) \cdot \omega T_{tr} \approx \int_{-\pi}^{\pi} \sin\left(\left(\frac{\omega_k}{\omega} + 1 \pm n\right) + \theta\right) d\beta \quad (15)$$

$$\sum_{l=1}^M \sin\left(\left(\frac{\omega_k}{\omega} + 1 \pm n\right) \beta_{2l-1} + \theta\right) \cdot \omega T_{tr} \approx \int_{-\pi}^{\pi} \sin\left(\left(\frac{\omega_k}{\omega} + 1 \pm n\right) + \theta\right) d\beta \quad (16)$$

Substituting (15), (16) into (14), we can get (17), given at the bottom of this page.

Similarly,  $b^{(2,1)}$  can be expressed as (18). By using the same method, we can obtain  $a_n^{(3,1)}$  and  $b_n^{(3,1)}$ , shown in (19) and (20) respectively.

$$a_n^{(2,1)} \approx \frac{1}{4\pi(V_{trm} - V_{trl})} \sum_{k=1}^{\infty} U_k \cos \phi_k \cdot \int_{-\pi}^{\pi} \left[ \begin{array}{l} U_B \sin \left[ \left( \frac{\omega_k}{\omega} - n + 1 \right) \beta + \theta \right] \\ + U_B \sin \left[ \left( \frac{\omega_k}{\omega} - n - 1 \right) \beta - \theta \right] \\ - (V_{trm} + V_{trl}) \cos \left( \frac{\omega_k}{\omega} - n \right) \beta \end{array} \right] d\beta \quad (17)$$

$$b_n^{(2,1)} = \frac{1}{2} \left[ \begin{array}{l} \sum_{j=1}^M \frac{1}{\pi} \int_{\alpha_{2j}}^{\alpha_{2j+1}} \sum_{k=1}^{\infty} U_k \cos \phi_k \cos(\omega_k \pm n) \frac{\alpha_{2j+1} + \alpha_{2j}}{2} \sin n \alpha d\alpha \\ + \sum_{l=1}^M \frac{1}{\pi} \int_{\alpha_{2l-1}}^{\alpha_{2l}} \sum_{k=1}^{\infty} -U_k \cos \phi_k \cos(\omega_k \pm n) \frac{\alpha_{2j+1} + \alpha_{2j}}{2} \sin n \alpha d\alpha \end{array} \right]$$

$$= \frac{1}{4\pi(V_{trm} - V_{trl})} \sum_{k=1}^{\infty} U_k \cos \phi_k \int_{-\pi}^{\pi} \left[ \begin{array}{l} U_B \cos \left( \left( \frac{\omega_k}{\omega} + 1 - n \right) \beta + \theta \right) \\ - U_B \cos \left( \left( \frac{\omega_k}{\omega} - 1 - n \right) \beta - \theta \right) \\ + \sin \left( \frac{\omega_k}{\omega} - n \right) \beta (V_{trm} + V_{trl}) \end{array} \right] d\beta \quad (18)$$

$$a_n^{(3,1)} = \frac{1}{4\pi(V_{trm} - V_{trl})} \sum_{i=1}^{\infty} U_k \sin \phi_k \int_{-\pi}^{\pi} \left[ \begin{array}{l} -U_B \cos \left( \left( \frac{\omega_k}{\omega} - n + 1 \right) \beta + \theta \right) \\ + U_B \cos \left( \left( \frac{\omega_k}{\omega} - n - 1 \right) \beta - \theta \right) \\ - \sin \left( \frac{\omega_k}{\omega} - n \right) \beta (V_{trm} + V_{trl}) \end{array} \right] d\beta \quad (19)$$

$$b_n^{(3,1)} = \frac{1}{4\pi(V_{trm} - V_{trl})} \sum_{k=1}^{\infty} U_k \sin \phi_k \int_{-\pi}^{\pi} \left[ \begin{array}{l} U_B \sin \left( \left( \frac{\omega_i}{\omega} + 1 - n \right) \beta + \theta \right) \\ - U_B \sin \left( \left( \frac{\omega_i}{\omega} - 1 - n \right) \beta - \theta \right) \\ - \cos \left( \frac{\omega_i}{\omega} - n \right) \beta (V_{trm} + V_{trl}) \end{array} \right] d\beta \quad (20)$$

$$u_a = \frac{U_D U_B \sin(\omega t + \theta)}{V_{trm} - V_{trl}} + \frac{1}{2} \sum_{k=1}^{\infty} \left( \frac{U_k U_B (\sin((\omega_k + \omega)t + \theta - \phi_k) - \sin((\omega_k - \omega)t - \theta - \phi_k))}{V_{trm} - V_{trl}} \right)$$

$$= \frac{U_D U_B \sin(\omega t + \theta)}{V_{trm} - V_{trl}} + \sum_{k=1}^{\infty} \left( \frac{U_k \cos(\omega_k t - \phi_k) U_B \sin(\omega t + \theta)}{V_{trm} - V_{trl}} \right)$$

$$= \frac{U_D U_B \sin(\omega t + \theta)}{V_{trm} - V_{trl}} + \sum_{k=1}^{\infty} \frac{U_k U_B [\sin(\omega_k t + \omega t - \phi_k + \theta) - \sin(\omega_k t - \omega t - \phi_k - \theta)]}{2(V_{trm} - V_{trl})} \quad (21)$$

Substituting (11), (12), (17), (18), (19), (20) into (3), we can obtain (21). Obviously,  $u_a$  contains of a fundamental component, lower harmonics of  $f_k \pm f_{\sin}$  ( $k = 1, 2, \dots, f_k = \omega_k / 2\pi, f_{\sin} = \omega / 2\pi$ ), and harmonics above the switching frequency generated by triangular-wave SPWM operation. Then there is a relationship between  $u_a$  and  $v_{dc}$  which is expressed as follows:

$$u_a = T(\theta) \cdot v_{dc} \quad (22)$$

Where  $T(\theta)$  is the switching function of triggering pulses. Substituting the second step in (21) into (22), we can get the following:

$$T(\theta) = \frac{U_B \sin(\omega t + \theta)}{V_{trm} - V_{trl}} \quad (23)$$

## 2. Analysis of Output Voltage Using MWR-SPWM Technique

From above analysis, we can add some component to standard modulation wave to offset the influence on output ac

$$u_a = (T'(\theta) + T''(\theta)) \cdot (U_D + \sum_{k=1}^{\infty} U_k \cos(\omega_k t - \phi_k)) = T'(\theta) \cdot U_D \quad (26)$$

$$T''(\theta) = -\frac{\sum_{k=1}^{\infty} U_k \cos(\omega_k t - \phi_k)}{U_D + \sum_{k=1}^{\infty} U_k \cos(\omega_k t - \phi_k)} \cdot T'(\theta) = -\frac{v_{dc} - U_D}{v_{dc}} T'(\theta) \quad (27)$$

Substituting (23) into (27), we obtain the following:

$$T''(\theta) = -\frac{v_{dc} - U_D}{v_{dc}} \cdot \frac{U_B \sin(\omega t + \theta)}{V_{trm} - V_{trl}} \quad (28)$$

When  $T''(\theta)$  is compared with  $T'(\theta)$ ,  $k$  can be

voltage from dc voltage's fluctuation. Based on this idea, we propose a new modulation wave as follows:

$$u_s = k + u_{s1} \quad (24)$$

We consider that  $u_s$  consists of two independent parts, one is  $u_{s1}$ , another is  $k$ . When (24) is chosen as modulation wave, the switching function  $T(\theta)$  can be expressed as follows:

$$T(\theta) = T'(\theta) + T''(\theta) \quad (25)$$

Where  $T'(\theta)$  is the component of switching function when modulation wave is  $u_{s1}$  which is shown in (23);  $T''(\theta)$  is the component of switching function when modulation wave is  $k$ .

When the new modulation wave is adopted we hope that the harmonics of  $u_a$  can be eliminated effectively, we can obtain (26), given at the bottom of this page. Therefore, we can obtain (27).

obtained by homogeneity theorem.

Therefore, when the new modulation wave  $u_s$  is adopted  $u_a$  only contains fundamental component in low frequency band.

So, when power system is balanced system, new

modulation wave  $u_s$  is adopted that can eliminate the influence of  $6nf_0$  harmonics from three-phase diode

$$k = -\frac{v_{dc} - U_D}{v_{dc}} u_{s1} \quad (29)$$

$$u_a \approx \frac{U_D U_B \sin(\omega t + \theta)}{V_{trm} - V_{trl}} \quad (30)$$

#### IV. SIMULINK AND EXPERIMENTAL RESULT

In order to verify the analyses and the simulation results, a 2-kVA experimental novel inverter that adopts above proposed topology was set up in laboratory. The diode bridge rectifier is connected with a three-phase unbalanced supply. The circuit parameters used in experiment is the same with the ones in simulation.

Figure 4 and Figure 5 show the load phase current waveforms with general SPWM and MWR-SPWM technique respectively. Figure 6 and Figure 7 show the

bridge output voltage to harmonics of converter output voltage so as to not use bulky dc filter capacitor.

output voltage spectrum by using general SPWM and MWR-SPWM technique respectively. Obviously, the novel ac/dc/ac converter can eliminate harmonics of output voltage effectively. The experimental results are in full agreement with theoretical analyses and simulation results.

#### V. CONCLUSIONS

The proposed novel inverter has such advantages as simpler structure, higher reliability, and higher performance. Moreover, because an MWR-SPWM technique is adopted to eliminate low harmonics in output voltage, not only the bulky dc filter capacitor is greatly decreased or even removed, but also the size of output filter is reduced accordingly. The simulation and experimental results prove the validity of the analysis and the feasibility of the proposed MWR-SPWM technique.

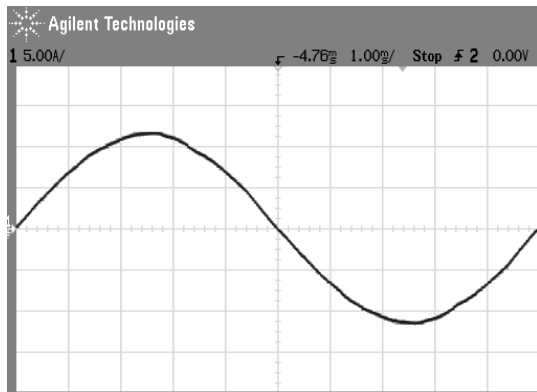


Figure 4. Current waveform using general SPWM technique

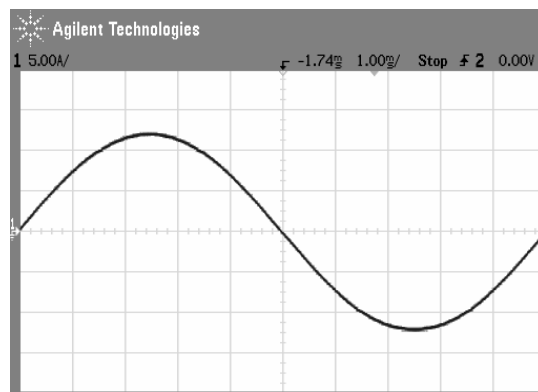


Figure 5. Current waveform by using MWR-SPWM technique

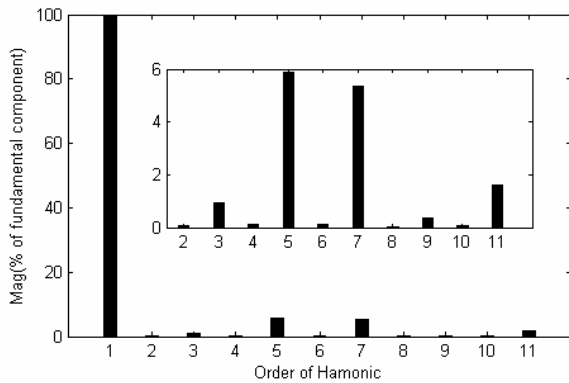


Figure 6. The spectrum of using general SPWM technique

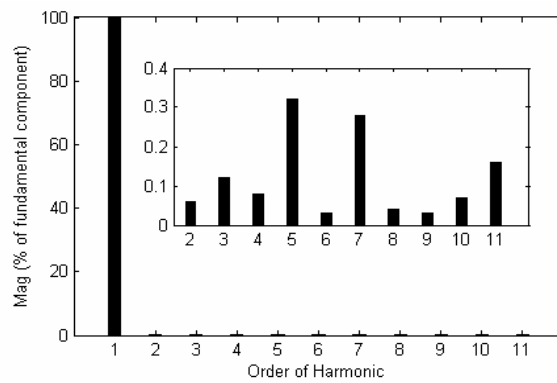


Figure 7. The spectrum of using MWR-SPWM technique

**Correspondence to:**

Wang Shuwen, Fang Junlong  
 Harbin Institute of Technology  
 Harbin, Heilongjiang 150001, China  
 Email: [wswtr@163.com](mailto:wswtr@163.com)

**Information of Authors:**

- Wang Shuwen** (1975-) male. He is presently studying at Harbin Institute of Technology for his PhD. In 2002, he joined the Department of Electrical Engineering at NEAU. His research interests include PWM technique, harmonic suppression, and static var compensators.
- Ji Yanchao** (1962-) male. He has been a full-time professor of Electric Engineering at Harbin Institute, since 1993. His research fields include FACTS, static var generators, and generalized active filters.

**REFERENCES**

- Habetler T G A space vector-based Rectifier Regulator for AC/DC/AC Converters [J]. IEEE Trans. On Power Electronics, 1999,8(1):30~36.

- Hur Namho, Jung Junhwan, Nam Kwanghee. Fast Dynamic DC-link Power balancing Scheme for a PWM converter-inverter System[A]. IECON' 99 Proceedings[C]. The 25<sup>th</sup> Annual conference of the IEEE, 1999, 2:767~772
- Jung Jinhwan, Lim Sunkyoung, Nam Kwanghee. A Feed-back Linearizing Control Scheme for a PWM Converter –inverter Having a very Small DC-link Capacitor[J].IEEE Trans. on Ind. Appl., 1999,35(5):1124~1131
- Li Li, D. Czarkowski, Yaguang Liu and P. Pillay, “Multilevel selective harmonic elimination PWM technique in series-connected voltage inverters,” IEEE Trans. Ind. Applicat., vol. 36, pp. 160-170, Jan/Feb. 2000.
- Toshiji Kato, “Sequential homotopy-based computation of multiple solutions for selected harmonic elimination in PWM inverters,” IEEE Trans. Cir. and Sys.—I: Fundamental Theory and Application, vol. 46 pp. 586-593, May.1999.
- L. M. Malesani, L. Rossetto, P. Tenti, and P. Tomasin, “AC/DC/AC PWM converter with reduced energy storage in the DC link,” IEEE Trans. Ind. Applicat., vol.31, pp. 287-292, Mar/Apr.1995.
- N. Hur, Jinhwan Jung, Kwanghee Nam, “A fast dynamic DC-link power-balancing scheme for a PWM converter-inverter system,” IEEE Trans. Ind. Applicat., vol. 48, pp. 794-803, Aug.2001.



## Microbiological and Nutritional Qualities of Dairy Products: Nono and Wara

Roseline E. Uzeh \*, Regina E. Ohenhen \*\*, Ayodeji K. Rojugin \*

\* Department of Botany and Microbiology, University of Lagos, Nigeria. Telephone: 002348051217750.  
Email: [roseline\\_uzeh@yahoo.com](mailto:roseline_uzeh@yahoo.com)

\*\* Department of Microbiology, Ambrose Alli University, Ekpoma, Nigeria. Telephone: 00234803355312.  
Email: [drginaohen@yahoo.co.uk](mailto:drginaohen@yahoo.co.uk)

**ABSTRACT:** The microbiological and nutritional qualities of two fermented dairy products: nono and wara were investigated. Bacteria and fungi were isolated from both products. The bacteria isolated include *Acinetobacter mallei*, *Alcaligenes faecalis*, *Bacillus cereus*, *Enterobacter aerogenes*, *Enterobacter cloacae*, *Micrococcus spp*, *Serratia spp*, *Flavobacterium spp*, *Staphylococcus aureus* and *Klebsiella licquifasciens*. The fungal isolates were *Aspergillus niger*, *Aspergillus fumigatus*, *Penicillium chrysogenum*, *Rhizopus spp*, *Fusarium moniliforme*, and *Trichoderma reesii*. The mean total plate count of nono was  $3.55 \times 10^8$  cfu/ml, while that of wara was  $4.55 \times 10^8$  cfu/g. The mean coliform count was  $4.25 \times 10^7$  cfu/ml for nono and  $2.40 \times 10^7$  cfu/g for wara. While the mean fungal count was  $12.9 \times 10^6$  cfu/ml for nono and  $1.31 \times 10^7$  cfu/g for wara. The respective moisture content and total titratable acid were higher in nono (86.03%, 1.37%) than in wara (55.68%, 0.48%). Wara was of a higher pH (4.64), than nono (2.87). Wara had higher values respectively for fat, ash, and protein (18.55%, 1.5%, and 23%) than nono (3.68%, 0.97%, and 6.40%), while the carbohydrate level was lower in wara (1%) than in nono (2.9%). Nono and in particular, wara, are of good protein sources. However, the range of microorganisms isolated from both products pose serious threat to food safety, and the need to ensure the microbiological safety of these products can not be over emphasized. [Nature and Science. 2006;4(3):37-40].

**Keywords:** Nono; wara; microbiological and nutritional qualities; food safety

### INTRODUCTION

Nono and wara are local dairy products that are produced and widely consumed in many African countries, including Nigeria. Mainly the Fulanis produce milk locally in Nigeria and the excess milk is processed into these products for preservation (Akinyele *et al.*, 1999). Nono and wara are produced in homes, especially in villages where shelf-life and safety of the products are not considered. They are however sold to both rural and urban people as food. Nono is produced from non-pasteurized cow milk collected in a container called calabash and allowed to ferment naturally for 24 h (Eka and Ohaba, 1977; Olasupo *et al.*, 1996). Wara is a white soft non-ripened cheese made by the addition of a plant extract (*Calotropis procera*) to the non-pasteurized whole milk from cattle (Adeyemi and Umar, 1994).

Poor hygiene, practiced by handlers of these products, may lead to introduction of pathogenic microorganisms into the products and since they do not undergo further processing before consumption, these foods may pose risk to their consumers.

This research is aimed at isolating and identifying microorganisms present in nono and wara in addition to determining the nutritional and some physicochemical

qualities of nono and wara. These will help to ascertain the microbial and product quality of nono and wara.

### MATERIALS AND METHODS

#### Collection of samples

Nono samples were purchased from hawkers at Yaba, Okoko, Idiaraba, Sabo, and Mile 12 markets and the samples were labeled A, B, C, D, and E respectively. While wara samples were purchased from markets in Orile, Oshodi, Mushin, Ketu, and Agege, all in Lagos state, Nigeria, and the samples were labeled F, G, H, I, and J respectively.

#### Determination of the physicochemical parameters of nono and wara

##### Moisture content

A clean platinum dish was dried in an oven and cooled in a desiccator. The cooled dish was weighed. From the nono sample 5 g was weighed and spread on the dish, the dish containing the sample was weighed. It was then transferred into the air oven at  $105^{\circ}\text{C}$  to dry for about 3h. A pair of tongs was used to transfer the dish into a desiccator, allowed to cool and weighed. The dish was returned into the oven for 30 min and again cooled in a desiccator and weighed (AOAC, 1980). The process

was repeated until a constant weight was obtained. This was done for other samples.

### Hydrogen ion concentration (pH)

In order to obtain the pH of the samples, 5 g each was weighed and suspended in 10 ml of distilled water. The pH was determined with a pH meter.

### Nutritional analysis

The carbohydrate was determined according to Anthrone reaction method (Southgate, 1976). Protein was analyzed for by the Microkjedhal estimation of nitrogen, using a conversion factor of %N x 6.25. Determination of the ash content was done according to AOAC (1980) method, while that of fat was done as described by Pearson (1976).

### Determination of crude fiber

The nono and wara samples to be analyzed were defatted using petroleum ether. From the defatted sample 1 g was weighed into 500 ml beaker containing 100 ml of trichloroacetic acid. The content of the beaker was boiled and refluxed for 4 min. It was cooled and filtered with filter paper (Whatman No.1). The residues were washed six times in hot distilled water and once with mentholated spirit. The filter paper together with the sample was transferred into a porcelain crucible and dried in an oven overnight at 100°C, after which it was cooled in a desiccator, weighed, ashed in a muffle furnace at 600°C for 4h and weighed again after cooling. The loss in weight during incineration was equivalent to the amount of crude fiber.

### Microbiological analysis

This was done both quantitatively and qualitatively. Samples were diluted serially using sterile distilled water as diluent. From appropriate dilutions 1ml each was plated in duplicate using the pour plate method.

Media used include nutrient agar, MacConkey agar, and potato dextrose agar. The nutrient and MacConkey agar plates were incubated at 37°C for 24 h, while the potato dextrose agar plates were incubated at 25°C for 48-72 h. After incubation, developed colonies were counted, and representative colonies were sub cultured to obtain pure cultures of isolates.

### Identification of microbial isolates

Identification of the bacterial isolates was based on cultural, morphological, and biochemical characteristics following standard methods (Buchanan and Gibbons, 1974) while that of fungi was also based on cultural and morphological characteristics and standard methods were followed (Talbot, 1971; Bryce, 1992).

### RESULTS

The moisture and total titratable acid were higher in nono than in wara, and the pH of wara was higher than that of nono (Table 1). From the nutritional analysis, wara had higher values for fat, ash and protein than nono. Carbohydrate was however more in nono than in wara. Crude fiber was not detected in both products (Table 2).

The mean total plate count of nono was  $3.55 \times 10^8$  cfu/ml while that of wara was  $4.55 \times 10^8$  cfu/g. The mean coliform count was  $4.25 \times 10^7$  cfu/ml for nono and  $2.40 \times 10^7$  cfu/g for wara. While the mean fungal count was  $12.9 \times 10^6$  cfu/ml for nono and  $1.31 \times 10^7$  cfu/g for wara (Tables 3a and 3b). The bacteria isolated from the products were *Acinetobacter mallei*, *Alcaligenes faecalis*, *Bacillus cereus*, *Enterobacter aerogenes*, *Enterobacter cloacae*, *Micrococcus* spp, *Serratia* spp, *Flavobacterium* spp, *Staphylococcus aureus*, and *Klebsiella licquifasciens* (Table 4). The fungal isolates include *Aspergillus niger*, *Penicillium chrysogenum*, *Rhizopus* spp, *Fusarium moniliforme*, *Trichoderma reesii*, and *Aspergillus fumigatus*.

Table 1. Physicochemical parameters of nono and wara

Parameters	Nono	Wara
Moisture (%)	86.03	55.68
Total titratable acid (%)	1.37	0.48
pH	2.87	4.64

Table 2. Nutritional content of nono and wara

Parameters ( % )	Nono	Wara
Fat	3.68	18.55
Ash	0.97	1.50
Crude fiber	not detected	not detected
Protein	6.40	23.00
Carbohydrate	2.90	1.00

Table 3a. Microbial count of nono

Locations	Total plate count (x 10 <sup>8</sup> cfu/ml)	Coliform count (x 10 <sup>7</sup> cfu/ml)	Fungal count (x 10 <sup>6</sup> cfu/ml)
A	2.65	3.80	9.5
B	1.75	2.10	5.0
C	2.25	5.20	8.5
D	1.80	4.10	18.5
E	9.30	6.00	23.5
Mean	3.55	4.25	12.9

Table 3b. Microbial count of wara

Locations	Total plate count (x 10 <sup>8</sup> cfu/g)	Coliform count (x 10 <sup>7</sup> cfu/g)	Fungal count (x 10 <sup>7</sup> cfu/g)
F	1.50	1.55	1.00
G	10.90	2.65	1.15
H	3.90	2.40	1.90
I	3.50	3.20	1.35
J	3.70	2.20	1.15
Mean	4.55	2.40	1.31

Table 4. Bacteria isolated from nono and wara

Bacterial isolates	Nono	Wara
<i>Acinetobacter mallei</i>	-	+
<i>Alcaligenes faecalis</i>	-	+
<i>Bacillus cereus</i>	+	+
<i>Enterobacter aerogenes</i>	+	-
<i>Enterobacter cloacae</i>	-	+
<i>Micrococcus</i> spp	+	+
<i>Serratia</i> spp	-	+
<i>Flavobacterium</i> spp	+	-
<i>Staphylococcus aureus</i>	+	+
<i>Klebsiella licuifasciens</i>	-	+

Key: + = Present; - = Absent

## DISCUSSION

The nutritional content of nono and wara shows that they are of appreciable nutritional status especially in the protein content. The dairy products particularly wara are good sources of protein. Higher protein content was observed in wara than in nono. This could be due to accumulation of the protein through expulsion of the whey, which does not occur in nono production.

The results obtained from the microbial analysis of nono and wara show that both products were contaminated with microorganisms of public health concern. The high total bacterial and coliform count in both products may be a consequence of the low level of hygiene maintained during the processing and sale of the products. This includes the handlers, quality of water used and the utensils. During the sale of wara, dirty hands and spoons are dipped into the bowl for product selection by both hawkers and consumers. The exposure of both wara and nono while they are displayed for sale in bowls can serve as source of

contamination. The detection of *Enterobacter aerogenes*, *Enterobacter cloacae*, *Klebsiella*, and *Serratia* species in nono and wara as the case may be, indicates possible faecal contamination. Being enteric bacteria, their presence indicates poor hygienic practices among handlers of nono and wara. Due to the significance of the faecal-oral route transmission for many bacterial food-borne diseases, basic hygiene measures assume a decisive importance in food safety management (Untermann, 1998).

Other bacteria isolated include *Acinetobacter*, *Alcaligenes*, *Flavobacterium*, *Micrococcus* species, and *Staphylococcus aureus*. *Alcaligenes* and *Flavobacterium* have been implicated in the spoilage of milk and its products at even refrigerator temperatures. *Acinetobacter* species are known to cause ropiness of milk and secretion of extracellular enzymes both at psychrophilic and mesophilic temperatures (Gilmour and Rowe, 1990).

*Bacillus cereus* which is known to be highly resistant to environmental stress due to its sporing

nature was also isolated, and *B.cereus* is known to be of public health importance since it is pathogenic. The detection of *Staphylococcus aureus* is also of public health importance because of its ability to cause a wide range of infections especially food-borne intoxication. This organism was equally isolated by Olasupo *et al.* (2002) from wara and kunun-zaki, a cereal based, non-alcoholic beverage.

The fungal isolates: *Aspergillus*, *Penicillium*, *Rhizopus*, *Fusarium*, and *Trichoderma* species which were isolated are known spore formers, which therefore means that they can easily contaminate the dairy products which are usually exposed during processing, storage, and hawking. They are major spoilage organisms of carbohydrate foods (Rhodes and Fletcher, 1966). However, their growth can result in the production and accumulation of mycotoxins which are of public health and economic importance.

Microbiological standards have not been put in place for the two locally processed dairy products: nono and wara in Nigeria, and even in most African countries where they are consumed. This is also applicable to many other locally processed foods in Nigeria. The isolation of coliforms and some other food pathogens from these dairy products pose serious threat to food safety, especially locally processed foods in Nigeria. Due to the fact that nono and wara are ready-to-eat foods which are consumed without further processing, great attention should therefore be given to the microbiological safety of these products because their direct consumption may cause health hazard to the consumers.

**Correspondence to:**

Roseline E. Uzeh  
Department of Botany and Microbiology  
Universty of Lagos

Akoka, Lagos, Nigeria

Telephone: +234-805-121-7750

E-mail: [roseline\\_uzeh@yahoo.com](mailto:roseline_uzeh@yahoo.com)

**REFERENCES**

1. Adeyemi, I. A. and Umar, S. Effect of method of manufacture on quality characteristics of kunun-zaki, a millet-based beverage. Nigerian Food Journal. 1994; 12: 34-41.
2. Akinyele, B.J, Fawole, M.O and Akinyosoye, F.A. Microorganisms associated with fresh cow milk, wara, and nono; two local milk products hawked by Fulani women in Ilorin, Kwara state, Nigeria. Nigerian Food Journal. 1999; 17: 11-17.
3. A.O.A.C. Official Methods of Analysis. 13<sup>th</sup> ed. Washington DC: Association of Official Analytical Chemist. 1980.
4. Bryce,K. The fifth kingdom. Mycologue Publications, Ontario. 1992; 412pp.
5. Buchanan, R.E. and Gibbons, N.E. Bergey's Manual of Determinative Bacteriology. 8<sup>th</sup> ed. The Williams and Wilkins Co., Baltimore. 1974.
6. Eka, O.U. and Ohaba, J.A. Microbiological examination of Fulani milk (nono) and butter (manshanu). Nigerian Journal of Science. 1977; 11: 113-122.
7. Gilmour, A and Rowe, M.T. Microorganisms associated with milk. In Dairy microbiology: The microbiology of milk, eds. Robison, R.K, 2<sup>nd</sup> edition, vol. 1. Applied science, London .1990; pp 37-75.
8. Olasupo, N.A., Akinsanya, S.M., Oladele, O.F. and Azeez, M.K. Evaluation of nisin for the preservation of nono, a Nigerian fermented milk product. Journal of Food Processing and Preservation. 1996; 20: 71-78.
9. Olasupo, N.A., Smith, S.I. and Akinsinde K.A. Examination of the microbial status of selected indigenous fermented foods in Nigeria. Journal of Food Safety. 2002. 22: 85-93.
10. Pearson, D. The chemical analysis of foods 6<sup>th</sup> ed., New York: Chemical Publishers Co. 1976.
11. Rhodes, A. and Flecher, D.L. Principles of industrial microbiology, Pergamam press, Oxford, 1966; pp 119.
12. Southgate, D. A. T. Determination of food carbohydrates. Applied Science Publishers Limited, London. 1976. pp 68-70.
13. Talbot, P.H.R. Principles of fungal taxonomy. Macmillan Press, London. 1971. 274pp
14. Utermann, F. Microbial hazards of food. Food Controll. 1998; 9: 119-126.

# The Study of a Novel Microstrip Antenna Being Used for the Estimation of Sample Material Dielectric Coefficient under Electromagnetic Wave at 2.4 GHz

Yu-Min Li<sup>1</sup>, Chia-ching Chu<sup>1</sup>, Yuan-Tung Cheng<sup>2</sup>, Hsien-Chiao Teng<sup>3</sup>, Shen Cherng<sup>1</sup>

<sup>3</sup> Department of Electrical Engineering, Chinese Military Academy, Fengshan, Taiwan, 830 ROC

<sup>2</sup> Department of Elewctronics, Chengshiu University, Niasong, Taiwan, 833 ROC

<sup>1</sup> Department of Electrical Engineering, Chengshiu University, Niasong, Taiwan, 833 ROC

**ABSTRACT:** A new microstrip antenna named as jacket antenna is proposed for estimating the sample material dielectric coefficient under electromagnetic wave at 2.4 GHz. Clipping sample material to the jacket antenna will cause the changing of operation frequency and bandwidth that being sensitive to the dielectric coefficient of the clipping material. [Nature and Science. 2006;4(3):41-44].

**Keywords:** microstrip antenna; dielectric coefficient; operation frequency

## 1. INTRODUCTION

A single structure of metal radiation patch microstrip antenna has been studied very well [1, 2]. In this article, a new microstrip antenna named jacket antenna is proposed for the use of estimating the sensitivity of dielectric coefficient of the clipping sample material to respond to the electromagnetic wave at 2.4 GHz. The patch of the antenna is slotted for adjusting the bandwidth to sense the loss tangent of the sample material dielectric coefficient [3, 4]. The antenna ground is sized to reduce the cross-polarization of the radiation pattern. Inexpensive FR4 substrate is used for convenience [5, 6]. Double side and single side metal-modified FR4 plates are provided as sample materials for being standardized the radiation pattern and the antenna gain. Extra check-shape radiator is connected to microstrip antenna for the direction gain adjustment. The measurement of the radiation pattern as well as HFSS simulation reveals the dispersive relation of the sample material to respond to the electromagnetic

wave at 2.4 GHz.

## 2. ANTENNA DESIGN

The proposed design of a jacket antenna is depicted as in Figure 1. Sample material can be clipped on the slotted patch between end point of check-shape radiator and the substrate.

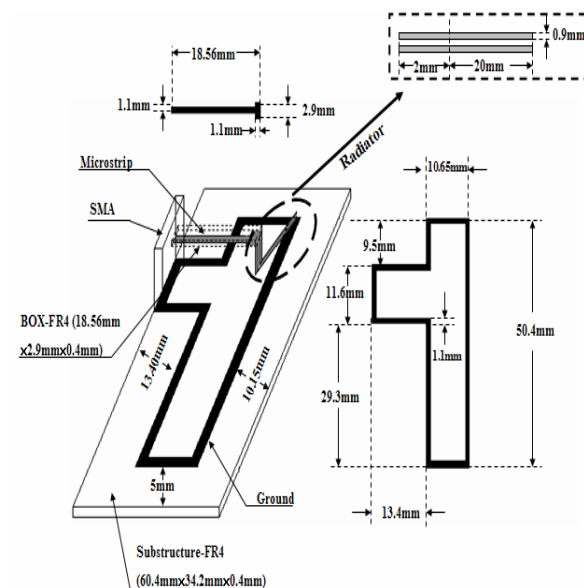


Figure 1. The geometry of the jacket antenna

T-type patch microstrip ground was printed on the 18.56 mm×2.9 mm×0.4 mm FR4 substrate. By using a small microstrip line as the transition between radiator and signal, SMA connector connected to a microstrip radiator. The most optimization of the radiator is 20 mm in length. The test sample materials were proposed and depicted in Figure 2.

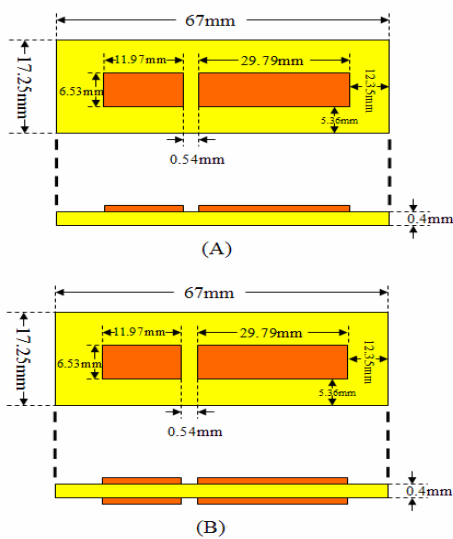


Figure 2. Design of test sample materials:  
 (A) single side FR4 plate with specific size of metal and slot line printed  
 (B) double side FR4 plate with specific size of metal and slot line printed

Since the effective dielectric coefficient of the test sample can be adjusted by microstrip printed on FR4 plates, standard material samples were designed for estimation of the dielectric coefficient of the interested materials.

### 3. EXPERIMENTAL RESULTS AND DISCUSSIONS

Figure 3 depicts the measurement for the return

loss of the jacket antenna. The low band operation frequency of the jacket antenna is at 2.65 GHz. However, single side with microstrip printed test sample shifted the operation frequency to 2.4 GHz and increased the bandwidth (BW) from 4.91% to 12.58%. In comparison, the double side with microstrip printed test sample shifted the operation frequency to the same frequency at 2.4 GHz with increasing bandwidth (BW) from 4.91% to 13.81%. The effective dielectric coefficient of the test sample of single side microstrip moved to 3 and the loss tangent to 1.5 being increased. In contrary, the effective dielectric coefficient of the test sample of double side microstrip moved to 3 also but being increased the loss tangent to 2.

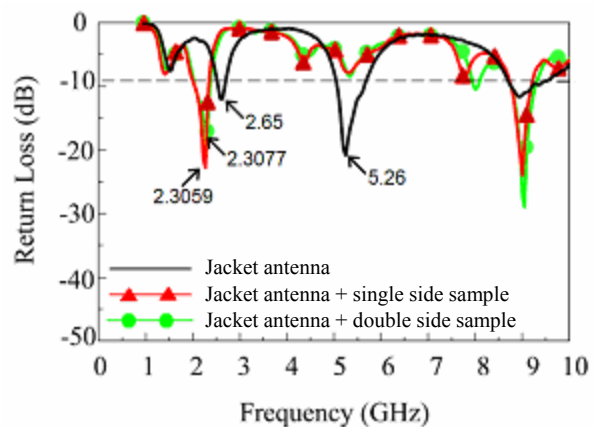


Figure 3. The return loss of the jacket antenna and that with clipped test samples

Table 1. The results of the antenna measurement

	Operation frequency GHz	DB	BW
Jacket antenna	2.65	-11.97	4.91%
with single side microstrip test A	2.40	-22.547	12.58%
with double side microstrip test B	2.40	-21.252	13.81%

The test sample material B can be regarded as a parallel plate waveguide but experimentally showing no significant effect to the operation frequencies. The radiation patterns at the two operation frequencies of the proposed jacket antenna and the jacket antenna with both clipped sample materials of A and B are plotted in Figure 4 and Figure 5. Table I listed the basic measurements. The gains of the jacket antenna and the antenna clipped with both sample materials A and B are shown in Figure 6. Different sample material clearly affected the gain levels of the jacket antenna operated at lower frequency band. The shift of the band frequency caused by clipped sample material indicated the altering of the electromagnetic wave propagation in sample material may be resulted from the changing of the current density on the check-shape reflector. The further study of the dispersive effect of the sample materials will be discussed in next publication.

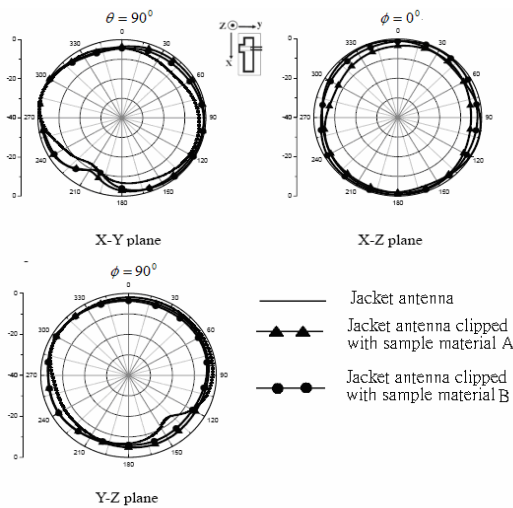


Figure 4. Measured radiation patterns of the E-Phi at 2.65 GHz of jacket antenna and 2.4 GHz of the clipped sample materials

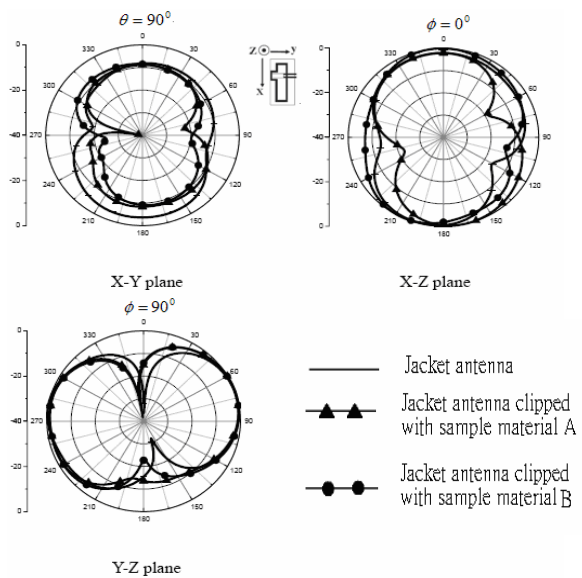


Figure 5. Measured radiation patterns of the E-Theta at 2.65 GHz of jacket antenna and 2.4 GHz of the clipped sample materials.

#### 4. CONCLUSION

According to the measurement, the jacket antenna clipped sample material can significantly affect the operation frequencies and the antenna gains of the jacket antenna. The HFSS simulation of the dispersive dielectric coefficient of the sample material [7, 8] supports the loss tangent of the effective dielectric coefficient of the sample material is 2 which is 50% down of the FR4 plate.

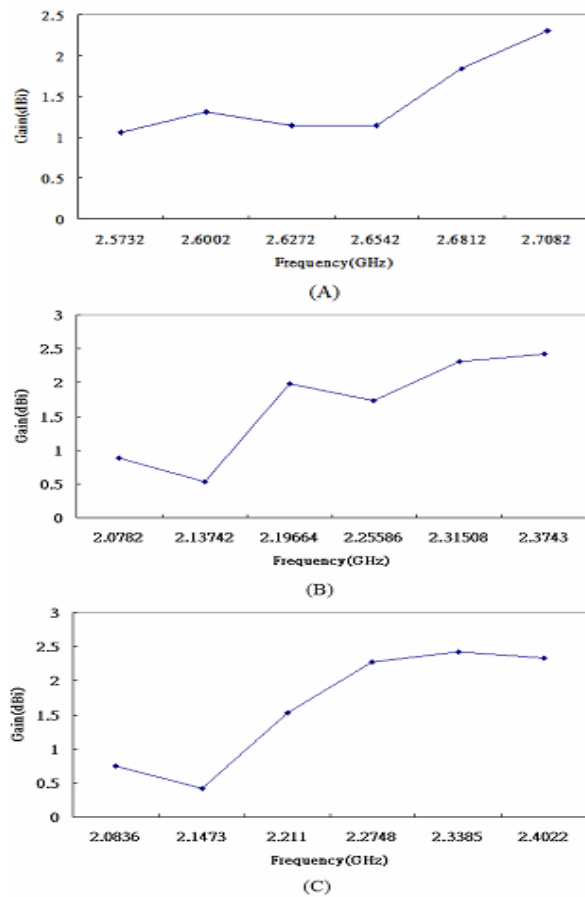


Figure 6. The measurement of the antenna gain. (A) Jacket antenna (B) Jacket antenna with clipped sample material A (C) Jacket antenna with clipped sample material B.

**Correspondence to:**

Shen Cherng, P.E., Ph.D.

Associate Professor

Department of Electrical Engineering

Chengshiu University

Niausong, Kaohsiung, 833, Taiwan, ROC

Phones: 011-886-7732-0480;

011-886-929-370-970 (cellular)

[cherngs@csu.edu.tw](mailto:cherngs@csu.edu.tw)

[cherng@msu.edu](mailto:cherng@msu.edu)

**Received:** August 1, 2006

**References**

1. Tang CL, Chou JY, Wong KL. Broadband dual-frequency v-shape patch antenna. *Microwave and Optical Technology Letters*. 2000;25:121-123.
2. Maci S, Gentili GB. Dual-frequency patch antennas. *IEEE Antennas Propagat Mag* 1999;39:13-20.
3. Chu CC, Li YM, Teng HC, Cherng S. The permittivity frequency-dependent response of a ceramic material to electromagnetic waves at 2 GHz. in press 2006.
4. Andersen JB, Vaughan RG. Transmitting, receiving, and scattering properties of antennas. *IEEE Antennas and Propagation Magazine*. 2003;45(4):93-98.
5. Esselle, KP. A low-profile rectangular dielectric-rectangular antenna, *IEEE Trans. Antennas Propagat*. 1996;44:1296-1297.
6. Mongia RK. Reduced size metalized dielectric resonator antennas, in *IEEE Antennas Propagat.-S/URSI Symp. Digest*, Montreal, Canada. 1997:2202-2205.
7. Maeda T, Morooka T. Radiation efficiency measurement of electrically small antennas using radio waves scatterers. *IEEE Antennas Propagat Int. Symp. Dig*. 1988:324-327.
8. Ansoft Corporation HFSS. <http://www.ansoft.com/products/hf/hfss>. 2004.



## Extra Dimentions, Brane Worlds, and the Vanishing of Axion Contributions to Inflation?

A. W. Beckwith

[projectbeckwith2@yahoo.com](mailto:projectbeckwith2@yahoo.com)

**Abstract:** We examine the implications of the 5<sup>th</sup> Randall Sundrum Brane world dimension in terms of setting initial conditions for chaotic inflationary physics. Our model pre supposes that the inflationary potential pioneered by Guth is equivalent in magnitude in its initial inflationary state to the effective potential presented in the Randall - Sundrum model We also pre suppose an axion contribution to chaotic inflation with a temperature dependence which partly fades out up to the point of chaotic inflation being matched to a Randall – Sundrum effective potential. This is done by use of the Bogomolnyi inequality to re scale and re set initial conditions for the chaotic inflationary potential. One of potential systems embedded in the Ruandal-Sundrum brane world is a model with a phase transition bridge from a tilted washboard potential to the chaotic inflationary model pioneered by Guth which is congruent with the slow roll criteria. If the axion wall contribution is due to Di Quarks, this is equivalent to tying in **baryogenesis** to the formation of chaotic inflation initial conditions, with the Randall-Sundrum brane world effective potential delineating the end of the dominant role of di quarks, due to baryogenesis, and the beginning of inflation. [Nature and Science. 2006;2(3):45-50].

### INTRODUCTION

The 5<sup>th</sup> dimension of the Randall-Sundrum brane world is of the genre, for  $-\pi \leq \theta \leq \pi$

$$x_5 \equiv R \cdot \theta$$

This lead to an additional embedding structure for typical GR fields, assuming as one may write up a scalar potential ‘field ‘with  $\phi_0(x)$  real valued, and the rest of it complex valued as:

$$\phi(x^\mu, \theta) = \frac{1}{\sqrt{2 \cdot \pi \cdot R}} \cdot \left\{ \phi_0(x) + \sum_{n=1}^{\infty} [\phi_n(x) \cdot \exp(i \cdot n \cdot \theta) + C.C.] \right\}$$

This scalar field makes its way to an action integral structure which will be discussed later on, which Sundrum used to forming an effective potential. Our claim in this analysis can also be used as a way of embedding a Bogomolnyi inequality reduced effective potential in this structure, with the magnitude of the Sundrum potential forming an initial condition for the second potential of the following phase transition .

$$\begin{aligned} \tilde{V}_1 &\rightarrow \tilde{V}_2 \\ \phi(\text{increase}) \leq 2 \cdot \pi &\rightarrow \phi(\text{decrease}) \leq 2 \cdot \pi \\ t \leq t_p &\rightarrow t \geq t_p + \delta \cdot t \end{aligned}$$

The potentials  $\tilde{V}_1$ , and  $\tilde{V}_2$  were described in terms of **S-S\*** di quark pairs nucleating and then contributing to a chaotic inflationary scalar potential system. Here,

$$m^4 \approx (1/100) \cdot M_P^4 \tag{1}$$

$$\tilde{V}_1(\phi) = \frac{M_P^4}{2} \cdot (1 - \cos(\phi)) + \frac{m^4}{2} \cdot (\phi - \phi^*)^2$$

$$\tilde{V}_2(\phi) \propto \frac{1}{2} \cdot (\phi - \phi_c)^2 \tag{2}$$

We should keep in mind that  $\phi_c$  in Eqn 3a is an equilibrium value of a true vacuum minimum of Eqn. 3a after tunneling. In the potential system given as Eqn, (3a) we see a steadily rising scalar field value which is consistent with the physics of Figure 1 . In the potential system given by Eqn. (3b) we see a reduction of the ‘height of a scalar field which is consistent with the chaotic inflationary potential overshoot phenomena We should note that  $\phi^*$  in Eq (3a) is a measure of the onset of quantum fluctuations. **Appendix I** is a discussion of Axion potentials which we claim is part of the contribution of the potential given in Eqn. (3a) Note that the tilt to the potential given in Eqn. (3a) is due to a quantum fluctuation. As explained by Guth for quadratic potentials<sup>2</sup>,

$$\phi^* \equiv \left( \frac{3}{16 \cdot \pi} \right)^{\frac{1}{4}} \cdot \frac{M_P^{\frac{3}{2}}}{m^{\frac{1}{2}}} \cdot M_P \rightarrow \left( \frac{3}{16 \cdot \pi} \right)^{\frac{1}{4}} \cdot \frac{1}{m^{\frac{1}{2}}} \quad - \partial_\mu \partial^\mu \phi + \frac{\partial_\theta^2}{R^2} \phi - m_5^2 \phi = K \cdot \frac{\delta(\theta)}{R} + K \cdot \frac{\delta(\theta - \pi)}{R} \quad (3c)$$

This in the context of the fluctuations having an upper bound of

$$\tilde{\phi} > \sqrt{\frac{60}{2 \cdot \pi}} M_P \approx 3.1 M_P \equiv 3.1$$

Here,  $\tilde{\phi} > \phi_C$ . Also, the fluctuations Guth had in mind were modeled via<sup>3</sup>

$$\phi \equiv \tilde{\phi} - \frac{m}{\sqrt{12 \cdot \pi \cdot G}} \cdot t$$

In the potential system given by Eqn. (3b) we see a reduction of the ‘height’ or magnitude of a scalar field which is consistent with the chaotic inflationary potential overshoot phenomena mentioned just above. This leads us to use the Randall-Sundrum effective potential, in tandem with tying in baryogenesis to the formation of chaotic inflation initial conditions for Eqn. (3b), with the Randall-Sundrum brane world effective potential delineating the end of the dominant role of di quarks, due to baryogenesis, and the beginning of inflation. The role of the Bogomolnyi inequality is to introduce, from a topological domain wall stand point a mechanism for the introduction of baryogenesis in early universe models, and the combination of that analysis, plus matching conditions with the Randall-Sundrum effective potential sets us up for chaotic inflation.

### How to form the Randall-Sundrum effective potential

The consequences of the fifth dimension mentioned in Eqn. (1) above show up in a simple warped compactification involving two branes, i.e. a Planck world brane, and an IR brane. This construction with the physics of this 5 dimensional system allow for solving the hierarchy problem of particle physics, and in addition permits us to investigate the following five dimensional action integral.

$$S_5 = \int d^4 x \cdot \int_{-\pi}^{\pi} d\theta \cdot R \cdot \left\{ \frac{1}{2} \cdot (\partial_M \phi)^2 - \frac{m_5^2}{2} \cdot \phi^2 - K \cdot \phi \cdot [\delta(x_5) + \delta(x_5 - \pi \cdot R)] \right\}$$

This integral, will lead to the following equation to solve.

Here, what is called  $m_5^2$  can be linked to Kalusa Klein ‘excitations’ via (for  $n > 0$ )

$$m_n^2 \equiv \frac{n^2}{R^2} + m_5^2 \quad (3d)$$

This is for a compactification scale, for  $m_5 \ll \frac{1}{R}$ , and after an ansatz of the following is used:

$$\phi \equiv A \cdot [\exp(m_5 \cdot R \cdot |\theta|) + \exp(m_5 \cdot R \cdot (\pi - |\theta|))]$$

We then obtain after a non trivial vacuum averaging

$$\langle \phi(x, \theta) \rangle = \Phi(\theta)$$

$$S_5 = - \int d^4 x \cdot V_{eff}(R_{phys}(x))$$

This is leading to an initial formulation of

$$V_{eff}(R_{phys}(x)) = \frac{K^2}{2 \cdot m_5} \cdot \frac{1 + \exp(m_5 \cdot \pi \cdot R_{phys}(x))}{1 - \exp(m_5 \cdot \pi \cdot R_{phys}(x))}$$

Now, if one is looking at an addition of a 2<sup>nd</sup> scalar term of opposite sign, but of equal magnitude

$$S_5 = - \int d^4 x \cdot V_{eff}(R_{phys}(x)) \rightarrow - \int d^4 x \cdot \tilde{V}_{eff}(R_{phys}(x))$$

This is for when we set up an effective Randall – Sundrum potential looking like

$$\tilde{V}_{eff}(R_{phys}(x)) = \frac{K^2}{2 \cdot m_5} \cdot \frac{1 + \exp(m_5 \cdot \pi \cdot R_{phys}(x))}{1 - \exp(m_5 \cdot \pi \cdot R_{phys}(x))} + \frac{\tilde{K}^2}{2 \cdot \tilde{m}_5} \cdot \frac{1 - \exp(\tilde{m}_5 \cdot \pi \cdot R_{phys}(x))}{1 + \exp(\tilde{m}_5 \cdot \pi \cdot R_{phys}(x))} \quad (4)$$

This above system has a meta stable vacuum for a given special value of  $R_{phys}(x)$  We will from now on use this as a ‘minimum’ to compare a similar action

integral for the potential system given by Eqn. (3) above.

**How to compare the Randall-Sundrum effective potential minimum with an effective potential minimum involving the potential of Eqn. (3) above**

A Randall – Sundrum effective potential, as outlined above would give a structure for embedding an earlier than axion potential structure which would be a primary candidate for an initial configuration of dark energy. This structure would by baryogenesis be shift to dark energy. The Sundrum effective potential at a critical value of  $R_{phys}(x)$  would be

$$\tilde{V}_{eff}(R_{phys}(x)) \approx \text{constant} + \frac{1}{2} \cdot (R_{phys}(x) - R_{critical})^2 \propto \tilde{V}_2(\tilde{\phi}) \propto \frac{1}{2} \cdot (\tilde{\phi} - \phi_C)^2$$

Let us now view a toy problem involving use of a S-S' pair which we may write as<sup>4</sup>

$$\phi \equiv \pi \cdot [\tanh b(x - x_a) + \tanh b(x_b - x)]$$

This is for a di quark pair along the lines given when looking at the first potential system.

Now for the question the paper is raising., Does a reduction of axion wall mass for the first potential system due to temperature dependence shed light upon the Wheeler De Witts equations<sup>5</sup> modification by Ashtekar<sup>6</sup> in a early universe quantum bounce ?

Kolb's book also gives a temperature dependence of axions which is<sup>7</sup>

$$m_{axion}(T) \cong .1 \cdot m_{axion}(T=0) \cdot (\Lambda_{QCD} / T)^{3.7}$$

We should note that  $\Lambda_{QCD}$  is the enormous value of the cosmological constant which is  $10^{120}$  larger than what it is observed to be today. However, if axions are involved in the formation of instaton physics for early universe nucleation, then Eqn. (14) tells us that as can be expected for very high initial temperatures that axions are without mass but exist as an energy construct. Does this process if it occurs lend then to the regime where there is a bridge between classical applications of the Wheeler De Witt equation to the quantum bounce condition raised by Ashtekar<sup>6</sup> ?

**Tie in with di quark potential systems, and the classical Wheeler De-Witt equation**

We previously found problems with previous calculations of the cosmological constant as seen in the current QCD calculations<sup>8</sup> which we believe are solved by the inclusion of temperature dependent behavior of the axion wall mass. In doing so, though, we now need to raise the question of a transition from a regime where the classical Wheeler De Witt equation holds, as in n=2 versions of scalar potential as shown by Eqn. (2b) above to where it breaks down, as shown by Abbay Ashtekar's quantum bounce discretized version of the same Wheeler De Witt equation. Let us first review classical De Witt theory which incidently ties in with inflationary n= 2 scalar potential field cosmology.

In the common versions of Wheeler De Witt theory a potential system using a scale radius  $R(t)$ , with  $R_0$  as a classical turning point value<sup>5</sup>

$$U(R) = \left( \frac{3 \cdot \pi \cdot c^3 \cdot R_0}{2 \cdot G} \right)^2 \cdot \left[ \left( \frac{R}{R_0} \right)^2 - \left( \frac{R}{R_0} \right)^4 \right] \tag{13a}$$

Here we have that

$$R_0 \sim c \cdot t_0 \equiv l_p \equiv c \cdot \sqrt{\frac{3}{\Lambda}} \sim 7.44 \times 10^{-36} \text{ meters}$$

As well as

$$\sqrt{\frac{3}{\Lambda}} \equiv t_p \sim 2.48 \times 10^{-44} \text{ sec}$$

This assumes in doing it that one is looking at a Hamiltonian system for a wave functional with  $\Psi(R)$  obeying a Hamiltonian system with energy set equal to zero, so

$$\hat{H} \cdot \Psi(R) = 0 \Rightarrow \left[ -\hbar^2 \cdot \frac{\partial^2}{\partial \cdot R^2} + U(R) \right] \cdot \Psi(R) = 0$$

Now, Alfredo B. Henriques<sup>9</sup> presents a way in which one can obtain a Wheeler De Witt equation based upon

$$\tilde{H} \cdot \Psi(\phi) = \left[ \frac{1}{2} \cdot (A_\mu \cdot p_\phi^2 + B_\mu \cdot m^2 \cdot \phi^2) \cdot \Psi(\phi) \right]$$

Using a momentum operator as give by

$$\hat{p}_i = -i \cdot \hbar \cdot \frac{\partial}{\partial \cdot \phi}$$

This is assuming a real scalar field  $\phi$  as well as a ‘scalar mass’  $m$  based upon a derivation originally given by Thieumann<sup>10</sup>. The above equation given by Theumann, and secondarily by Henriques<sup>9</sup> lead directly to considering the real scalar field  $\phi$  as leading to a prototype wave functional for the  $\phi^2$  potential term as given by

$$\psi_\mu(\phi) \equiv \psi_\mu \cdot \exp(\alpha_\mu \cdot \phi^2)$$

As well as an energy term

$$E_\mu = \sqrt{A_\mu \cdot B_\mu} \cdot m \cdot \hbar$$

$$\alpha_\mu = \sqrt{B_\mu / A_\mu} \cdot m \cdot \hbar$$

This is for a ‘cosmic’ Schrodinger equation as given by

$$\tilde{H} \cdot \psi_\mu(\phi) = E_\mu(\phi)$$

This has

$$A_\mu = \frac{4 \cdot m_{pl}}{9 \cdot l_{pl}^9} \cdot (V_{\mu+\mu_0}^{1/2} - V_{\mu-\mu_0}^{1/2})^6$$

And

$$B_\mu = \frac{m_{pl}}{l_{pl}^3} \cdot (V_\mu)$$

Here  $V_\mu$  is the eigenvalue of a so called volume operator<sup>6</sup>, and the interested readers are urged to consult with the cited paper to go into the details of this, while at the time noting  $m_{pl}$  is for Planck mass, and  $l_{pl}$  is for Planck length, and keep in mid that the main point made above, is that a potential operator based upon a quadratic term leads to a Gaussian wavefunctional with an exponential similarly dependent upon a quadratic  $\phi^2$  exponent. We do approximate solitons via the evolution of Eqn. (9), and so how we reconcile higher order potential terms in this approximation of wave functionals is extremely important.

Now Ashtekar in his arXIV article<sup>11</sup> make reference to a revision of this momentum operation along the lines of basis vectors  $|\mu\rangle$  by

$$\hat{p}_i |\mu\rangle = \frac{8 \cdot \pi \cdot \gamma \cdot l_{pl}^2}{6} \cdot \mu |\mu\rangle$$

With the advent of this re definition of momentum we are seeing what Ashtekar works with as a symplectic structure with a revision of the differential equation assumed in Wheeler – De Witt theory to a form characterized by<sup>11</sup>

$$\frac{\partial^2}{\partial \phi^2} \cdot \Psi \equiv - \Theta \cdot \Psi \tag{19}$$

$$\Theta \text{ in this situation is such that} \tag{19a}$$

$$\Theta \neq \Theta(\phi) \tag{19b}$$

Also, and more importantly this  $\Theta$  is a difference operator, allowing for a treatment of the scalar field as an ‘emergent time’, or ‘internal time’ so that one can set up a wave functional built about a Gaussian wavefunctional defined via

$$\max \tilde{\Psi}(k) = \tilde{\Psi}(k) \Big|_{k=k^*} \tag{19c}$$

$$\text{This is for a crucial ‘momentum’ value} \tag{19d}$$

$$p_\phi^* = - \left( \sqrt{16 \cdot \pi \cdot G \cdot \hbar^2 / 3} \right) \cdot k^*$$

And

$$\phi^* = -\sqrt{3/16 \cdot \pi G} \cdot \ln |\mu^*| + \phi_0 \tag{19e}$$

Which leads to, for an initial point in ‘trajectory space’ given by the following relation  $(\mu^*, \phi_0) =$  (initial degrees of freedom [dimensionless number]  $\sim$  eigenvalue of ‘momentum’, initial ‘emergent time’)

So that if we consider eigenfunctions of the De Witt (difference) operator, as contributing toward

$$e_k^s(\mu) = (1/\sqrt{2}) \cdot [e_k(\mu) + e_k(-\mu)]$$

With each  $e_k(\mu)$  an eigenfunction of Eqn. (12a) above, with eigenvalues of Eqn. (12a) above given by  $\omega(k)$ , we have a potentially numerically treatable

early universe wave functional data set which can be written as

$$\Psi(\mu, \phi) = \int_{-\infty}^{\infty} dk \cdot \tilde{\Psi}(k) \cdot e_k^s(\mu) \cdot \exp[i\omega(k) \cdot \phi]$$

This equation above has a ‘symmetry’ as seen in Figure 1 of Ashtekar’s PRL article ‘about  $\phi$ , reflecting upon a quantum bounce for a preceding universe prior to the ‘big bang’ contracting to the singularity and a ‘rebirth’ as seen by a different ‘branch of Eqn. (28b) emerging for a ‘growing’ set of values of  $\phi$ .

**Does the formation of temperature dependence of axion walls help delineate a regime where the Wheeler De Witt equation holds classically ?**

How does this relate to what was done in our earlier di quark modeling of dark energy? The following claim is made that a vanishing of the axion wall mass  $m_{axion}(T) \equiv .1 \cdot m_{axion}(T=0) \cdot (\Lambda_{QCD} / T)^{3.7} \xrightarrow{T \rightarrow \infty} \epsilon^+ \Rightarrow$  transition from the 1<sup>st</sup> to the 2<sup>nd</sup> potentials as given by Eqn. (3a) and Eqn. (3b) that one is seeing a collapse of the di quark contributions to the 1<sup>st</sup> potential in a transition given by Eqn. (3) to a potential scheme which is in some respects similar to the quadratic inflationary potential referred to by Henrique’s, which has a Gaussian wave functional. as given by Eqn. (9) In terms of phase evolution and change of potentials this would be similar to Eqn. (1) above. This would be in tandem with a cancellation of di quark contributions to Eqn. (2a) in which  $\phi_F$  is for the ‘false vacuum’ value of the scalar potential given in Eqn. (2a), and  $\phi_T$  is for finding the true minimum value of Eqn. (2a) so that<sup>6</sup> as seen in the condensed matter template given earlier where the change in a least action integral

$$\Psi \propto \exp(-\int dx_{space} d\tau_{Euclidian} L_E)$$

$$L_E \geq |Q| + \frac{1}{2} \cdot (\phi - \phi_0)^2 \{ \} \xrightarrow{Q \rightarrow 0} \frac{1}{2} \cdot (\phi - \phi_0)^2 \cdot \{ \}$$

Where

$$\{ \} = 2 \cdot \Delta \cdot E_{gap}$$

This leads, if done correctly to the quadratic sort of potential contribution as given by  $\psi_\mu(\phi) \equiv \psi_\mu \cdot \exp(\alpha_\mu \cdot \phi^2)$  in, At the same time it

raises the question of if or not when there is a change from the 1<sup>st</sup> to the 2<sup>nd</sup> potential system, if or not we can

still work with  $\psi_\mu(\phi) \equiv \psi_\mu \cdot \exp(\alpha_\mu \cdot \phi^2)$  in a general sense in the regime of quantum bounces. (22b)

**Conclusion**

We are presenting a question which may be of relevance to JDEM research. Namely if Ashtekar is correct in his quantum geometry<sup>6</sup>, and the break down of early universe conditions not permitting the typical application of the Wheeler De Witt equation, then what do we have to verify it experimentally? The axion wall dependence so indicated above may provide an answer to that, and may be experimentally measurable via Kadotas pixel reconstructive scheme.<sup>12</sup>

Furthermore, we also argue that the semi classical analysis of the initial potential system as given by Eqn (2) above and its subsequent collapse is de facto evidence for a phase transition to conditions allowing for dark energy to be created at the beginning of inflationary cosmology.<sup>13,14</sup> This builds upon an earlier paper done by Kolb in minimum conditions for reconstructing scalar potentials<sup>15,16,17,18</sup>. It also will necessitate reviewing other recent derivation bound to the cosmological constant in cosmology model in a more sophisticated manner than has been presently done<sup>19,20</sup>. In doing so, it may be appropriate to try to reconcile A. Ashtekar’s approach involving a discretization of the Wheeler De Witt equation with the bounce calculations in general cosmology pioneered by Hackworth and Weinberg<sup>21</sup>.

**APPENDIX I.**

**Forming an axion potential term as part of the contribution to Equation 2A**

Kolb’s book<sup>7</sup> has a discussion of an Axion potential given in his Eqn. (10.27) (23)

$$V(a) = m_a^2 \cdot (f_{PQ} / N)^2 \cdot (1 - \cos[a / (f_{PQ} / N)])$$

(23a)

Here, he has the mass of the Axion potential as given by  $m_a$  as well as a discussion of symmetry breaking which occurs with a temperature  $T \approx f_{PQ}$ . Furthermore, he states that the Axion goes to a massless regime for high temperatures, and becomes massive as the temperature drops. Due to the fact that Axions were cited by Zhitinisky in his QCD ball formation<sup>22</sup>, this is worth considering, and this potential is part of Eqn. (6a) with the added term giving a tilt to this potential system, (23b)

due to the role quantum fluctuations play in inflation. Here,  $N > 1$  leads to tipping of the wine bottle potential, and  $N$  degenerate CP-conserving minimal values. The interested reader is urged to consult section 10.3 of Kolb's Early universe book for details<sup>7</sup>.

### Correspondence to:

A. W. Beckwith

Email: [projectbeckwith2@yahoo.com](mailto:projectbeckwith2@yahoo.com)

PACS numbers: 03.75.Lm, 11.27.+d, 98.65.Dx, 98.80.Cq, 98.80.-k

### References

1. Guth. Ar XIV: astro-ph/0002156 v1 7 Feb 2000, A. Guth . arXIV :astro-ph/0002186 v1 8 Feb 2000, A. H. Guth, *Phys. Rev. D* 23, 347-356 (1981)
2. A.H. Guth, E. Weinberg, *Nucl. Phys.*, v. B212, p. 321, 1983.
3. A.W. Beckwith arXIV math-ph/0411045, 'A New Soliton-Anti Soliton Pair Creation Rate Expression Improving Upon Zener Curve Fitting for I-E Plots', Submitted to *Mod.Phys.Lett.B* to be published in June 2006 as author was notified in e mail from the editor of *Mod Phys Lett B*;
4. W. Beckwith , 'Making An Analogy Between a Multi-Chain Interaction in Charge Density Wave Transport and the Use of Wavefunctionals to Form S - S' Pairs'. Published in *Int.J.Mod.Phys.B*19:3683-3703,2005
5. A.W. Beckwith , An Open Question : Are Topological Arguments Helpful In Setting Initial Conditions For Transport Problems In Condensed Matter Physics ? , Published in *Mod.Phys.Lett.B*29:233-243,2006
6. M. Dalarsson, and N. Dalarsson,, *Tensors, Relativity, and Cosmology,* Elsevier press, 2005
7. Ashtekar, T. Pawlowiski, and P. Singh, ' Quantum nature of the big bang' Published in *P R.L.* 96, 121301 ( 2006 )
8. The Early universe, by E.W.Kolb, and M. S. Turner, Westview Press, 1990
9. Volovik, arXIV gr-qc/0604062 v2 16 April 2006 : ' *Vacuum Energies; Myths and Reality*'
10. arXIV gr-qc/0601134 'Loop quantum cosmology and the Wheeler-De Witt equation', by A B. Henriques Classical and quantum gravity **15** (1998), 1281 by T. Thieumann ; arXIV gr-qc / 9705019
11. A, Ashtekar, T. Pawlowski, P. Singh 'Quantum Nature of the Big Bang: An Analytical and Numerical Investigation I' arXIV gr-qc/0604013
12. K. Kadota, S. Dodelson, W. Hu, and E. D. Steward ;arXIV:astro-ph/0505185 v1 9 May 2005
13. The reader is referred to a white paper proposal for reconstruction of potentials from an algorithm devised by Kadota et al of FNALs astroparticle theoretical physics division, which the author myself, cited as being useful in data reconstruction of an appropriate early universe scalar potential system. This proposal was accepted as a legitimate inquiry for study by the DETF headed by Dr. Kolb as of June 23, 2000
14. A.W. Beckwith , arXIV gr-qc/0511081 , 'How S-S' Di Quark Pairs Signify an Einstein Constant Dominated Cosmology , and Lead to new Inflationary Cosmology Physics' ; Published in *Electron.J.Theor.Phys.*9:7-33,2006
15. E.W. Kolb. "Deducing the Value of the Cosmological Constant During Inflation from Present-Day Observations," in *The Cosmological Constant and the Evolution of the Universe*, K. Sato, T. Suginoara, and N. Sugiyama, eds., (Universal Academy Press, Tokyo), p. 169.
16. E.W. Kolb. "From the Big Bang to Now, and the Journey Back," *Proceedings of the 1995 Valencia Meeting on Dark Matter and the Universe*, J. W. Valle, ed., in press (1996).
17. E.W. Kolb. "The Inflation Potential from Present Day Observations," in *Trends in Astrophysics*, L. Bergstrom, P. Carlson, P. O. Huth, and H. Snellman, eds., (North-Holland, 1995), p. 118.
18. E.W. Kolb. "Lectures on Inflation," in the *Proceedings of the 1995 Varenna Summer School*, in press (1996)
19. E.W. Kolb. "Potential Reconstruction," in *Frontier Objects in Astrophysics and Particle Physics*, F. Giovannelli and G. Mannocchi, eds., (Editrice Compositori, Bologna, 1995) p. 3
20. G. Gurzadyan and She-Sheng Xue , *Modern Physics letters A* , Vol 18, No.8 ( 2003) pp. 561-568, ' *On The Estimation of the Current Value of the Cosmological constant*'
21. C. Hackworth and E.J. Weinberg arXIV hep-th/0410142 v21 12 Oct 2004 ' Oscillating bounce solutions and vacuum tunneling in de Sitter spacetime'
22. A.R. Zhitnisky, arXIV: astro-ph/0204218 v1 12 April 2002 Dark Matter as Dense Color Superconductor'

## Hydrocarbon Degrading Potentials of Bacteria Isolated from a Nigerian Bitumen (Tarsand) Deposit

Bola O. Oboh<sup>1</sup>, Matthew O. Ilori<sup>2\*</sup>, Joseph O. Akinyemi<sup>1</sup>, Sunday A. Adebuso<sup>2</sup>

<sup>1</sup>Department of Cell Biology and Genetics, University of Lagos, Akoka Yaba, Lagos, Nigeria

<sup>2</sup>Department of Botany and Microbiology, University of Lagos, Akoka Yaba, Lagos, Nigeria

**Abstract:** In an effort at developing active microbial strains that could be of relevance in bioremediation of petroleum contaminated systems in Nigeria, fifteen hydrocarbon degrading bacteria and fungal species were isolated from three bitumen deposits. The predominant species belonged to the genera *Pseudomonas* and *Aspergillus*. The ability of *Pseudomonas stutzeri*, *Pseudomonas mullei* and *Alcaligenes* sp. to degrade naphthalene, kerosene and diesel was studied. The results show maximal increase in optical densities and total viable counts concomitant with decrease in pH of the culture media. Typical generation times vary between 0.64 and 1.09 d, 0.97 and 3.03 d, 0.88 and 2.97 d respectively for kerosene, diesel and naphthalene. All the isolates utilized the hydrocarbons as sole carbon and energy sources equally well; there was no statistical difference ( $P > 0.05$ ) in the utilization rates, thus suggesting close genetic similarities in respect of oil degradation capabilities. The study revealed for the first time, the types of microorganisms that are associated with Nigerian bitumen deposit and their potential to degrade oil. The knowledge of the potentials of these isolates to degrade hydrocarbons will increase the possibilities of developing models and strategies for removing hydrocarbon pollutants from the environment. [Nature and Science. 2006;4(3):51-57].

**Keywords:** bacteria; bitumen; degrade; Nigerian; hydrocarbon

### Introduction

Tarsand is composed of sand, heavy oil and clays that are rich in minerals and water. The heavy oil in tarsand is called bitumen. Nigeria is richly endowed with many natural resources; the most important are crude oil, gas and bitumen. Of all the three natural resources, only the crude oil has been well developed and it contributes about 90 % of the country's foreign earnings (Adegoke et al., 1991). The Nigerian bitumen belt lies on the onshore areas of the Eastern Dahomey (Benin) Basin. The probable reserve of bitumen and heavy oil in the entire Nigerian belt is about 120 x 4.3 Km (Adegoke and Ibe, 1982).

The clay content of the Nigerian deposit is very low averaging about 5 % and heavy oil extracted from the deposits has an API gravity ranging between 5.00° and 14.6°. Physical properties reported include softening point (44 -52 °C), ductility (0.1 – 1.3 mm), penetration (80 – 100 mm), hydrocarbon content (7.2 % by wt - 18.2 % by wt), resins (32.12 % by wt - 34.0 % by wt) and sulphur (5.00 ppm to 10.00 ppm). Furthermore, the Nigerian bitumen possesses relatively large quantity of naphthenes, aromatics and asphaltenes that are similar to the conventional oil. This makes the Nigerian bitumen a very useful alternative source of petroleum hydrocarbon and a potential feedstock for petrochemical industries (Adegoke et al., 1991).

The high demand for petroleum and associated products during the last ten decades has made petroleum spills inevitable consequences of oil production and refining. Despite fluctuations in its prices, oil will remain a major source of energy in the next several decades because a reliable alternative has not yet been found. As a result, the problem of pollution during production and transportation of oil would remain a major issue. Microbial degradation appears to be the most environmentally friendly method of removal of oil pollutant since other methods such as surfactant washing and incineration lead to introduction of more toxic compounds to the environment. Hydrocarbon-degrading microorganisms are widely distributed in marine, freshwater, and soil ecosystems (Atlas and Bartha, 1973). The ability to isolate high numbers of certain oil-degrading microorganisms from an environment is commonly taken as an evidence that those organisms are the active degraders of that environment (Okerentugba and Ezeronye, 2003). Although, hydrocarbon degraders may be expected to be readily isolated from a petroleum-polluted environment, the same degree of expectation may be anticipated for microorganisms isolated from a total unrelated environment. There is an extensive body of knowledge on mineralization or degradation of hydrocarbons by microorganisms (Ojomu et al., 2005; Adenipekun and Fasidi, 2005). Most of these organisms, majority of

which are bacteria have been characterized and classified using cultural, biochemical and molecular techniques. Bacteria have evolved millions of years ago regulatory systems that ensure the synthesis of enzymes so that the initial attack on these compounds is induced only when required.

In a recent study, Ojo (2006) reported the capability of native bacterial population to mineralize petroleum hydrocarbons in wastewater. Similarly, Okoh (2003) demonstrated degradation rates of different strains of *Pseudomonas aeruginosa* on crude oil with evidence of significant reduction of major peak components of the oil. The organisms also showed multiple antibiotic resistance thus, the authors concluded that this could be an important factor to consider in their eventual use in bioremediation program. Virtually all of these studies utilized organisms isolated from petroleum contaminated sites and degradation competencies were only tested on crude oil. In this report however, we chose to isolate hydrocarbon degraders from bitumen deposits in Nigeria. Degradation potentials of the obtained isolates were not only demonstrated on crude oil, and petroleum feedstocks including kerosene, and diesel but naphthalene which is usually less degradable compared to the petroleum fractions. The results from this investigation would be useful for the prediction of the bioremediation mechanisms of these microbial isolates.

## Materials and Methods

### Chemicals

Escaros blend crude oil, petroleum feedstocks including kerosene and diesel obtained were all obtained from Chevron (Nigeria) Limited. Naphthalene was provided by the Department of Botany and Microbiology, University of Lagos.

### Collection of bitumen and soil samples

The bitumen used was obtained from three different communities namely, Agbabu, Ilubirin and Mile 2, all in Odigbo Local Government Area of Ondo State, Nigeria. Three sets of samples were collected from these locations i) "core bitumen" represented bitumen samples seeping out directly from installation pipes; ii) "surface bitumen" represented bitumen samples collected from surfaces of installed pipes and; iii) "control samples" represented relatively undisturbed soils in the vicinities of these sampling stations. All samples were collected in two replicates and treated immediately.

### Isolation and characterization of hydrocarbon-degrading microorganisms

The bacterial species indigenous to the bitumen and soil samples were isolated by spread plate technique using 0.1 ml aliquots of appropriate dilution into

nutrient agar slants. Individual cultures were identified by morphological and biochemical techniques using the taxonomic scheme of Bergey's Manual of Determinative Bacteriology (Holt et al., 1994).

The fungi species were also isolated from the samples in similar manner to bacteria but using potato dextrose agar (PDA) into which streptomycin (50 mg/ml) has been added to suppress bacterial growth. The microscopic and macroscopic features of the hyphal mass, morphology of cells and spores, nature of the fruiting bodies among other criteria were used for identification.

The obtained cultures of bacteria and fungi were screened for hydrocarbon utilization using crude oil as model substrate.

### Growth of bacterial isolates on hydrocarbon substrate

Time-course degradation of kerosene, diesel and naphthalene was performed in mineral salts medium previously described by Mills et al. (1978). The medium was dispensed in 99 ml quantities into 250 ml Erlenmeyer flasks. Each flask was supplemented with 1 ml or 1 g as the case may be of selected carbon source and seeded with axenic cultures of isolates. The flasks were cultivated in a gyratory shaker incubator programmed at 120 rpm and 30 °C. The optical density (OD<sub>600nm</sub>), total viable count (TVC) and pH of the culture fluids were monitored at determined time intervals as biodegradation indices.

## Results and Discussion

The morphological and biochemical characterization of the bacterial isolates obtained from the different sites revealed the following genera: *Pseudomonas*, *Bacillus*, *Alcaligenes* and *Citrobacter*. All the isolates were motile, rod-shaped and Gram-negative with the exception of *Bacillus subtilis*. Most were indole-negative, urea and citrate utilizers. Majority of the organisms were isolated from the core bitumen while the predominant species were mainly *Pseudomonas* (Table 1). The fungi isolates were mainly *Aspergillus* species. Others were *Trichoderma*, *Penicillium*, *Rhizopus* and *Rhodotorula* species (Table 1). All of these isolates were able to grow on crude petroleum as the sole source of carbon and energy when screened for hydrocarbon utilization. Interestingly, this same group of organisms have been implicated in hydrocarbon degradation, particularly *Pseudomonas* and *Alcaligenes* by several workers (Amund and Adebiji, 1991; Atlas, 1992; Nwachukwu and Ugoji, 1995; Nwachukwu, 2001).

Figures 1-3 show the degradation potentials of *Pseudomonas stutzeri*, *P. mullei* and *Alcaligenes* sp. on petroleum cuts and naphthalene under aerobic batch conditions. The growth dynamics of the organisms was



determined by the optical densities, total viable counts and the pH of the culture media. Our results showed that the isolates grew maximally on the four hydrocarbon substrates when supplied as the sole source of carbon and energy. The growth profiles showed that none of the bacterial isolates exhibited lag phases. This observation has been reported previously (Amund, 1984; Okerentugba and Ezeronye, 2003), and can be attributed to genetic make up due to the constitutive expression of hydrocarbon catalysing enzymes or physiological owing to previous exposure to exogenous hydrocarbons present in the bitumen deposits. Typical doubling times and specific growth rates on diesel ranged from 0.97 – 3.05 d and 0.23 – 0.71 d<sup>-1</sup> respectively (Table 2).

The utilization of the hydrocarbons resulted in increase in cell densities with a concomitant visual gradual reduction in the oil layer and complete disappearance of the oil with prolonged incubation. The reduction in pH of the culture fluids in the experimental flasks within the 8-day incubation period further confirmed chemical changes of the hydrocarbon substrates which must have been precipitated by microbial enzymes (Atlas and Bartha, 1972). Microbial degradation of hydrocarbons often leads to production of organic acids and other metabolic products (Nwachukwu and Ugoji, 1995; Okpokwasili and James, 1995). Thus, the acids probably produced account for the reduction in pH levels.

Of particular significance was the growth data obtained on naphthalene, an aromatic hydrocarbon that is relatively recalcitrant to aerobic degradation (Table 2). These values are comparable to those obtained for kerosene and diesel. It would appear that these organisms have aromatic degradation capabilities and could be relied upon for the destruction of both alkane and aromatic components inherent in crude petroleum.

On the basis of the growth data, we could infer that kerosene was slightly preferred by the isolates contrary to the reports of Amanchukwu et al. (1989) and Okpokwasili and James (1995). However, statistical analysis showed no significant difference ( $P > 0.05$ ) in the degradation competence of the isolates on the four hydrocarbon substrates, thus suggesting possession of similar catabolic properties. This observation also confirmed the close genetic similarities of isolates in respect of oil degradation capabilities particularly of the *Pseudomonas* strains.

It is evident from this investigation that oil degrading microorganisms could readily be isolated from bitumen deposits without the need for time consuming traditional enrichment protocols. Further understanding of the metabolic process of these organisms on the hydrocarbons will increase possibilities of developing models and strategies for removing hydrocarbon pollutants from oil impacted environment.

Table 1. Hydrocarbon-utilizing microbial species isolated from various samples

<b>ISOLATES</b>	<b>Source</b>
<i>Pseudomonas stutzeri</i>	Core
<i>Pseudomonas putida</i>	Core
<i>Pseudomonas mellei</i>	Surface, core
<i>Bacillus subtilis</i>	Surface, core
<i>Alcaligene sp.</i>	Surface, core
<i>Aspergillus fumigatus</i>	Surface, soil
<i>Aspergillus oryzae</i>	Surface
<i>Aspergillus wentii</i>	Soil
<i>Aspergillus flavus</i>	Soil
<i>Aspergillus niger</i>	Core, surface
<i>Trichodema sp.</i>	Core
<i>Penicillium notatum</i>	Core, surface, soil
<i>Rhizopus stolonifer</i>	Surface
<i>Rhodotorula sp.</i>	Core

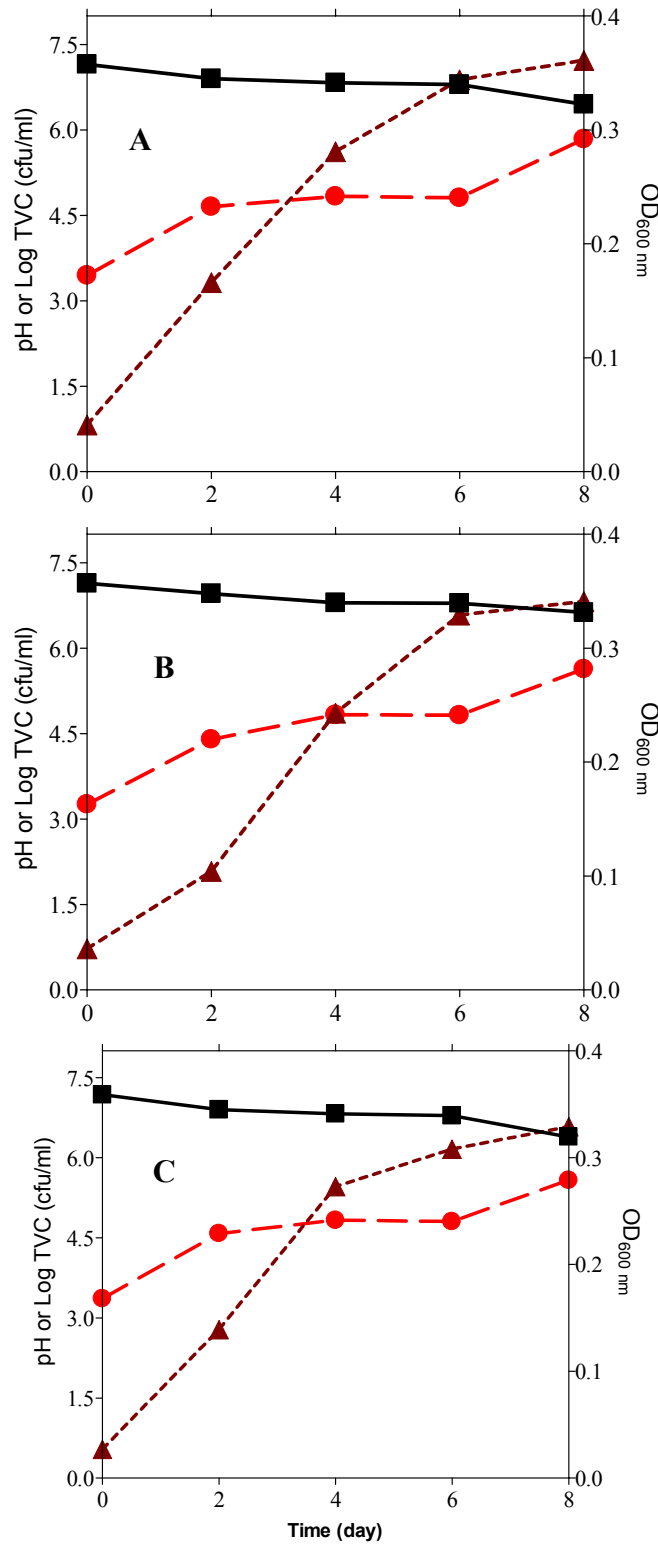


Figure 1. Growth Profiles of *Pseudomonas stutzeri* (A), *Pseudomonas mellei* (B) and *Alcaligenes* sp. on Kerosene. ●, Log TVC (cfu/ml); ▲, OD<sub>600nm</sub>; ■, pH of culture fluids.

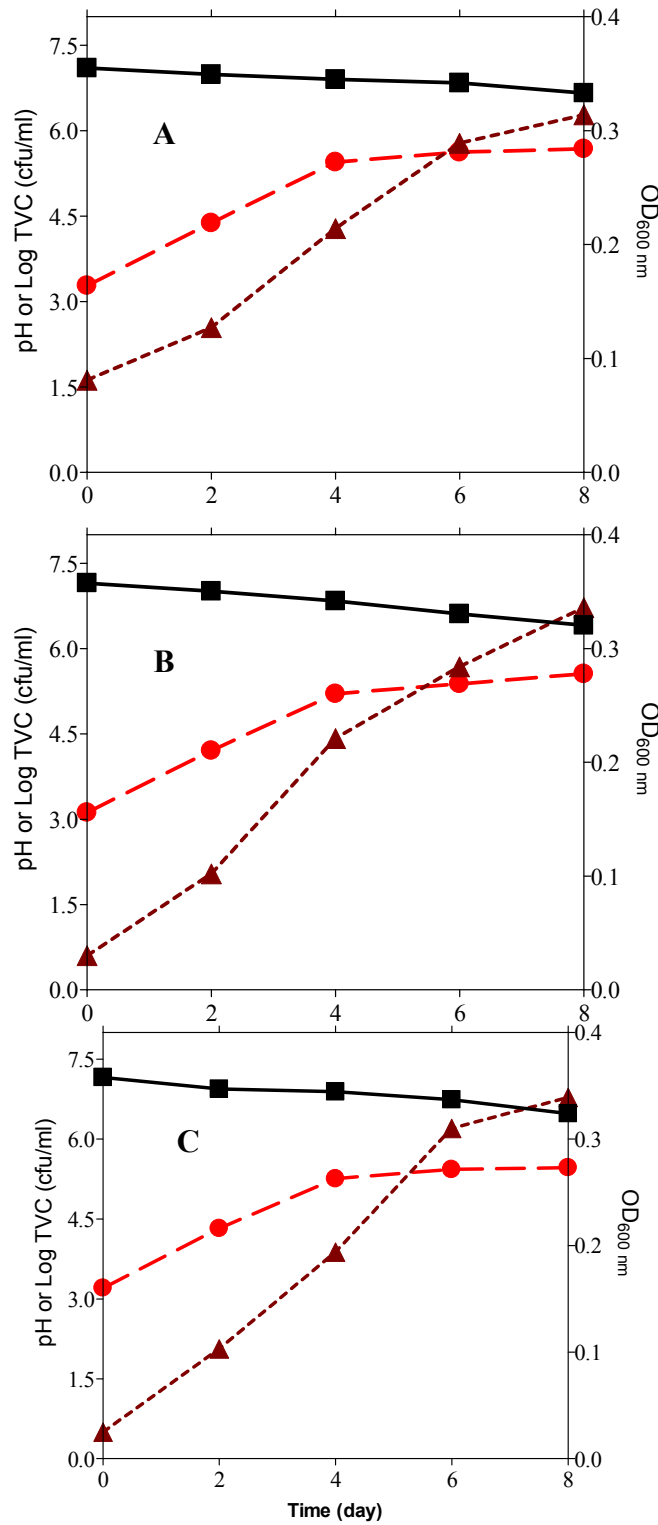


Figure 2. Growth Profiles of *Pseudomonas stutzeri* (A), *Pseudomonas mellei* (B) and *Alcaligenes* sp. on Diesel. ●, Log TVC (cfu/ml); ▲, OD<sub>600nm</sub>; ■, pH of culture fluids.

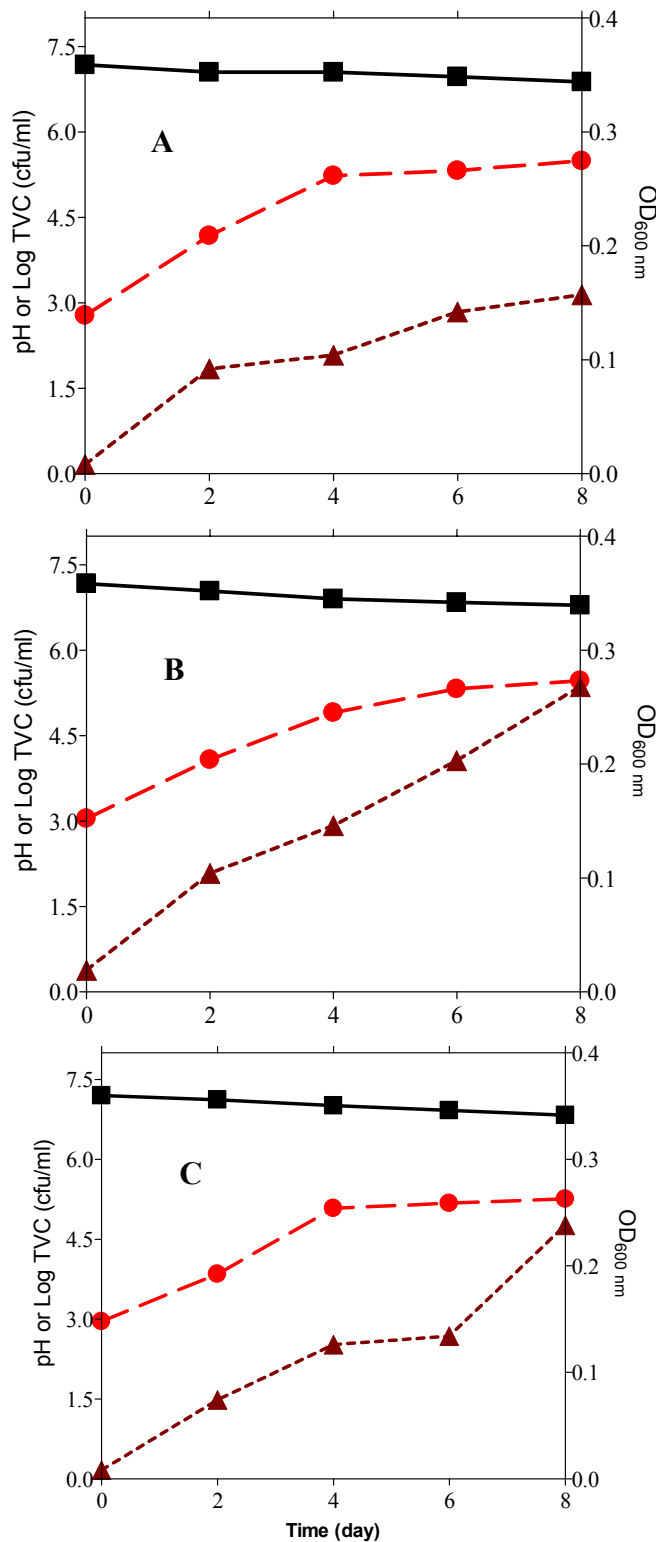


Figure 3. Growth Profiles of *Pseudomonas stutzeri* (A), *Pseudomonas mellei* (B) and *Alcaligenes* sp. on Naphthalene. ●, Log TVC (cfu/ml); ▲, OD<sub>600nm</sub>; ■, pH of culture fluids.

Table 2. Growth potentials of hydrocarbon-utilizing bacteria

Isolate	Kerosene		Diesel		Naphthalene	
	$\mu$ (d <sup>-1</sup> ) <sup>a</sup>	Tg (d) <sup>b</sup>	$\mu$ (d <sup>-1</sup> ) <sup>a</sup>	Tg (d) <sup>b</sup>	$\mu$ (d <sup>-1</sup> ) <sup>a</sup>	Tg (d) <sup>b</sup>
<i>Pseudomonas stutzeri</i>	1.08	0.64	0.24	2.91	0.79	0.88
<i>Pseudomonas putida</i>	0.79	0.88	0.3	2.34	0.25	2.76
<i>Pseudomonas mullei</i>	0.68	1.02	0.71	0.97	0.71	0.98
<i>Bacillus subtilis</i>	0.67	1.03	0.23	3.05	0.23	2.96
<i>Alcaligenes</i> sp.	0.64	1.09	0.23	3.03	0.23	2.97

<sup>a</sup>specific growth rate, <sup>b</sup>mean generation time

#### Correspondence to:

Dr. Matthew O. Ilori

Department of Botany and Microbiology

University of Lagos

Akoka, Yaba, Lagos, Nigeria

Phone: (234)-8023195170

E-mail: [olusojiilor@yahoo.com](mailto:olusojiilor@yahoo.com)

#### References

- Adegoke OS, Ibe EC. The Tar sand and heavy crude resources of Nigeria. Proc. 2<sup>nd</sup> Intern. Conf. on heavy crude and Tar sands. Caracas, Venezuela, Ch. 1982; 32:280-285.
- Adegoke OS, Omatsola ME, Coker JL. The geology of the Nigerian Tar-sands. In: Heavy Crude and Tarsands Hydrocarbons for the 21<sup>st</sup> Century. Proc. 5<sup>th</sup> UNITAR Intern. Conf. on Heavy Crude and Tar Sands. 1991:369-835.
- Adenipekun CO, Fasidi IO. Bioremediation of oil-polluted soil by *Lentinus subnudus*, a Nigerian white-rot fungus. Afr J Biotechnol 2005;4(8): 796-798.
- Amanchukwu SC, Obafemi A, Okpokwasili GC. Hydrocarbon degradation and utilization by a palm-wine yeast isolate. FEMS Microbiol Lett 1989;57: 151-154.
- Amund OO, Adebisi AG. Effect of viscosity on the biodegradability of automotive lubricating oils. Tribol Intern 1991;24: 235-237.
- Atlas RM, Bartha R. Degradation and mineralization of petroleum by two bacteria isolated from coastal waters. Biotechnol Bioeng 1972;14: 297-308
- Atlas RM. Petroleum microbiology. In: Encyclopedia of Microbiology. Baltimore, USA: Academic Press. 1992: 363-369.
- Atlas RM, Bartha R. Abundance, distribution and oil degradation potential of microorganisms in Raritan Bay. Environ Pollut 1973;4: 291-300.
- Holt JG, Krieg NR, Sneath PHA, Stanley JT, William ST. Bergey's Manual of Determinative Bacteriology. Baltimore, USA: William and Wilkins. 1994.
- Mills AL, Breuil C, Colwell RR. Enumeration of petroleum-degrading marine and estuarine microorganisms by the most probable number method. Canad J Microbiol 1978;24: 552-557.
- Nwachukwu SU, Ugoji EO. Impacts of crude petroleum spills on microbial communities of tropical soils. Intern J Ecol Environ Sci 1995;21: 169-176.
- Nwachukwu SCU. Bioremediation of sterile agricultural soils polluted with crude petroleum by application of the soil bacterium, *Pseudomonas putida*, with inorganic nutrient supplementations. Curr Microbiol 2001;42(2):231-236.
- Okerentugba PO, Ezeronye OU. Petroleum degrading potentials of single and mixed microbial cultures isolated from rivers and refinery effluent in Nigeria. Afr J Biotechnol 2003;2:288-292.
- Ojo OA. Petroleum-hydrocarbon utilization by native bacterial population from a wastewater canal Southwest Nigeria. Afr J Biotechnol 2006;5(4): 333-337.
- Ojumu TV, Bello OO, Sonibare JA, Solomon BO. Evaluation of microbial systems for bioremediation of petroleum refinery effluent in Nigeria. Afr J Biotechnol 2005;4(1): 31-35.
- Okpokwasili GC, James WA. Microbial contamination of kerosene, gasoline, and crude oil and their spoilage potentials. Material u Organismen 1995;29:147-156.
- Okoh AI. Biodegradation of Bonny light crude oil in soil microcosms by some bacterial strains isolated from crude oil flow stations saver pits in Nigeria. Afr J Biotechnol (2003);2(5):104-108.

## Physiological and Biochemical Studies of $\beta$ -Carotene on Thrombosis and Thrombosis

Kuan-Jiunn Shieh, Mei-Ying Chuang

Department of Chemistry, Chinese Military Academy, Fengshan, Kaohsiung, Taiwan 830, ROC,  
[chemistry0220@gmail.com](mailto:chemistry0220@gmail.com), 011-886-7742-9442

**Abstract:**  $\beta$ -Carotene is one of antioxidant micronutrients that can be favorably manipulated without side effects. Basic research provides a plausible mechanism by which antioxidant is associated with reducing the risk of atherosclerosis. The purpose of this study was to understand better the effects of  $\beta$ -carotene on atherosclerosis and thrombosis by using the atherosclerotic rabbit model. Twenty-four New Zealand White rabbits were divided into 4 groups: normal rabbits as control-control (Group I, n=4); atherosclerosis, non-thrombus triggered and non- $\beta$ -carotene treatment as control (Group II, n=4); atherosclerosis, thrombus triggered by Russell's viper venom and histamine but non- $\beta$ -carotene treatment (Group III, n=8); atherosclerosis, thrombus triggering and  $\beta$ -carotene (30 mg/kg, i.v.) treatment (Group IV, n=8). Atherosclerosis was induced by a balloon surgery with feeding a high cholesterol diet (1%). After rabbits were sacrificed isolated carotid arteries were placed in a dual perfusion chamber and tissues were kept in liquid nitrogen for biochemical measurements. Both carotid arteries from each rabbit were perfused with oxygenated physiologic buffered solution at 37°C and 60 mmHg. Baseline vasodilation was determined using norepinephrine (NE,  $1 \times 10^{-6}$  M) precontraction, and pharmacological challenge was performed with acetylcholine (Ach,  $1 \times 10^{-5}$  M) and sodium nitroprusside (SN,  $1 \times 10^{-5}$  M). Vessel diameter was measured by a computer planimetry system. Metallothionein, glucose, protein and glucose-6-phosphatase in the tissues and serum were measured after the rabbits were sacrificed.  $\beta$ -Carotene reduced thrombosis triggering. The vasodilation activity of artery responded to norepinephrine, acetylcholine and sodium nitroprusside was Group I>Group II>Group IV>Group III (inter-group ratio of the arterial vasodilation after pharmacological challenge was 1.2-3.5,  $p < 0.01-0.05$ ).  $\beta$ -Carotene reduced liver, kidney and heart metallothionein content of atherosclerotic rabbits. Group III had higher serum glucose content than Group IV. There was no significant difference of glucose and protein content in aorta arteries among 4 groups.  $\beta$ -Carotene has potential pharmacological effects on atherosclerotic animal. [Nature and Science. 2006;4(3):58-64].

**Keywords:** atherosclerosis;  $\beta$ -carotene; thrombosis; vasoconstriction

**Abbreviation:** Ach: acetylcholine; EDTA: ethylenediamine-tetraacetic acid; G-6-Pase: glucose-6-phosphatase; LDL: low-density lipoproteins; MT: metallothionein; NE: norepinephrine; PBS: physiologic buffered saline solution; RVV: Russell's viper venom; SEM: scanning electron microscopy; SN: sodium nitroprusside; TEM: transmission electron microscopy

### 1. Introduction

The model of plaque disruption and thrombosis developed by Constantinides et al in the early sixties was based on simulating the conditions often thought to be the main triggers for acute cardiovascular events (Constantinides, 1981). These include a hypercoagulable state and vasospasm. Based on this hypothesis various agents were tested independently and in combination to achieve a disrupted plaque with a superimposed platelet rich thrombus overlying a disrupted plaque. These included epinephrine and vasopressin etc. However, the best combination includes histamine, a vasoconstrictor agent in rabbits and Russell's viper venom (RVV), an activator of the coagulation Factors Va and Xa. Each alone could not produce a significant number of events but in combination resulted in about 72% event rate (Hung,

2002). The original model called for a two-year preparation by feeding rabbits a high cholesterol diet alternating with a normal diet. This double lipemic exposure approach seemed to create a lesion similar to that seen in humans, a lipid rich core with a fibrous cap. At the end of this period, RVV and histamine were given at 48 and 24 hours prior to sacrifice to induce a trigger for plaque disruption and thrombosis. A modification of the model was made by endothelial debridement to accelerate the atherosclerotic process as described by Baumgartner et al (2000). Using this approach it was possible to prepare the rabbits within a 6 months period and maintain the same event rate demonstrated by Constantinides (1989). Because it is not entirely clear what effects the triggering has on the vasomotor function in this model, we tested arteries by pharmacological challenges in a dual organ chamber.  $\beta$ -

Carotene is one of antioxidant micronutrients that can be favorably manipulated without side effects. Basic research provides a plausible mechanism by which antioxidant is associated with reducing the risk of atherosclerosis. To understand better the effects of  $\beta$ -carotene on atherosclerosis and thrombosis, we used  $\beta$ -carotene on the atherosclerotic rabbit model to try and see if it could change the event rate and alter the vasomotor function.

## 2. Materials and Methods

### 2.1 Study Groups

Twenty-four, male, New Zealand White rabbits weighing between 2.5 to 3.2 kg were divided into 4 groups (Table 1). The method of establishing the atherosclerotic rabbit model and thrombus triggering were described previously.

### 2.2 Atherosclerosis Inducing

Briefly, the control-control group (Group I) consisted of four normal white rabbits that were fed a regular diet for 6 months. Rabbits in Groups II, III and IV (n= 4, 8 and 8, respectively) underwent balloon deendothelialization and were then maintained on a 1% cholesterol enriched diet alternating with regular diet every month for a total of 6 months. Under general anesthesia (ketamine 50 mg/kg and xylazine 20 mg/kg, i.m.) balloon-induced deendothelialization of the aorta was performed using a 4F Fogarty arterial embolectomy catheter introduced through the right femoral artery cutdown. The catheter was advanced in a retrograde fashion to the ascending aorta and pulled back three times.

### 2.3 Pharmacological Triggering

Only the atherosclerotic rabbits (Groups II, III and IV) had pharmacological triggering since previous studies have not shown thrombosis to occur in normal arteries. Thrombus triggering was induced by RVV (0.15 mg/kg, i.p., Sigma Chemical Co., St. Louis, MO, USA) and histamine (0.02 mg/kg, i.v., 30 min after RVV, Sigma Chemical Co., St. Louis, MO, USA) given at 48 and 24 hours prior sacrifice. In Group IV,  $\beta$ -carotene (30 mg/kg, i.v., BASF Corporation, Mount Olive, NJ, USA) given 8 days prior to sacrifice. Heparin sulfate (1000 IU/rabbit, i.v., Sigma Chemical Co., St. Louis, MO, USA) was given 30 min prior to sacrifice to prevent postmortem clotting. Rabbits were sacrificed with an overdose i.v. injection of pentobarbital (Abbot Laboratories, North Chicago, IL, USA). Tissue samples from the heart, liver and kidney were stored immediately in liquid nitrogen until biochemical measurements.

### 2.4 Quantitation of Thrombosis

The total surface area of the aorta, the surface area of aorta covered with atherosclerotic plaque and the surface area of aorta covered with *ante mortem* thrombus were measured. The surface area was measured from images obtained by a digital camera. The digitized images were calibrated by use of a graticule. Surface area was measured by use of a customized quantitative image analysis package. Also, the number of thrombi on the aortic arch to the distal common iliac branches was counted.

### 2.5 Artery Diameter Respond Evaluation

After rabbits were sacrificed both carotid arteries were isolated from each rabbit and placed in a dual organ chamber and perfused with oxygenated physiologic buffered solution (PBS) (NaCl 119 mM, KCl 4.7 mM, CaCl<sub>2</sub> 2 mM, NaH<sub>2</sub>PO<sub>4</sub> 1.2 mM, MgSO<sub>4</sub> 1.2 mM, NaHCO<sub>3</sub> 22.6 mM, glucose 11.1 mM and Na<sub>2</sub>EDTA 0.03 mM) at 60 mmHg and 2.5 ml/minute flow rate at 37°C. Baseline vasodilation was determined using norepinephrine (NE,  $1 \times 10^{-6}$  M) precontraction and pharmacological challenge was then performed with acetylcholine (Ach,  $1 \times 10^{-5}$  M) and sodium nitroprusside (SN,  $1 \times 10^{-5}$  M) successively. Vessel diameter was measured by a computer planimetry system (Figure 1). The data were calculated according to the formulas: Ach-NE (%)=(Ach-NE)/NE $\times$ 100 and SN-NE (%)=(SN-NE)/NE $\times$ 100 separately, where Ach, NE and SN represented the diameter (mm) of the arteries that were perfused by the PBS containing a corresponding chemical.

### 2.6 Metallothionein (MT)

Metallothionein concentration as an index of oxidation was measured with Cd-hemoglobin saturation method (Eaton, 1991). Tissues were removed and rinsed in ice-cold Tris-HCl buffer (0.05 M, pH 8.6) then homogenized in 3 volume of the Tris-HCl buffer. The homogenate was centrifuged at 8,000 $\times$ g for 10 minutes at 4°C and the supernatant fraction was heated for 90 seconds at 100°C. The heated samples were centrifuged at 8,000 $\times$ g for 5 minutes at 4°C to remove precipitates. 100  $\mu$ l of 400 ppm CdCl<sub>2</sub> solution was added into 200  $\mu$ l of the supernatant and allowed to incubate at room temperature for 10 minutes. 150  $\mu$ l of 2% bovine hemoglobin solution (w/v) was added into the sample, then the sample was mixed and heated in boiling water for 2 minutes. The boiled samples were placed in ice for 3 minutes and centrifuged at 8,000 $\times$ g for 5 minutes at 4°C. Another 150  $\mu$ l of 2% hemoglobin was added into the supernatant, then heating, cooling and centrifuging were repeated, and the supernatant was collected. The Cd concentration in the supernatant was measured using a flame atomic absorption equipment and MT

concentration was calculated from the Cd concentration measured in the supernatant (1 mg Cd represented 8.93 mg MT).

### 2.7 Glucose-6-phosphatase (G-6-Pase)

G-6-Pase measurement was followed Harper method (Harper, 1965). Briefly, 0.1 ml of tissue homogenate (100 mg tissue/ml) in citrate buffer (0.1 M, pH 6.5) was added into a test tube and incubated at 37°C for 5 minutes. 0.1 ml of glucose-6-phosphate (0.08 M) was added and the sample was incubated at 37°C for 5 minutes, then 5 ml of trichloroacetic acid (10%, w/v) was added and centrifuged at 9,000 $\times$ g at 4°C for 5 minutes. 1 ml of the supernatant was taken into a test tube and 5 ml of ammonium molybdate solution (2 mM) then 1 ml of reducing solution (42 mM 1-amino-2-naphthol-4-sulphonic acid, 560 mM SO<sub>3</sub>) was added. The sample was incubated at room temperature for 30 minutes then absorption was measured at 660 nm.

### 2.8 Glucose Concentration

Sigma Glucose Diagnostic Kit (Sigma Chemical Co., St. Louis, MO, USA) was used. The method of the instruction by Sigma was followed for this evaluation.

### 2.9 Light and Electron Microscopy

Arterial tissue specimen were examined with light and electron microscope.

### 2.10 Statistical Analysis

With Jandel Scientific program, SigmaStat (Sigma Chemical Co., St. Louis, MO, USA) was used for data statistical analysis.  $P < 0.05$  was considered statistically significant difference. Measured data were reported as mean $\pm$ SD. The student t-test was used for comparison.

## 3. Results

### 3.1 Aorta

The measurement results of the rabbit aortas are showed in Table 2. The average surface area of aorta of the four groups was 1660 $\pm$ 257 mm<sup>2</sup>. There was no significant difference for surface area of aorta within the four groups (Table 2).

All the rabbits that were fed a 1% cholesterol diet and underwent endothelial debridement had visible diffuse atherosclerosis. Half of triggered rabbits developed thrombosis. The ratio of the thrombus surface area on the aorta in Group III rabbits to that on the aorta in Group IV rabbits was 1.56 (78.6 $\pm$ 38.9 vs 50.3 $\pm$ 25.9,  $p < 0.05$ ). Group II rabbits developed atherosclerosis, but no thrombus because rabbits of this group had no thrombus triggering by RVV and histamine. Table 2 also showed that the number of thrombi in Group III rabbits was two times as that in  $\beta$ -carotene treatment

rabbits (Group IV) (5.0 $\pm$ 4.3 vs 2.3 $\pm$ 1.3,  $p < 0.05$ ). Group I rabbits got neither atherosclerosis nor thrombus.

The average of glucose and protein content in aorta of the 4 rabbit groups were 1.3 $\pm$ 0.3 mg/g and 10.1 $\pm$ 0.8 mg/g respectively. There were no significant difference for glucose and protein content among the 4 rabbit groups (Table 2).

### 3.2 Artery Diameter

In this experiment, the contraction diameter of rabbit left and right carotid arteries using NE precontraction and pharmacological challenge with Ach and SN were measured (Table 3). There was no significant difference between left and right carotid arteries. The data in Table 3 were the average of left and right carotid arteries.

The vasodilation range of pharmacological challenge with Ach and SN to NE was 10-40% and it represented the following order: Group I > Group II > Group IV > Group III. Inter-group ratios of the arterial vasodilation after pharmacological challenge were 1.2 to 3.5 for Ach-NE ( $p < 0.005$  to  $p < 0.05$ ) and 1.1 to 3.2 for SN-NE ( $p < 0.01$  to  $p < 0.05$ ) (Table 3).

### 3.3 Metallothionein (MT)

MT in liver, kidney and heart tissues of Group III rabbits was significantly higher than that in Group I (ratios were: liver 3.3,  $p < 0.03$ ; kidney 4.3,  $p < 0.02$ ; heart 8.9,  $p < 0.05$ ), Group II (ratios were: liver 1.9,  $p < 0.05$ ; kidney 1.6,  $p < 0.05$ ; heart 1.6,  $p < 0.05$ ) and Group IV (ratios were: liver 2.5,  $p < 0.03$ ; kidney 1.3,  $p < 0.05$ ; heart 2.2,  $p < 0.05$ ) rabbits. There were no significant differences for MT content among the 4 groups in aorta, carotid and femoral arteries (Table 4).

### 3.4 Glucose, Protein, Glucose-6-phosphatase (G-6-Pase) and Lipid-liver

The results of glucose in the blood, total protein in the blood and in liver tissue, the activity of G-6-Pase in the liver tissue and lipid-liver disease happening were evaluated and shown in Table 5.

The serum glucose content in the 4 groups was Group III > Group II > Group IV > Group I ( $p < 0.05$ -0.01). Serum glucose of Group III rabbits was significantly higher than that of Group IV rabbits ( $p < 0.03$ ) and there was no significant difference between Group II and Group III rabbits. There was no significant difference for the both serum and liver protein content among the 4 rabbit groups. Liver G-6-Pase of non- $\beta$ -carotene rabbits was significantly higher than that of other 3 groups ( $p < 0.05$ ) and there was no significant difference for liver G-6-Pase among the 3 groups. Serum cholesterol of Group I was significantly lower than that of the other 3 groups and there was no significant difference among the 3 groups. About a half of atherosclerotic rabbits (38-50%) got lipid-liver



disease and there was no lipid-liver happening in the Group I (Table 5).

### 3.5 Light and Electron Microscopy Observation

Thrombi were observed on the atherosclerotic rabbit aortas after the thrombus triggering. Using the electron microscopy observation, the plaques, irregular cell surface and ulceration with blood cells and clotting fibers could be seen on the lamina surface of the endothelium layer. It seems that there was no significant change could be observed between Group IV and Group III. Comparing with Group I, all treated groups could be

seen increased elastin number, degenerated organelles, irregular density, bundles of microfibrils, some longitudinal and others in cross-section. These changes were more prominent in Group III than Group IV. Endothelium can be seen clearly attaching on thick internal elastin lamella in Group II and Group IV, but it was hardly to be found in Group III. In Group IV, prominent vacuoles were presented which were considered as lipid. In Group III, the impression of morphological architectural and subcellular organs seems to be more irregular and imparity than that in the droplets of rest groups.

Table 1. Preparation of the four rabbit groups

Groups	Treatments	n	Normal Diet	Cholesterol Diet (1%)	Balloon Trauma	RVV and Histamine	$\beta$ -Carotene
I	Control-control	4	Yes	No	No	No	No
II	Control	4	Yes	Yes	Yes	No	No
III	Non- $\beta$ -carotene	8	Yes	Yes	Yes	Yes	No
IV	$\beta$ -Carotene	8	Yes	Yes	Yes	Yes	Yes

Table 2. Evaluations of rabbit aortas

Groups	Surface Area (mm <sup>2</sup> )	Weight (g)	Thrombus Surface (mm <sup>2</sup> )	Thrombus Number	Glucose Content (mg/g)	Total Protein (mg/g)
I	1550±181	1.62±0.55	0	0	1.1±0.1	10.4±1.7
II	1881±233	3.92±0.28	0	0	1.0±0.4	10.0±2.0
III	1664±285	3.48±0.21	78.6±38.9	5.0±4.3	1.4±0.3	11.0±1.1
IV	1545±193	3.76±0.46	50.3±25.9	2.3±1.3	1.6±0.9	9.1 ±1.1
Average	1660±257	3.20±1.07	32.2±39.0	1.8±2.4	1.3±0.3	10.1±0.8

Table 3. Diameter of rabbit carotid artery response to vascular regulating chemicals (mm)

Groups	NE (1×10 <sup>-6</sup> M)	Ach (1×10 <sup>-5</sup> M)	SN (1×10 <sup>-5</sup> M)	Ach-NE (%)	SN-NE (%)
I	13.98±2.34	18.21±2.81	18.83±2.45	35.27±29.76	39.38±26.07
II	18.56±7.16	20.94±2.98	21.88±2.96	16.80±14.91	20.30±15.22
III	18.05±3.39	19.68±3.64	20.21±3.62	9.98±9.68	12.43±11.84
IV	16.52±3.22	18.75±3.32	19.16±3.29	14.30±10.02	16.93±11.37
Average	16.78±2.06	19.40±1.20	20.02±1.37	19.09±11.15	22.26±11.86

Ach-NE (%)=(Ach-NE)/NE×100; SN-NE (%)=(SN-NE)/NE×100. Ach, NE and SN here are diameter (mm) of the arteries perfused by the PBS containing a corresponding chemical.

Table 4. Metallothionein in rabbit tissues ( $\mu\text{g-MT/g-wet tissue}$ )

Groups	Liver	Kidney	Heart	Aorta artery	Carotid artery	Femoral artery
I	136.6 $\pm$ 54.4	46.3 $\pm$ 0.6	6.4 $\pm$ 0.5	4.0 $\pm$ 0.3	4.5 $\pm$ 0.8	3.3 $\pm$ 0.7
II	239.8 $\pm$ 46.1	126.5 $\pm$ 17.1	36.1 $\pm$ 25.1	8.0 $\pm$ 2.9	4.9 $\pm$ 1.3	5.1 $\pm$ 0.9
III	447.5 $\pm$ 200.1	200.9 $\pm$ 123.7	56.7 $\pm$ 21.7	5.9 $\pm$ 0.5	5.4 $\pm$ 0.9	4.3 $\pm$ 0.7
IV	189.5 $\pm$ 50.5	149.3 $\pm$ 15.4	25.5 $\pm$ 2.6	4.2 $\pm$ 0.3	5.8 $\pm$ 1.1	4.1 $\pm$ 0.9
Average	274.6 $\pm$ 158.4	120.8 $\pm$ 158.4	31.2 $\pm$ 21.0	5.5 $\pm$ 1.9	5.2 $\pm$ 0.6	4.2 $\pm$ 0.7

Table 5. Glucose, total protein, glucose-6-phosphatase and lipid-liver

Groups	Serum Glucose (mg/dl)	Serum Protein (mg/ml)	Liver Protein (mg/g)	Liver G-6-Pase (mol/min/g)	Serum Cholesterol (mg/l)	Lipid-liver Disease (%)
I	101.55 $\pm$ 4.27	35.91 $\pm$ 0.29	13.48 $\pm$ 2.76	10.47 $\pm$ 3.06	1837 $\pm$ 306	0
II	151.59 $\pm$ 34.75	32.44 $\pm$ 4.61	11.37 $\pm$ 1.14	11.28 $\pm$ 2.67	4208 $\pm$ 712	50
III	160.41 $\pm$ 20.41	33.07 $\pm$ 1.75	12.13 $\pm$ 2.31	16.34 $\pm$ 3.51	4196 $\pm$ 615	38
IV	136.46 $\pm$ 13.95	33.04 $\pm$ 1.43	11.56 $\pm$ 3.10	12.02 $\pm$ 2.19	4257 $\pm$ 683	38
Average	137.50 $\pm$ 25.93	33.63 $\pm$ 1.56	12.14 $\pm$ 0.95	12.53 $\pm$ 2.62	3625 $\pm$ 1192	32

## Discussions

Atherosclerosis, or "hardening of the arteries", is the process that causes heart attacks and most strokes. It is characterized by the progressive build-up of fatty plaques in blood vessels. One major component of the atherosclerotic plaque is cells loaded with cholesterol called foam cells. It is currently believed that cholesterol, especially the low-density lipoproteins (LDL), must be modified or oxidized before they can be taken up to cause foam cells. Antioxidants such as vitamin C, vitamin E, and carotenoids can prevent the oxidative modification of LDL in the laboratory. This has given rise to the concept that these vitamins could decrease the risk of heart disease by preventing oxidation of LDL in the body. Myocardial infarction in human cases a triggering activity such as physical exertion precipitates the acute onset of the disorder (Mittleman 1993; Muller 1989; Tofle1990), but it is difficult to be studied in human. Therefore, a suitable animal model has been created recently (Abela, 1995). This study demonstrated that vulnerable plaques could be produced, the plaque disruption and platelet-rich arterial thrombus formation could be triggered pharmacologically in the atherosclerotic rabbits that has been described in a previous paper (Abela, 1995). Rabbits in the three groups which were balloon induced arterial injury and then maintained in an alternative 1% of cholesterol diet for a total of six months clearly caught atherosclerosis. The aorta artery weight of the atherosclerotic rabbits was 2.25 times heavier than that of normal rabbits ( $p < 0.01$ ) (Table 2). This model is a useful method to get atherosclerotic animal for the

related scientific research purpose.

When cells use oxygen for energy purpose, they produce by-products called free radicals. Free radicals damage cells and tissues during a process called oxidation - a factor in many chronic illnesses, including some forms of cancer, cataracts, arthritis and cardiovascular disease. LDL, known as the "bad cholesterol", is actually a protein that carries cholesterol throughout the body. The cholesterol carried by LDL deserves its bad reputation, however. It often ends up in our arteries, causing clots that can lead to heart attacks. Oxidation of LDL-cholesterol contributes to the plaque build-up in arteries, a process called atherosclerosis that can cause blockages and reduced blood flow. The process also plays a role in the loss of elasticity in arteries. Antioxidants help to neutralize free radicals and prevent them from causing cellular damage. Once oxidized, the cholesterol is less apt to be expelled by the body's cleaning mechanisms and more likely to be stored in arteries. Taking antioxidants, such as  $\beta$ -carotene, may lower a person's risk of developing heart disease. Free glucose in blood is the important energy resource and precursor resource for the various requirements including anti-oxidation in animal body. One of the problems for atherosclerotic rabbits is that their free radical and oxidation conditions are changed under the disease. Free radical modification of serum that is not the solely increased level of lipoprotein oxidation products in blood lipoproteins is an important cause for cholesterol accumulation in cells, and apparently for their transformation into foam cells during atherosclerosis (Jacob, 1996). Once altered by

free radical oxidation, plasma lipoproteins undergo dramatic change, both in the manner in which they can interact with cells and in the ways in which they influence cell functions (Chisolm, 1991). This study showed that the average aorta weight of Groups II, III and IV was about 2.25 times heavier than that of Group I ( $p < 0.01$ ) and the average total aorta cholesterol of Groups II, III and IV was about 6 times as that of Group I ( $p < 0.01$ ) (Table 2). One of the reasons that  $\beta$ -carotene improves the atherosclerotic condition in experimental rabbits maybe that  $\beta$ -carotene balances the adverse function of free radical and oxidation from high cholesterol.

In animal liver, glycogen is broken down into glucose-1-phosphate by liver phosphorylase and then converted into glucose-6-phosphate. Glucose-6-phosphate is dephosphorylated by G-6-Pase to yield free D-glucose, which passes into the systemic blood to be transported to other tissues. The non- $\beta$ -carotene rabbits have higher free glucose concentration in the blood hints that they have higher requirement for the free glucose. For this phenomenon, the explanation is not clear, and the energy metabolism may be involved. The  $\beta$ -carotene treatment let the glucose concentration down hints that  $\beta$ -carotene compensates the requirement of the free glucose amount (Table 5).

MT is a ubiquitous class of low molecular weight and cysteine-rich proteins (about 1/3 of amino acid in MT is cysteine) binding unusually high amounts of metal ions, such as Ag, Cd, Cu, Hg and Zn. The most conspicuous biological feature of MT is its inducibility by a variety of agents and conditions. The biosynthesis of MT is induced by various factors such as heavy metals, certain hormones, cytokines, growth factors, tumor promoters, coldness, heat, hunger, radiation and diseases (Brady, 1982). Most of the inducing factors of MT biosynthesis are adverse factors. MT is thought to play an important role the homeostasis of metal ions and to be involved in the detoxification of heavy metals, scavenge free radical, etc. (Kagi, 1991). The accurate functions of MT in atherosclerosis are not clear. One study examined the supplementation of  $\beta$ -carotene on metal ion-dependent and metal ion-independent induced oxidation of LDL and it showed that  $\beta$ -carotene would not inhibit the LDL oxidation (Gaziano, 1995). The phenomenon that the non- $\beta$ -carotene rabbits have higher MT level in the various tissues shows that the balloon-induced arterial injury, high cholesterol diet and injection of RVV/histamine could enhance the biosynthesis of MT or keep MT from the degradation. That the amount of MT in the Group IV was similar to that in Group II and Group I rabbits but much lower than that in Group III rabbits showed that  $\beta$ -carotene made some compensation function for the MT induced requirement, such as free radical scavenge and anti-

oxidation (Table 4).

In this study, the results showed that the arteries from  $\beta$ -carotene treatment rabbits had the similar contraction response to Ach and SN as the arteries from control-control and control rabbits (Table 3). Since those rabbits are in later atherosclerotic stage, it seems to that the  $\beta$ -carotene shows a protective function on the balloon-induced arterial injury and a 1% cholesterol diet treatment is not only in the early stage of atherosclerosis but also in the late stage of atherosclerosis. Explanation seems to be involved in endothelium function as reported before (Abela, 1995). The vascular endothelium plays a central role in the regulation of vascular function. In particular, the local release of endothelium-derived relaxing factor regulates vascular tone and prevents platelet adhesion to the vascular wall. The atherosclerotic rabbits with hyper-cholesterol ichemia can significantly induce endothelium dependent relaxation function (Jayakody, 1988). Also there was a report showing that imbalance vascular oxidative stress and antioxidant protection is involved in the development of the vascular dysfunction in atherosclerosis (Keaney, 1995). The antioxidative function of  $\beta$ -carotene seems to effecting on the activity of the endothelium in the atherosclerotic rabbit arteries.

The activity of G-6-Pase in liver of these four rabbit groups had the consistent magnitude result with glucose content in blood (Table 5). This hinted that the alteration of glucose level in blood was adjusted by the activity of G-6-Pase in liver. It was not clear whether the  $\beta$ -carotene inhibited G-6-Pase expression or inhibits the activity of G-6-Pase, or other more complex procedure.

Carotenoid pigments are widely distributed in nature, where they play an important role in protecting cells and organisms against oxidation and free radical (Palozza, 1992). As the most important one of the carotenoid pigments,  $\beta$ -carotene is the most well known antioxidant of the carotenoid family. Carotenoids are natural plant pigments that produce the bright and vibrant colors that associate with fresh fruits and vegetables.  $\beta$ -Carotene supplies the bright orange color of carrots, apricots, cantaloupe, sweet potatoes and acorn squash. In addition to giving plants a bright color,  $\beta$ -carotene is a potent antioxidant. Epidemiological studies have shown the more fruits and vegetables we eat, the lower our risk of heart disease se will get. A strong association between  $\beta$ -carotene consumption from foods and risk of heart disease has also been described.

Our study suggests that  $\beta$ -carotene has important function in prevention of atherosclerotic plaque disruption and arterial thrombosis in atherosclerotic rabbit model. It is provided pilot information for management in human atherosclerosis.

**Correspondence to:**

Kuan-Jiunn Shieh

Department of Chemistry

Chinese Military Academy

Fengshan, Kaohsiung, Taiwan 830, ROC

Email: [chemistry0220@gmail.com](mailto:chemistry0220@gmail.com)

Telephone: 011-886-7742-9442

**References**

1. Baumgartner I, von Aesch K, Do DD, Triller J, Birrer M, Mahler F. Stent placement in ostial and nonostial atherosclerotic renal arterial stenoses: a prospective follow-up study. *Radiology* 2000;216(2):498-505.
2. Brady FO. The physiological function of metallothionein. *TIBS* 1982;8:143-5.
3. Chisolm GM. Antioxidants and atherosclerosis: a current assessment. *Clin Cardiol* 1991;14 (Supple 1):125-30.
4. Constantinides P. Overview of studies on regression of atherosclerosis. *Artery* 1981;9(1):30-43.
5. Constantinides P. The role of arterial wall injury in atherogenesis and arterial thrombogenesis. *Zentralbl Allg Pathol* 1989;135(6):517-30.
6. Eaton DL, Cherian MG. Determination of metallothionein in tissues by cadmium-hemoglobin affinity assay. In Riordan JF, Vallee BL, eds: *Methods Enzymol (Vol 205, Metallobiochemistry Part B: Metallothionein and Related Molecules)*. New York, USA: Academic Press, Inc. 1991:83-8.
7. Gaziano JM, Hatta A, Flynn M, Johnson EJ, Krinsky NI, Ridker PM, Hennekens CH, Frei B. Supplementation with  $\beta$ -carotene *in vivo* and *in vitro* does not inhibit low density lipoprotein oxidation. *Atherosclerosis* 1995;112(2):187-95.
8. Harper AE. Measurement of enzyme activity: Glucose-6-phosphatase; In *Methods of Enzymatic Analysis*. New York, USA: Academic Press. 1965:788-92.
9. Hung DZ, Wu ML, Deng JF, Yang DY, Lin-Shiau SY. Multiple thrombotic occlusions of vessels after Russell's viper envenoming. *Pharmacol Toxicol* 2002;91(3):106-10.
10. Jacob RA, Burri BJ. Oxidative damage and defense. *Am J Clin Nutr* 1996;63(6):985s-990s.
11. Jayakody L, Kappagoda T, Senaratne MP, Thomson AB. Impairment of endothelium-dependent relaxation: an early marker for atherosclerosis in the rabbit. *Br J Pharmacol* 1988;94(2):335-46.
12. Kagi JHR. Overview of Metallothionein; In Riordan JF, Vallee BL, eds: *Methods Enzymol (Vol 205, Metallobiochemistry Part B: Metallothionein and Related Molecules)*. New York, USA: Academic Press, Inc. 1991:613-26.
13. Keaney JF, Vita JA. Atherosclerosis, oxidative stress, and antioxidant protection in endothelium-derived relaxing factor action. *Prog Cardiovasc Dis* 1995;38(2):129-54.
14. Kim JC, Chung TH. Direct determination of free cholesterol and individual cholesterol esters in serum by high pressure liquid chromatography. *Korean J Biochem* 1984;16:69-77.
15. Mittleman MA, Maclure M, Tofler GH, Sherwood JB, Goldberg RJ, Muller JE. Triggering of acute myocardial infarction by heavy physical exertion. Protection against triggering by regular exertion. *N Engl J Med* 1993;329(23):1677-83.
16. Muller JE, Tofler GH, Stone PH. Circadian variation and triggers of onset of acute cardiovascular disease. *Circulation* 1989;79(4):733-43.
17. Palozza P, Krinsky NI. Antioxidant effects of carotenoids *in vivo* and *in vitro*: An overview; In Packer L, ed. *Methods Enzymol (Vol 213, Carotenoids Part A: Chemistry, Separation, Quantitation, and Antioxidation)*. New York, USA: Academic Press, Inc. 1992:403-20.
18. Prince MR, LaMuraglia GM, MacNichol EF Jr. Increased preferential absorption in human atherosclerotic plaque with oral  $\beta$ -carotene. *Circulation* 1988;78(2):338-44.
19. Tofler GH, Stone PH, Maclure M, Edelman E, Davis VG, Robertson T, Antman EM, Muller JE. Analysis of possible triggers of acute myocardial infarction. *Am J Cardiol* 1990;66(1):22-7.
20. Witztum JL, Young SG, Elam RL, Carew TE, Fisher M. Cholestyramine-induced changes in low density lipoprotein composition and metabolism. I. Studies in the guinea pig. *J Lipid Res* 1985;26(1):92-103.

## Utilisation of Alicyclic Compounds by Soil Bacteria

Olukayode O. Amund, Matthew, O. Ilori\*, Sunday A. Adebuseye, and K. I. Musa

Department of Botany and Microbiology, University of Lagos, Akoka, Yaba, Lagos, Nigeria  
Phone: (234) 802-319-5170, E-mail: [olusojiilori@yahoo.com](mailto:olusojiilori@yahoo.com)

**Abstract:** Alicyclic compounds are recalcitrant hydrocarbons, they are a major component of crude oil and their fraction in the oil may be as high as 37%. They are used as industrial chemicals and are obtained via extraction from petroleum or by synthesis. A number of alicyclic compounds are, in addition to the petrogenic source, continually synthesized biologically as constituents of plants and microorganisms. Despite the wide occurrence of these compounds in nature, very little works had been carried out on their utilization by microorganisms. Species of *Pseudomonas*, *Acinetobacter*, *Arthrobacter* and *Nocardia* able to utilize cyclohexanone as sole carbon source were isolated from soil by enrichment technique. The isolates also grew on cyclohexanol, succinic and acetic acids as sole carbon sources. DNA profiles of the organisms did not reveal the presence of any plasmid. Growth in acriflavin-supplemented broth did not result in loss of ability to utilize the compounds. The genetic control of alicyclic metabolism in these organisms appeared to be chromosomal in nature. [Nature and Science. 2006;4(3):65-68].

**Keywords:** Hydrocarbons; Alicyclic; Degradation; Bacteria; Microorganisms

### Introduction

Alicyclic hydrocarbons are the most resistant molecules to microbial attack among saturated hydrocarbons (Sikkema *et al.*, 1995; Ko and Lebeault, 1999), and are major components of 'drilling oils' (Chaîneau *et al.*, 1995). These are becoming increasingly important as industrial solvents to replace benzene (Sikkema *et al.*, 1995). Studies have shown that the alkanes are the most susceptible to attack followed by the isoalkanes with cycloalkanes as the most recalcitrant (Perry, 1984; Leahy and Colwell, 1990). The wide spread occurrence of alicyclic hydrocarbons in the biosphere over the preceding millions of years suggests that the capability for utilization of these compounds as sole source of carbon and energy would be broadly distributed over the microbial world but this is not so. Where one can readily demonstrate  $10^6$  bacteria capable of growth of n-hexadecane thrive in a gram of soil, reports on the successful enrichment for axenic cultures of cycloalkane-utilizing organisms are limited. Their very low water solubility and potential membrane toxicity to microbes are some of the reasons for their persistence and paucity of reports concerning their biodegradation (Anderson *et al.*, 1980; Sikkema *et al.*, 1995). Ilori (1999) reported the ability of lagoon water isolates identified as species of *Pseudomonas*, *Acinetobacter*, *Vibrio*, *Micrococcus* and *Flavobacterium* to utilise cyclohexanol as sole source of carbon and energy. To our knowledge, only *Brevibacterium* sp. strain HCU (Brzostowicz *et al.*, 2000) has been reported to grow on cyclohexanone while reports on the potentials of other organisms to utilise the compound as sole source of carbon and energy is scanty. This work

reports the ability of some soil microorganisms to utilize cyclohexanone as sole source of carbon and energy.

### Materials and Methods

#### Isolation of and identification of organisms

Cotton wool pieces were soaked in cyclohexanone, wrapped with aluminium foil and sterilised by autoclaving. One of the cotton wool was buried in an uncontaminated soil around Faculty of Science while another one was buried in spent oil-polluted soil at the AP filling station in University of Lagos. The cotton wool pieces were removed after 3 weeks and incubated in an enrichment medium described by Murray *et al.* (1974) for one week on rotary shaker (50 rpm) at 30 °C. Aliquots of the culture was thereafter plated on cyclohexanone agar and incubated at room temperature for one week. Pure cultures were obtained from this by picking distinct colonies and streaking each on separate cyclohexanone agar plates before transferring onto cyclohexanone slants. Identification of isolates was as described by Holt *et al.* (1994).

#### Growth on alicyclic compounds and organic acids

The isolates were tested for their ability to oxidize cyclohexanone, cyclohexanol, cyclohexane, succinic and acetic acids. These substrates were supplied in minimal salts medium as the sole carbon source at a concentration of 0.1%.

#### Screening for plasmids and curing

Screening for plasmids was as described by Birnboim and Doly (1979) while curing was as described by Miller (1972).

## Results

A mixed culture of bacteria, which grew on exogenously supplied cyclohexanone as sole source of carbon and energy were obtained. They were subsequently characterized and found to belong to four genera namely *Pseudomonas*, *Arthrobacter*, *Acinetobacter* and *Nocardia*. All the isolates grew on cyclohexanone, cyclohexanol, succinate and acetate (Table 1), while only the *Nocardia* species grew on cyclohexane.

The time course growth profile of the organisms on cyclohexanone is as shown in Figure 1. *Nocardia* sp had the best growth on the compound while the least growth was recorded with *Acinetobacter* sp. Figure 2 shows the content of the DNA extracts of the isolates after agarose gel electrophoresis. Growth in acriflavine supplemented nutrient broth for 48 h revealed that all the isolates retained the ability to grow on cyclohexanone.

Table 1. Growth of Isolates on Alicyclic Compounds and Organic Acids

Isolates	Cyclohexanone	Cyclohexanol	Cyclohexane	Succinate	Acetate
<i>Acinetobacter Calcoaceticus</i>	++	++	-	+	+
<i>Arthrobacter</i> sp.	+++	+++	-	+	+
<i>Pseudomonas fluorescens</i>	+++	+++	-	+	+
<i>Nocardia</i> sp.	+++	+++	+	++	+

+++ , Heavy growth; ++, moderate growth; +, poor growth; -, no growth.

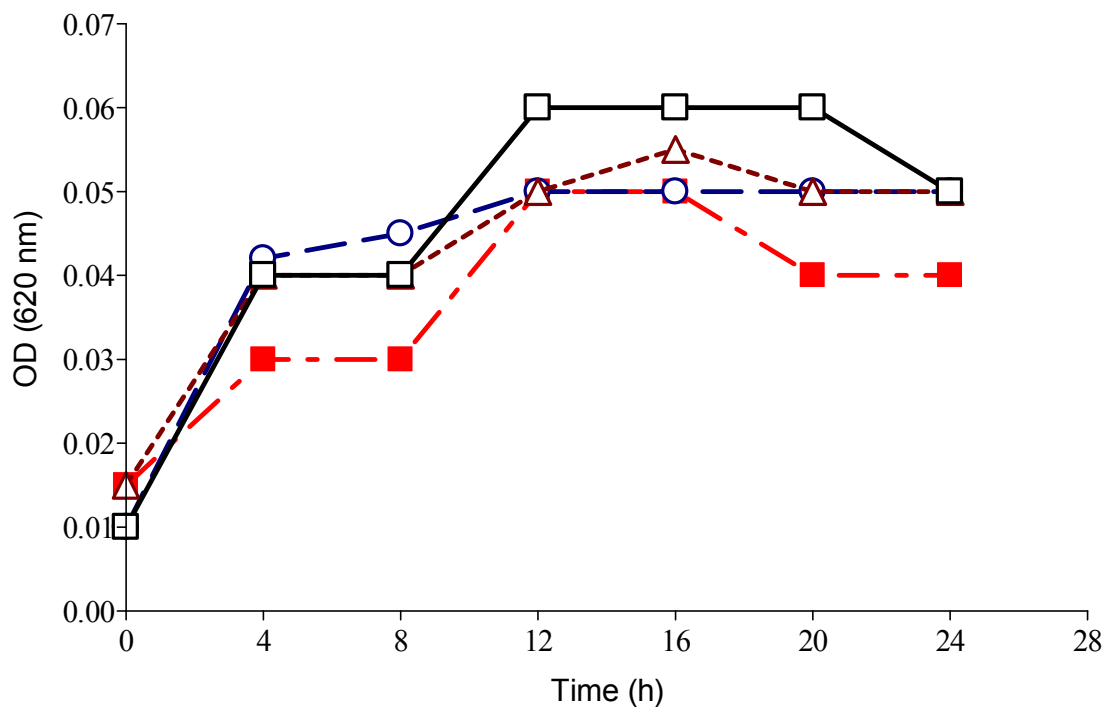


Figure 1. Growth Profile of the Isolates on Cyclohexanone. ○, *Pseudomonas fluorescens*; ■, *Acinetobacter calcoaceticus*; □, *Nocardia* sp.; Δ, *Arthrobacter* sp.

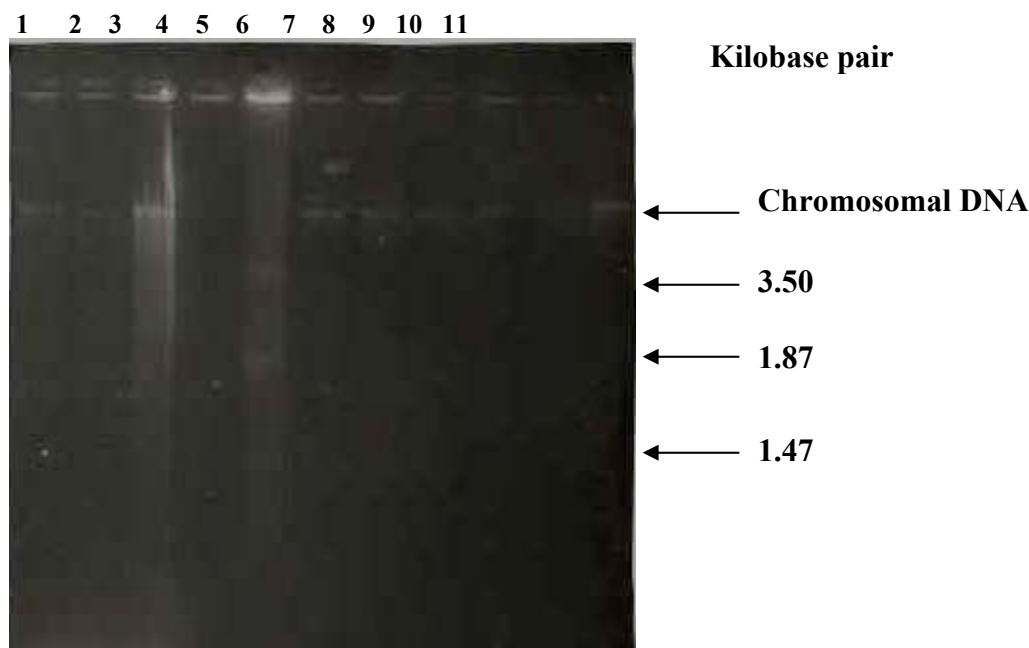


Figure 2. Agarose Gel Electrophoresis of DNA Extracts. Lanes: 1, 2, 4, 6, 7, 8, 9, *Pseudomonas* spp.; 3, *Nocardia* spp.; 5, *Escherichia coli* V517; 11, *Acinetobacter calcoaceticus*.

### Discussion

Alicyclic compounds are widely distributed in nature, they include monocyclic and other more complex terpenes, sterols and a wide range of more exotic molecules from pyrethrins. It is possible that, in natural mixed microbial populations, the degradation of such compounds may yield cyclohexanone or closely related compounds like cyclohexanol which are themselves not of significant natural occurrence as metabolic intermediates. The organisms grew on both cyclohexanone and cyclohexanol at nearly equivalent rates. This is similar to the findings of Donoghue and Trudgill (1975) who reported that this ability is compatible with a role for cyclohexanone in cyclohexanol oxidation. The failure of the organisms to grow on succinate and acetate at equivalent rates reflect the inability of these more polar compounds to penetrate the bacteria rapidly. Cyclohexane is a component of crude oil but reports of microorganisms able utilize this compound as sole source of carbon have been very few (Beam and Perry, 1973; Anderson *et al.*, 1980). Cyclohexane is very volatile and does not persist long enough for potential oxidizers to develop. Furthermore, the compound may be toxic to microorganisms in both liquid and vapour forms thereby making it resistant to microbial attack (Donoghue and Trudgill 1975; Sikkema *et al.*, 1995). The time course growth experiment showed that no appreciable period of time is required for the metabolism of cyclohexanone by the

organisms. The involvement of plasmid-encoded genes in the metabolism of both n-alkane and aromatic hydrocarbons has been documented (Chakrabarty, 1980; Foght and Westlake, 1996). No such report has however appeared on the catabolism of cycloalkanes. Therefore, cyclohexanone is probably catalysed by chromosomally encoded enzymes as shown by the results of plasmid screening and curing experiments.

### Conclusion

Many intermediates in the aliphatic and aromatic break-down by bacteria can be conveniently catabolized by chromosomally encoded enzymes.

### Corresponding Author:

Dr. Matthew O. Ilori  
Department of Botany and Microbiology  
University of Lagos  
Akoka, Yaba, Lagos, Nigeria  
Phone: (234)-8023195170  
E-mail: [olusojiilor@yahoo.com](mailto:olusojiilor@yahoo.com)

### References

1. Anderson MS, Hall RA, Griffin, M. Microbial metabolism of alicyclic hydrocarbons: cyclohexane metabolism by a pure strain of *Pseudomonas* sp. J Gen Microbiol 1980;119:89-94.
2. Beam HW, Perry JJ. Co-metabolism as a factor in microbial degradation of cyclo-paraffinic hydrocarbons. Arch Microbiol 1973;91:87-90.

3. Birnboim HC, Doly J. A rapid alkaline extraction procedure for screening recombinant plasmid DNA. *Nucleic Acids Res* 1979;7:1513-1523.
4. Brzostowicz PC, Gibson KL, Thomas SL, Blasko MS, Rouvière PE. Simultaneous identification of two cyclohexanone oxidation genes from an environmental *Brevibacterium* isolate using mRNA differential display. *J Bacteriol* 2000;182:4241-4248.
5. Chaîneau CH, Morel JL, Oudot J. Microbial degradation of chilling cuttings fuel oil hydrocarbons in an agricultural soil. *Environ Sci Technol* 1995;29:1613-1621.
6. Chakrabarty AM. Plasmids and dissimilation of synthetic environmental pollutants. In: Stuttard C, Rozee KR eds. *Plasmids and Transposons: Environmental Effects and Maintenance Mechanisms*, London, UK: Academic Press Inc. 1980:21-30.
7. Donoghue NA, Trudgill PW. The metabolism of cyclohexanol by *Acinetobacter* NCIB 9871. *J Biochem* 1975;60: 1-7.
8. Foght JM, Westlake DWS. Transposon and spontaneous deletion mutants of plasmids borne genes encoding polycyclic aromatic hydrocarbon degradation by a strain of *Pseudomonas fluorescens*. *Biodegradation* 1996;7:353-366.
9. Holt JG, Krieg NR, Sneath PHA, Stanley JT, William ST. *Bergey's Manual of Determinative Bacteriology*. Baltimore, USA: William and Wilkins. 1994.
10. Ilori MO. Utilisation of cyclohexanol by bacteria in a tropical estuarine water. *Folia Microbiol* 1999;44 (5): 553-556.
11. Ko SH, Lebeault JM. Effect of a mixed culture on co-oxidation during the degradation of saturated hydrocarbon mixture. *J Appl Microbiol* 1999;87:72-79.
12. Leahy JG, Colwell RR. Microbial degradation of hydrocarbons in the environment. *Microbiol Rev* 1990; 54:305-315.
13. Miller JH. *Experiments in Molecular Genetics*. Cold Spring Harbour Laboratory. New York, USA: 1972:104-105.
14. Murray JR, Scheikowski TA, McRae IC. Utilization of cyclohexanone and related substances by a *Nocardia* species. *Antonie van Leeuwenhoek* 1974;40:17-24.
15. Perry JJ. Microbial metabolism of cyclic alkanes. In: *Atlas RM ed Petroleum Microbiology*. New York, USA: Macmillan. 1984:61-97.
16. Sikkema J, deBont JAM, Griffin M. Mechanisms of membrane toxicity of hydrocarbon: isolation and properties of a cyclohexane degrading bacterium. *J Gen Microbiol* 1980;99:119-125.
17. Stirling LA, Watkinson RJ, Higgins IJ. Microbial metabolism of alicyclic hydrocarbons; isolation and properties of a cyclohexane-degrading bacteria. *Arch Microbiol* 1977;99:119-125.



## An *In Silico* Investigation into the Discovery of Novel *Cis*-acting Elements within the Intronic Regions of Human *PAX7*

\*Maika G. Mitchell<sup>1,2</sup>, Melanie Ziman<sup>1</sup>

<sup>1</sup> School of Exercise, Biomedical and Health Science, Edith Cowan University, Perth, Western Australia 6027,

<sup>2</sup> Email: [blackmam@mskcc.org](mailto:blackmam@mskcc.org)

<sup>2</sup> Sloan Kettering Institute (Memorial Sloan Kettering Cancer Center), New York City, New York 10021, USA

**Abstract:** PAX3 and PAX7 are homologous paired box family members expressed during early neural and myogenic development. Assays of mRNA expression have proven conclusively that PAX3 and PAX7 transcripts are present in embryonal and alveolar rhabdomyosarcoma, neuroblastoma, Ewing's sarcoma, and melanoma cell lines; the tumor-specific expression patterns correspond to expression patterns in corresponding embryonic cell lineages. The intronic regions of the PAX7 gene were analyzed using computational DNA pattern recognition methods. Several potential *cis*-regulatory motifs were identified in this investigation and one in particular that was common to both PAX7 and PAX3 and also to NF1, could have implications for the role of PAX7 in Alveolar Rhabdomyosarcoma and may be the cornerstone to more exciting, unique scientific investigations. **Methods:** In Silico biology methods are currently used in the pharmaceutical industry as an antecedent to wet chemistry and bench work. Here we employed several public online and offline programs/databases as tools to investigate the nucleotide sequences of the PAX7 gene. **Results:** Several potential *cis*-acting elements within the intronic regions of PAX7 were discovered through in silico biological methods. Transcription factors that could bind to these elements have also been identified and their association with cancer ascertained. Interestingly one *cis* element is found within a 155 bp sequence in intron 8 of PAX7 that surprisingly, is also found within intron 10 of PAX3 and is also found conserved within intron 23 of the NF-1 gene. **Discussion:** The use of In Silico Biology methods represent new, faster, cost-efficient techniques to identify novel regulatory elements that provide areas for more in depth in vitro investigations to confirm their functional effects. [Nature and Science. 2006;4(3):69-85].

**Keywords:** *PAX7*; *PAX3*; *cis* regulatory elements; *NF-1*; conserved sequences; ERMS; ARMS

**Abbreviations and notations:** TSS, transcription start site; *Cis*-acting element; ARMS, alveolar rhabdomyosarcoma; ERMS, embryonal rhabdomyosarcoma; NF-1, Neurofibromatosis factor 1; bp, base pair; TF, Transcription Factor; RD, Rhabdomyosarcoma; TSS, transcription start site

### INTRODUCTION

*Pax* genes derive their name from the paired box gene region which encodes a highly conserved Paired DNA binding domain. Paired domains are found in all members of the Pax family. There are four classes of *PAX* genes based not only on sequence but on genomic organization. Genes within a given class have intron/exon boundaries and encoding regions in common. *Pax3* and *Pax7* are closely related paired box family members expressed during early neural and myogenic development and have been implicated in the development of specific myogenic and neurogenic cell lineages (Glaser, et al., 1994; Relaix et al., 2004). Pax proteins are thought to function primarily by binding to enhancer DNA sequences and modifying the transcriptional activity of bound downstream target genes (Chi et al., 2002). Assays detailing human *PAX7* and *PAX3* mRNA expression show conclusively that transcripts of these genes are present in Alveolar Rhabdomyosarcoma, Embryonal Rhabdomyosarcoma, neuroblastoma, Ewing's sarcoma, and melanoma cell lines and reveal tumor-specific expression patterns that

correspond to those in corresponding embryonic cell lineages (Goulding, et al., 1991; Bennicelli et al., 1993; Macina et al., 1995; Schulte et al., 1997; Barr et al., 1999; Mercado et al., 2005).

The search for new regulatory elements in unreported regions of the *PAX7* gene would lead to a better understanding of the oncogenic pathways that activate this gene. In this study, the eight introns of *Homo sapiens PAX7* were scanned for new regulatory elements which may affect tumorigenesis in humans. We monitored the DNA repeat patterns of the eight introns in the time period from August 2005 to March 2006 to determine if updates to the NCBI database would affect the predicted outcomes for each query. The results for the eight introns of *PAX7* remained consistent in several repetitions of the experiment. We analyzed the intronic regions of this gene using computational DNA pattern recognition methods. We report here that several potential *cis*-regulatory motifs were identified in this way. The possible significance of all identified *cis* motifs for the *PAX7* gene were investigated using various web and offline databases that employ similar

statistical tests and parameters. Moreover, transcription factors likely to bind to the elements were identified and the association of these transcription factors with tumour cell function determined.

Specifically, one newly identified *cis* element was found in a conserved region of intron 8 of *PAX7*; the same sequence containing the *cis* element (ctccaccc) was also found in alternative intron 10 of *PAX3* and in the 3' region (in intron 23) of the tumor suppressor gene *Neurofibromatosis factor 1 (NF-1)*. The presence of this element has not previously been reported in association with the intronic regions of *PAX7* up to the date of submission of this publication (June 2006). The region of the *NF-1* gene that is present in intron 8 of *PAX7* and identified here by *in silico* data mining methods, has recently been linked to Embryonal Rhabdomyosarcoma (ERMS) (Hadjistilianou et al., 2002; Oguzkan et al., 2006) and Alveolar Rhabdomyosarcoma (ARMS) (Woodruff et al., 1993; Dei Tos et al., 1997) and confirmed as a significant role player in carcinogenesis in a recent publication using fluorescent-labeled microsatellite markers. (Oguzkan et al., 2006).

The conserved sequence containing the *cis* regulatory element identified in intron 8 of *PAX7*, may have arisen by insertion of a regulatory element in all three chromosomal regions or by homologous recombination between chromosome 1 (*PAX7*), chromosome 2 (*PAX3*) and/or chromosome 17 (*NF-1*). As a result of the similarly conserved intronic sequences present in all three genes, it is possible that the genes are similarly regulated by common transcription factors (TFs) proposed to bind to the common *cis* elements. Experimentation and *in vitro* studies that may prove the biological importance of these gene sequences, is currently underway.

## MATERIALS AND METHODS

### DNA Data-mining

#### Definition of *Cis* Elements

Before collecting meaningful data for the basis of this research, the first course of action for data mining is to define a *cis* element and second, to test several software applications that can be used to find *cis* elements. A *cis*-acting element controls the initiation, or the rate of transcription and translation of genes that reside on the same chromosome as itself. *Cis* elements contain the following features (Park et al., 2003):

A short consensus sequence ( $\geq 8$  base pairs long);

No fixed location but usually 100-200 bp upstream of the transcription start site or within 10 kb upstream or downstream or within intronic regions of a gene;

Can be located in a promoter or act as an enhancer or silencer;

It is assumed that a specific protein binds to the element and the presence of that protein is spatially and temporally regulated;

One consensus sequence is usually sufficient to confer a regulatory response but the sequence may be present as one of several consensus sequences close together or it may be present as tandem repeat units.

Knowledge of new *cis* elements in the intronic regions of *PAX7* (theoretical *cis* elements to be validated later by *in vitro* studies), may lead to a better understanding of the factors that lead to over-expression of the gene with resultant increased tumorigenicity (Lewin et al., 2000).

### The Selection of Databases used for the Computational Portion of the Research

Computational queries were performed against known, validated segments of sequences in order to quantitate a threshold of accuracy for all future evaluations of data. Automatic e-mail updates for the *PAX7* sequences for *Homo sapiens* (as well as for the *Homo sapiens PAX3* and *NF-1* gene) was set up within the National Center for Biotechnology Information database (NCBI, <http://www.ncbi.nlm.nih.gov>).

To determine functional significance, that is, biological properties of the newly identified *cis* elements, their position within sets of conserved sequences was determined by computational sequence alignment, a fundamental means of detecting biologically significant patterns in genes (Lewin et al., 2000). Multiple alignment methods were used to locate and align exons or introns of DNA in an attempt to locate and align similar subsequences. This approach has often been used to look for transcription factor binding sites in similarly regulated promoters (Liu et al., 1995; Frith et al., 2004; Chen et al., 2005).

### Programs Used for *In Silico* Investigations

The introns of *PAX7* were scrutinized for *cis* elements with eight separate programs which denote promoter areas, transcription factor binding sites and/or transcription start sites (TSS), DNA patterns, global and local nucleotide alignment and tandem repeats in submitted sequences. The names and functions of the programs used are:

#### 1) Mreps:

(<http://bioweb.pasteur.fr/seqanal/interfaces/mreps.html>)

- Mreps is a software package for identifying tandem repeats ( patterns that appear  $>1x$  in a given sequence) in DNA sequences.

#### 2) CLC Free Workbench version 2.2 by CLC

bioA/S: (<http://www.clcbio.com>) - The alignment software illustrates the conservation of all sequence positions below aligned sequences. The height of the bars in the view reflects how conserved that particular position is in the aligned sequence. If one position is 100% conserved the bar will be at full height. The

software uses a progressive alignment algorithm (Oguzkan et al., 2006) in order to create multiple alignments.

3) DNA Pattern Search – Softberry: (<http://www.softberry.com/>) - This program searches for significant patterns in the set of sequences.

4) PROSCAN Version 1.7 Web Promoter Scan Service: (<http://bimas.dcrf.nih.gov/molbio/proscan/>) - Predicts promoter regions based on homologies with putative eukaryotic Pol II promoter sequences. The site is serviced and maintained by Dr. Dan Prestridge at the Advanced Biosciences Computing Center, University of Minnesota.

5) Promoter 2.0 Prediction Server: (<http://www.cbs.dtu.dk/services/Promoter/>) – Promoter 2.0 predicts transcription start sites of vertebrate PolII promoters in DNA sequences. It has been developed as a frequently updated database of simulated transcription factors that interact with sequences in promoter regions. It builds on principles that are common to neural networks and genetic algorithms. The site is serviced and maintained by Steen Knudsen at The Center for Biological Sequence Analysis at the Technical University of Denmark.

6) TSSG - Recognition of human PolII promoter regions and transcription start sites from Softberry: (<http://www.softberry.com/>) - TSSG is the most accurate mammalian *cis* element prediction program.

7) CLC Gene Workbench v. 1.0.1 by CLC bioA/S: (<http://www.clcbio.com>) - Applying the Pattern Discovery helps identify unknown sequence patterns across single or multiple DNA and protein sequences. The discovery method is based on advanced hidden Markov models.

8) TRANSFAC® 7.0: (<http://www.gene-regulation.com/pub/databases.html#transfac>) - is a database of eukaryotic transcription factors, their genomic binding sites and DNA-binding profiles. This database was used to compare DNA patterns discovered during the data-mining stage of this research with known *cis*-acting elements and identify the transcription factors most likely to bind to them.

For each program, fasta files of the eight introns of *PAX7* were pasted into each program. The output was saved into a word document and/or a portable data file (PDF) for scrutiny and review.

## RESULTS

### 1. Prediction of novel *cis* regulatory regions by computer scans of intronic regions of *PAX7*:

The list of novel *cis*-acting elements found in each intron of *Homo sapiens PAX7* was created by analysis of:

1) The location of the *cis*-acting element in the sequence compared to the locality of known/previously identified *cis*-acting elements;

2) Comparison of the results from the different DNA patterning software programs;

3) Location of pattern to the proximity of start and stop codons or to exon/intron boundaries;

4) Comparisons of DNA patterns to those that exist for other *cis*-acting elements on the TRANSFAC Database v.5.0 (<http://transfac.gbf.de/TRANSFAC/index.html>).

Below are the results for each intron of *PAX7* obtained as a result of scanning the intronic sequences of *PAX7* using the software, databases and search criteria specified above. Table 9 contains a summary of the list of proposed *cis* elements for each intron of *PAX7* and table 10 lists the transcription factors that bind to each proposed *cis* elements.

### ***PAX7* INTRON ANALYSIS: INTRON 1**

*PAX7* intron 1 patterns found by Softberry Pattern Search Software: Found 5 pattern (s)

1) *Pattern 1*, Length = 10, 552bp - 561bp  
AAATAATAAT

2) *Pattern 2*, Length = 9, 552bp - 560bp  
AAATAATAA

3) *Pattern 3*, Length = 10, 553bp - 562bp  
AATAATAATT

4) *Pattern 4*, Length = 10, 554bp - 563bp  
ATAATAATTA

5) *Pattern 5*, Length = 10, 1322bp – 1331bp  
AATATAAAGT

#### Proscan: Version 1.7

*Cis* element region predicted on forward strand at 1094bp to 1344bp

TATA found at 1323bp, Est.TSS at 1353bp

#### Softberry TSSG:

2 promoter(s) are predicted .

Promoter position: 1350 LDF: TATA box at 1324bp  
TATAAAGT

Promoter position: 492 LDF: TATA box at 463bp  
TTTATATG

#### Promoter 2.0 Prediction Server:

Position (bp)	Score	Likelihood
600	0.638	Marginal prediction
1000	0.561	Marginal prediction
2000	0.629	Marginal prediction

CLC Gene Workbench v.1.0.1. Pattern Discovery Search (Table 1)

**Table 1: CLC Gene Workbench v.1.0.1. Pattern Discovery Search**

Sequence	Type	Pattern	Length	ModelScore	PatternScore	StartPos	EndPos
PAX7 INTRON 1	0	CGGGAGAG	8	3611.743 57871381 15	23.66548 94035726 6	619	627
PAX7 INTRON 1	0	GGCGAGAG	8	3611.743 57871381 15	19.06079 82311651 83	663	671
PAX7 INTRON 1	0	GGGGAGAC	8	3611.743 57871381 15	20.79577 19668466 12	746	754
PAX7 INTRON 1	0	GCGGAGAG	8	3611.743 57871381 15	18.98736 37802949 3	813	821
PAX7 INTRON 1	0	GGGGAGAG	8	3611.743 57871381 15	23.84288 65639622 6	1011	1019
PAX7 INTRON 1	0	CGGGAGAG	8	3611.743 57871381 15	23.66548 94035726 6	1161	1169
PAX7 INTRON 1	0	GAGGAGAG	8	3611.743 57871381 15	19.72943 65851499 8	1284	1292
PAX7 INTRON 1	0	CGGGAGAG	8	3611.743 57871381 15	23.66548 94035726 6	1470	1478
PAX7 INTRON 1	0	GGGGAGAC	8	3611.743 57871381 15	20.79577 19668466 12	2376	2384
PAX7 INTRON 1	1	TCTCGCCT CCT	11	3561.956 50273364 9	17.43936 06083101 53	1520	1531
PAX7 INTRON 1	1	CCTCCACT CCC	11	3561.956 50273364 9	22.26281 54940416 18	1553	1564
PAX7 INTRON 1	1	TCTCCCT CCC	11	3561.956 50273364 9	27.71272 83914939 93	1711	1722
PAX7 INTRON 1	1	TCACCCGT CCC	11	3561.956 50273364 9	21.64101 27969001 47	1993	2004
PAX7 INTRON 1	1	TCTCCCT CCC	11	3561.956 50273364 9	18.96284 22090329 83	2289	2300
PAX7 INTRON 1	1	TCTCCCT CCC	11	3561.956 50273364 9	27.71272 83914939 93	2595	2606
PAX7 INTRON 1	2	AACCCAGG GAGT	12	3517.911 84683555 8	24.39181 58111311 6	144	156
PAX7 INTRON 1	2	ACCCCGG GATT	12	3517.911 84683555 8	26.85349 84598473 5	406	418
PAX7 INTRON 1	2	AACCCGG GATT	12	3517.911 84683555 8	27.01549 03651027 92	1175	1187
PAX7 INTRON 1	2	ACCCCGG GATT	12	3517.911 84683555 8	23.80271 78007375 7	2484	2496

**Figure 1**

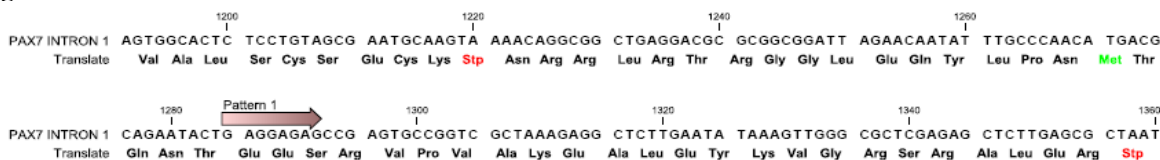


Figure 1: *Cis* regulatory region predicted by CLC Gene Workbench v. 1.0 – on forward strand at position 1094bp to 1344bp; **Pattern found within this *cis* regulatory region.**

## **PAX7 INTRON ANALYSIS: INTRON 2**

PAX7 intron 2 patterns found by Softberry Pattern Search Software: Found 5 pattern(s)

- 1) *Pattern 1*, Length = 10, Power: 1, 422bp - 431bp AAAGGATAAA
- 2) *Pattern 2*, Length = 10, Power: 1, 423bp - 432bp AAGGATAAAG
- 3) *Pattern 3*, Length = 10, Power: 1, 421bp - 430bp GAAAGGATAA
- 4) *Pattern 4*, Length = 9, Power: 1, 95bp - 103bp AGGAAAGTA
- 5) *Pattern 5*, Length = 9, Power: 1, 421bp - 429bp GAAAGGATA

Proscan: Version 1.7:

Processed Sequence: 572 bp. No *cis* element regions predicted.

Softberry programs:

0 promoter/enhancer(s) predicted

Promoter 2.0 Prediction Server:

No *cis* element predicted

CLC Gene Workbench v.1.0.1. Pattern Discovery Search ( Table 2)

**Table 2: CLC Gene Workbench v.1.0.1. Pattern Discovery Search**

Sequence	Type	Pattern	Length	ModelScore	PatternScore	StartPos	EndPos
PAX7 INTRON 2	0	CCCCACCC CACCT	13	786.0414 67692741 4	24.35138 44186404 78	361	374
PAX7 INTRON 2	0	CCCCATCC CATCT	13	786.0414 67692741 4	20.65919 82458401 87	525	538
PAX7 INTRON 2	0	CCCACCTC CACCT	13	786.0414 67692741 4	21.16756 03585959 1	553	566
PAX7 INTRON 2	1	ACTCCAG AT	10	762.1814 32865190 6	19.29041 15669702 67	122	132
PAX7 INTRON 2	1	ACCCCCAG CT	10	762.1814 32865190 6	22.55891 66334026 85	380	390
PAX7 INTRON 2	1	ACCACCAG CC	10	762.1814 32865190 6	19.29667 16934558 8	471	481

**Figure 2**

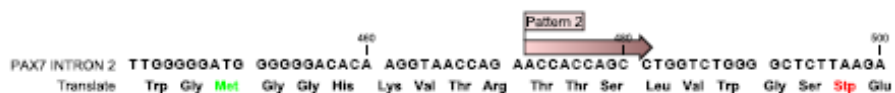


Figure 2: No *cis* element predicted, but 1 pattern found within 400-500 bps by CLC Gene Workbench v. 1.0.

**PAX7 INTRON ANALYSIS: INTRON 3**

PAX7 intron 3 patterns found by Softberry Pattern Search Software: *No patterns found*

Proscan: Version 1.7 No *cis* element regions predicted.

Softberry TSSG: No *cis* element regions predicted.

**Promoter 2.0 Prediction Server:**

Position	Score	Likelihood
200	0.557	Marginal prediction

**Proscan: Version 1.7:**

Processed Sequence: 996 Base Pairs. No *cis* element regions predicted.

**Softberry programs:**

0 promoter/enhancer(s) predicted.

**Table 3a: CLC Gene Workbench v.1.0.1. Pattern Discovery Search**

Sequence	Type	Pattern	Length	ModelScore	PatternScore	StartPos	EndPos
PAX7 INTRON 3	0	GGGAGGAA	8	1346.789 07869357 64	20.21155 43687426 32	122	130
PAX7 INTRON 3	0	GGAAGGAA	8	1346.789 07869357 64	19.68872 10488846 38	190	198
PAX7 INTRON 3	0	GGAAGGAA	8	1346.789 07869357 64	19.68872 10488846 38	205	213
PAX7 INTRON 3	0	GGGAGGAA	8	1346.789 07869357 64	20.21155 43687426 32	245	253
PAX7 INTRON 3	0	GGAAGGAA	8	1346.789 07869357 64	23.15276 12529448	256	264
PAX7 INTRON 3	0	GGAAGGTA	8	1346.789 07869357 64	17.53897 87215351 38	264	272
PAX7 INTRON 3	0	GGAAGGAA	8	1346.789 07869357 64	23.15276 12529448	272	280
PAX7 INTRON 3	0	GGAAGGAA	8	1346.789 07869357 64	23.15276 12529448	280	288
PAX7 INTRON 3	0	GGAAGGAA	8	1346.789 07869357 64	23.15276 12529448	292	300
PAX7 INTRON 3	0	GGAAGGAA	8	1346.789 07869357 64	23.15276 12529448	300	308
PAX7 INTRON 3	0	GGCAGGAA	8	1346.789 07869357 64	18.90215 99027119 7	328	336
PAX7 INTRON 3	0	GTAAGGAA	8	1346.789 07869357 64	18.32484 82073802 74	891	899

**Table 3b: 1 CLC Gene Workbench v.1.0.1. Pattern Discovery Search**

Sequence	Type	Pattern	Length	ModelScore	PatternScore	StartPos	EndPos
PAX7 INTRON 3	1	TGTGTGTG	8	1292.387 09900141 54	23.13529 16322799 7	564	572
PAX7 INTRON 3	1	TGTGTGTA	8	1292.387 09900141 54	18.44154 08128117 6	572	580
PAX7 INTRON 3	1	TGTGTGTG	8	1292.387 09900141 54	23.13529 16322799 7	580	588
PAX7 INTRON 3	1	TGTGTGTG	8	1292.387 09900141 54	23.13529 16322799 7	588	596
PAX7 INTRON 3	1	TGAGTGTG	8	1292.387 09900141 54	19.55980 93138332 24	635	643
PAX7 INTRON 3	1	TGTGGGTG	8	1292.387 09900141 54	19.42527 61692567 9	698	706
PAX7 INTRON 3	1	TGTGAGTG	8	1292.387 09900141 54	20.36494 47202190 47	785	793
PAX7 INTRON 3	1	TGTGTGTG	8	1292.387 09900141 54	23.13529 16322799 7	861	869
PAX7 INTRON 3	2	GTGGGAGA GAG	11	1266.019 80634617 55	21.30341 20449475 4	69	80
PAX7 INTRON 3	2	CTGTGAGA GAG	11	1266.019 80634617 55	21.04797 58203004 44	541	552
PAX7 INTRON 3	2	GTGTGAGT CAG	11	1266.019 80634617 55	22.96127 72583093 87	799	810

**Figure 3**

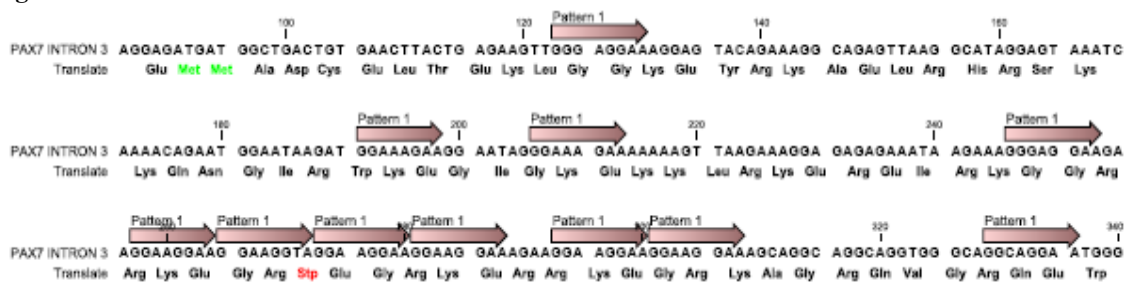


Figure 3: *Cis* regulatory region predicted by CLC Gene Workbench v. 1.0 on forward strand from 190-300bps; *Several patterns found within this region.*

**PAX7 INTRON ANALYSIS: INTRON 4**

PAX7 intron 4 patterns found by Softberry Pattern Search Software: Found 5 pattern(s)

- 1) *Pattern 1*, Length = 9, Power: 1, 916bp - 924bp CTTTCTCCC
- 2) *Pattern 2*, Length = 10, Power: 1, 948bp - 957bp CCTCTGCTCC
- 3) *Pattern 3*, Length = 10, Power: 1, 942bp - 951bp CTCGCTCCTC
- 4) *Pattern 4*, Length = 10, Power: 1, 916bp - 925bp CTTTCTCCCA
- 5) *Pattern 5*, Length = 10, Power: 1, 946bp - 955bp CTCCTCTGCT

Proscan: Version 1.7:

Processed Sequence: 1002bp. No *Cis* regulatory regions predicted.

Softberry programs:

0 promoter/enhancer(s) predicted

Promoter 2.0 Prediction Server:

Position (bp)      Score              Likelihood  
 200                  0.557                  Marginal prediction;  
 CLC Gene Workbench v.1.0.1. Pattern Discovery Search (Table 4a & 4b)

**Table 4a: CLC Gene Workbench v.1.0.1. Pattern Discovery Search**

Sequence	Pattern	Length	ModelScore	PatternScore	StartPos	EndPos
PAX7 INTRON 4	GGGAGGAA	8	1355.13354 91683985	20.2233399 74494554	122	130
PAX7 INTRON 4	GGAAAGAA	8	1355.13354 91683985	19.7005324 9513273	190	198
PAX7 INTRON 4	GGAAAGAA	8	1355.13354 91683985	19.7005324 9513273	205	213
PAX7 INTRON 4	GGGAGGAA	8	1355.13354 91683985	20.2233399 74494554	245	253
PAX7 INTRON 4	GGAAAGAA	8	1355.13354 91683985	23.1645652 2709397	256	264
PAX7 INTRON 4	GGAAAGTA	8	1355.13354 91683985	17.5507604 22396078	264	272
PAX7 INTRON 4	GGAAAGAA	8	1355.13354 91683985	23.1645652 2709397	272	280
PAX7 INTRON 4	GGAAAGAA	8	1355.13354 91683985	23.1645652 2709397	280	288
PAX7 INTRON 4	GGAAAGAA	8	1355.13354 91683985	23.1645652 2709397	292	300
PAX7 INTRON 4	GGAAAGAA	8	1355.13354 91683985	23.1645652 2709397	300	308
PAX7 INTRON 4	GGCAGGAA	8	1355.13354 91683985	18.9139383 07175883	328	336
PAX7 INTRON 4	GTAAGGAA	8	1355.13354 91683985	18.3366373 0150939	891	899
PAX7 INTRON 4	TGTGTGTG	8	1300.73142 67724823	23.1470854 38411686	564	572
PAX7 INTRON 4	TGTGTGTA	8	1300.73142 67724823	18.4533111 97633493	572	580
PAX7 INTRON 4	TGTGTGTG	8	1300.73142 67724823	23.1470854 38411686	580	588
PAX7 INTRON 4	TGTGTGTG	8	1300.73142 67724823	23.1470854 38411686	588	596
PAX7 INTRON 4	TGAGTGTG	8	1300.73142 67724823	19.5716325 08941946	635	643
PAX7 INTRON 4	TGTGGGTG	8	1300.73142 67724823	19.4371354 75261723	698	706
PAX7 INTRON 4	TGTGAGTG	8	1300.73142 67724823	20.3766870 37843958	785	793
PAX7 INTRON 4	TGTGTGTG	8	1300.73142 67724823	23.1470854 38411686	861	869
PAX7 INTRON 4	GTGGGAGAGA G	11	1274.34830 6284579	21.3126706 965328	69	80

**Table 3b:CLC Gene Workbench v.1.0.1. Pattern Discovery Search**

Sequence	Pattern	Length	ModelScore	PatternScore	StartPos	EndPos
PAX7 INTRON 4	CTGTGAGAGA G	11	1274.34830 6284579	21.0705243 20844594	541	552
PAX7 INTRON 4	GTGTGAGTCA G	11	1274.34830 6284579	22.9709269 59621153	799	810

**Figure 4**

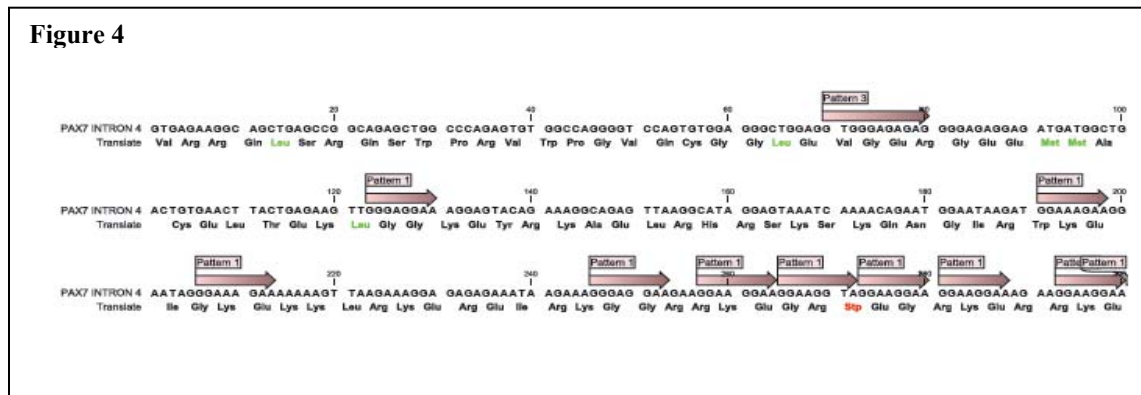


Figure 4: *Cis* regulatory region predicted by CLC Gene Workbench v. 1.0 on forward strand from 200-300bps; **Patterns found within this promoter region.**

**PAX7 INTRON ANALYSIS: INTRON 5**

PAX7 intron 5 patterns found by Softberry Pattern Search Software: Found 5 pattern(s)

- 1) *Pattern 1*, Length = 10, Power: 1, 5710bp - 5719bp TTTTTTTTAA
- 2) *Pattern 2*, Length = 10, Power: 1, 3023bp - 3032bp TATTTTTTTT
- 3) *Pattern 3*, Length = 10, Power: 1, 3024bp – 3033bp ATTTTTTTTT
- 4) *Pattern 4*, Length = 10, Power: 1, 50527bp – 50536bp TATTATTTTT
- 5) *Pattern 5*, Length = 10, Power: 1, 3760bp – 3769bp TATTATTTTT

From the four software programs used, many promoters were predicted (55382 bp).

Proscan: Version 1.7 : 100+ promoters predicted

Softberry TSSG: 23 promoter/enhancer(s) predicted

Promoter 2.0 Prediction Server: 45+ promoters predicted

CLC Gene Workbench v.1.0.1. Pattern Discovery Search (Table 5a & 5b)

**Table 5a: CLC Gene Workbench v.1.0.1. Pattern Discovery Search**

Sequence	Pattern	Length	ModelScore	PatternScore	StartPos	EndPos
PAX7 INTRON 5	GGGGCGGGG	9	76523.0283 0046571	24.1193467 05551376	383	392
PAX7 INTRON 5	GGGAAAGGG	9	76523.0283 0046571	22.4594208 77897016	813	822
PAX7 INTRON 5	GGGAAGGGG	9	76523.0283 0046571	24.9759799 17601167	1394	1403
PAX7 INTRON 5	AGGGAAGGG	9	76523.0283 0046571	23.9220253 5589768	1872	1881
PAX7 INTRON 5	AGGAAGAGG	9	76523.0283 0046571	22.4298595 59503228	1887	1896
PAX7 INTRON 5	TGGGGGAGG	9	76523.0283 0046571	24.1542085 83505895	2072	2081
PAX7 INTRON 5	AGGGAGAGG	9	76523.0283 0046571	24.4648905 8323772	2545	2554
PAX7 INTRON 5	GGAGAGGGG	9	76523.0283 0046571	22.984891 357242	2826	2835
PAX7 INTRON 5	AGGGAGGGG	9	76523.0283 0046571	26.4394753 9501827	3235	3244
PAX7 INTRON 5	GGGGCGGGG	9	76523.0283 0046571	24.1193467 05551378	3616	3625
PAX7 INTRON 5	GGGGGAGG	9	76523.0283 0046571	25.3889145 93891584	3698	3707
PAX7 INTRON 5	GGGAAGGGG	9	76523.0283 0046571	24.9759799 17601167	4008	4017
PAX7 INTRON 5	AGGAAGGGG	9	76523.0283 0046571	24.4044433 72167333	4096	4105
PAX7 INTRON 5	AGGGAGGGG	9	76523.0283 0046571	26.4394753 9501827	4144	4153
PAX7 INTRON 5	AGGGAGGGG	9	76523.0283 0046571	26.4394753 9501827	4437	4446
PAX7 INTRON 5	GGGGATGGG	9	76523.0283 0046571	23.5302248 92120843	4479	4488
PAX7 INTRON 5	GGAGAGGGG	9	76523.0283 0046571	22.984891 357242	4494	4503
PAX7 INTRON 5	AGGGGAGG	9	76523.0283 0046571	24.8173790 4782773	4633	4642
PAX7 INTRON 5	TGGAGGGGG	9	76523.0283 0046571	24.0938523 72435606	4830	4839
PAX7 INTRON 5	GGGAAGGGG	9	76523.0283 0046571	24.9759799 17601167	4954	4963
PAX7 INTRON 5	AGGGAGGGG	9	76523.0283 0046571	26.4394753 9501827	4967	4976

**Table 5b: CLC Gene Workbench v.1.0.1. Pattern Discovery Search**

Sequence	Pattern	Length	ModelScore	PatternScore	StartPos	EndPos
PAX7 INTRON 5	AGGGAAGGG	9	76523.0283 0046571	23.9220253 5589768	6028	6037
PAX7 INTRON 5	GGGGGAGG	9	76523.0283 0046571	25.3889145 93891584	6108	6117
PAX7 INTRON 5	GGGGAGGG	9	76523.0283 0046571	24.5469493 68321518	6366	6375
PAX7 INTRON 5	GGGGAGAGG	9	76523.0283 0046571	25.0364261 28971556	6484	6493
PAX7 INTRON 5	GGGGAGGGG	9	76523.0283 0046571	27.0110109 4163566	6546	6555
PAX7 INTRON 5	TGGAGGAGG	9	76523.0283 0046571	22.1192575 567714	6557	6566
PAX7 INTRON 5	AGGAAAGGG	9	76523.0283 0046571	21.8878943 32163185	6605	6614
PAX7 INTRON 5	GGGGAGGGG	9	76523.0283 0046571	27.0110109 4163566	6617	6626
PAX7 INTRON 5	AGGGAGGGG	9	76523.0283 0046571	26.4394753 9501827	6632	6641
PAX7 INTRON 5	TGGGAGAGG	9	76523.0283 0046571	23.8018101 18815887	6696	6678
PAX7 INTRON 5	CGGGAGGGG	9	76523.0283 0046571	22.0527674 0248411	6705	6714
PAX7 INTRON 5	AGGGAGGGG	9	76523.0283 0046571	26.4394753 9501827	6686	6695
PAX7 INTRON 5	GGGGAGAGG	9	76523.0283 0046571	25.0364261 28971556	6996	7005
PAX7 INTRON 5	GGGAAGGGG	9	76523.0283 0046571	22.0302914 9255880	7520	7529
PAX7 INTRON 5	AGGGAGAGG	9	76523.0283 0046571	24.4648905 8323772	7566	7575
PAX7 INTRON 5	TGGGAAGGG	9	76523.0283 0046571	23.2564448 9147584	7885	7894
PAX7 INTRON 5	AGGGAGAGG	9	76523.0283 0046571	24.4648905 8323772	8802	8811
PAX7 INTRON 5	GGGGTGGGG	9	76523.0283 0046571	24.6888666 7701248	9019	9028
PAX7 INTRON 5	GGGGTGGGG	9	76523.0283 0046571	24.6888666 7701248	10597	10606
PAX7 INTRON 5	GGGGGAGG	9	76523.0283 0046571	25.3889145 93891584	10608	10617
PAX7 INTRON 5	TGGCCGGGG	9	76523.0283 0046571	22.8847306 95386707	10627	10636
PAX7 INTRON 5	GGGGTGGGG	9	76523.0283 0046571	24.6888666 7701248	10847	10856
PAX7 INTRON 5	GGGGAGGGG	9	76523.0283 0046571	27.0110109 4163566	10968	10977

**Table 5c: CLC Gene Workbench v.1.0.1. Discovery Search**

Sequence	Pattern	Length	ModelScore	PatternScore	StartPos	EndPos
PAX7 INTRON 5	GGGGTAGGG	9	76523.0283 0046571	22.1823166 3706327	25740	25749
PAX7 INTRON 5	GGGGCAGGG	9	76523.0283 0046571	22.1447618 9288727	25769	25778
PAX7 INTRON 5	GGGAAGGGG	9	76523.0283 0046571	22.2403827 96853194	25803	25812
PAX7 INTRON 5	GGGAAGGGG	9	76523.0283 0046571	24.9759799 17601167	28076	28085
PAX7 INTRON 5	GGGAGGAGG	9	76523.0283 0046571	23.3538835 6992707	28096	28105
PAX7 INTRON 5	GGGGTAGGG	9	76523.0283 0046571	22.7242818 64348374	28311	28320
PAX7 INTRON 5	GGGGTGGGG	9	76523.0283 0046571	24.6988666 7701248	30246	30255
PAX7 INTRON 5	GGGAGTGGG	9	76523.0283 0046571	21.8556823 33076188	30590	30599
PAX7 INTRON 5	GGGAAGGGG	9	76523.0283 0046571	23.0013951 05237062	30917	30926
PAX7 INTRON 5	GGGGTGGGG	9	76523.0283 0046571	24.6988666 7701248	31772	31781
PAX7 INTRON 5	AGAGAGGGG	9	76523.0283 0046571	22.4169535 89990367	34790	34799
PAX7 INTRON 5	AGAGAGGGG	9	76523.0283 0046571	22.4169535 89990367	34852	34861
PAX7 INTRON 5	TGGAGGAGG	9	76523.0283 0046571	22.1192575 597714	34869	34878
PAX7 INTRON 5	TGGAAAGGG	9	76523.0283 0046571	23.7413639 07745498	35093	35102
PAX7 INTRON 5	GGGAGGAGG	9	76523.0283 0046571	23.3538835 6992707	35146	35155
PAX7 INTRON 5	AGAGGGGGG	9	76523.0283 0046571	22.7694420 54650376	35419	35428
PAX7 INTRON 5	GGGAAGAGG	9	76523.0283 0046571	23.0013951 05237062	35600	35609
PAX7 INTRON 5	TGGAGGAGG	9	76523.0283 0046571	22.1192575 597714	37913	37922
PAX7 INTRON 5	GGGGAGGGG	9	76523.0283 0046571	27.0110109 4163566	40031	40040
PAX7 INTRON 5	GGGGAGGGG	9	76523.0283 0046571	27.0110109 4163566	40119	40128
PAX7 INTRON 5	GGGGAGGGG	9	76523.0283 0046571	27.0110109 4163566	40134	40143
PAX7 INTRON 5	TGGGGGAGG	9	76523.0283 0046571	24.1542085 83505895	40147	40156
PAX7 INTRON 5	GGGAAAGGG	9	76523.0283 0046571	22.5198760 89667404	40159	40168

**Table 5d: CLC Gene Workbench v.1.0.1. Pattern Pattern Discovery Search**

Sequence	Pattern	Length	ModelScore	PatternScore	StartPos	EndPos
PAX7 INTRON 5	GGGAAGGGG	9	76523.0283 0046571	24.9759799 17601167	10687	10696
PAX7 INTRON 5	GGGGAGGGG	9	76523.0283 0046571	27.0110109 4163566	10827	10836
PAX7 INTRON 5	GGGACGGGG	9	76523.0283 0046571	22.0543156 8181682	10889	10898
PAX7 INTRON 5	GGGGTGGGG	9	76523.0283 0046571	24.6888666 7701248	11115	11124
PAX7 INTRON 5	GGGGAGAGG	9	76523.0283 0046571	25.0364261 28971556	11124	11133
PAX7 INTRON 5	GGGGTGGGG	9	76523.0283 0046571	24.6888666 7701248	11470	11479
PAX7 INTRON 5	AGGGGAAGG	9	76523.0283 0046571	22.3082900 07923582	12800	12809
PAX7 INTRON 5	GGGAGGAGG	9	76523.0283 0046571	23.3538835 6992707	13039	13048
PAX7 INTRON 5	AGGGTAGGG	9	76523.0283 0046571	22.1527463 181454	13764	13773
PAX7 INTRON 5	TGGGAGGGG	9	76523.0283 0046571	25.7783040 3147999	15811	15820
PAX7 INTRON 5	GGGAAAGGG	9	76523.0283 0046571	22.4594208 77897016	16755	16764
PAX7 INTRON 5	TGGGGAGGG	9	76523.0283 0046571	24.1542085 83505895	17078	17087
PAX7 INTRON 5	GGGGAGGGG	9	76523.0283 0046571	27.0110109 4163566	17957	17966
PAX7 INTRON 5	TGGGGGAGG	9	76523.0283 0046571	24.1542085 83505895	19023	19032
PAX7 INTRON 5	AGGGAGGGG	9	76523.0283 0046571	26.4394753 9501827	19070	19079
PAX7 INTRON 5	GGAGAAGGG	9	76523.0283 0046571	22.984891 357242	20863	20872
PAX7 INTRON 5	GGGGAGGGG	9	76523.0283 0046571	27.0110109 4163566	22964	22973
PAX7 INTRON 5	GGGGAGGGG	9	76523.0283 0046571	27.0110109 4163566	23759	23768
PAX7 INTRON 5	AGGGAGGGG	9	76523.0283 0046571	26.4394753 9501827	24434	24443
PAX7 INTRON 5	GGGGTGGGG	9	76523.0283 0046571	24.6888666 7701248	24457	24466
PAX7 INTRON 5	AGGGAGGGG	9	76523.0283 0046571	26.4394753 9501827	24677	24686
PAX7 INTRON 5	TGGGGGAGG	9	76523.0283 0046571	23.8917133 5691065	25475	25484
PAX7 INTRON 5	GGGGAGGGG	9	76523.0283 0046571	25.3284863 82591176	25495	25504



CLC Gene Workbench v.1.0.1. Pattern Discovery Search (Table 5e & 5f)

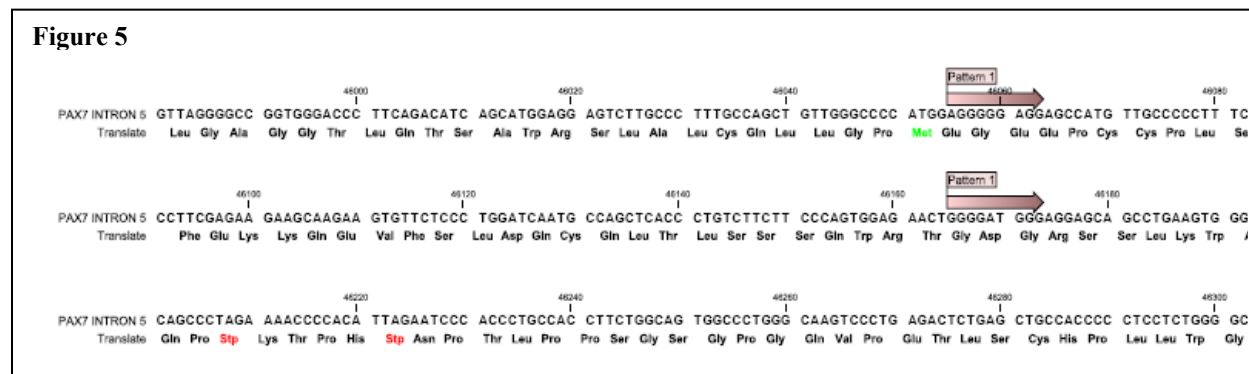


Figure 5: *Cis* regulatory region predicted by CLC Gene Workbench v. 1.0 on forward strand from 45000-46000bps; **Patterns found within this cis regulatory region.**

**PAX7 INTRON ANALYSIS: INTRON 6**

PAX7 intron 6: patterns found by Softberry Pattern Search Software: No patterns found

Proscan: Version 1.7

Promoter region predicted on forward strand in 1456 to 1706bps

Promoter region predicted on forward strand in 1791 to 2041bps

Promoter 2.0 Prediction Server:

Position	Score	Likelihood
1000	1.021	Highly likely prediction
3600	1.084	Highly likely prediction
4000	0.584	Marginal prediction
5400	1.262	Highly likely prediction
6800	0.660	Marginal prediction
7400	0.666	Marginal prediction

Softberry TSSG: 2 promoter/enhancer(s) predicted

Promoter Pos: 893 LDF: TATA box at 863bp AATATATG

Promoter Pos: 5092 LDF: TATA box at 5062bp TATAAATA

Softberry programs:

Promoter Pos: 5092 LDF: TATA box at 5062bp TATAAATA

CLC Gene Workbench v.1.0.1. Pattern Discovery Search ( Table 6)

Sequence	Pattern	Length	ModelScore	PatternScore	StartPos	EndPos
FAX7 INTRON 6	AAAAAGAAA	9	12025.4642 6286368	21.4214355 81383303	590	599
FAX7 INTRON 6	AAGAATAAA	9	12025.4642 6286368	21.3297510 59130928	2216	2225
FAX7 INTRON 6	AAAAATACA	9	12025.4642 6286368	20.1493917 32709592	2344	2353
FAX7 INTRON 6	ATAAATAAA	9	12025.4642 6286368	25.3323885 9500065	2510	2519
FAX7 INTRON 6	ATAAATAAA	9	12025.4642 6286368	25.3323885 9500065	2522	2531
FAX7 INTRON 6	ATAAATAAA	9	12025.4642 6286368	25.3323885 9500065	2534	2543
FAX7 INTRON 6	ATAAATAAA	9	12025.4642 6286368	25.3323885 9500065	2546	2555
FAX7 INTRON 6	TAAATAAA	9	12025.4642 6286368	23.4171905 68406124	2557	2566
FAX7 INTRON 6	ATAAATCAA	9	12025.4642 6286368	21.4455845 28654944	2566	2575
FAX7 INTRON 6	AAAAAAAAA	9	12025.4642 6286368	25.0080904 7125887	3255	3264
FAX7 INTRON 6	AAAAAAAAA	9	12025.4642 6286368	25.0080904 7125887	3267	3276
FAX7 INTRON 6	ATAAAAAAG	9	12025.4642 6286368	18.2065123 46481908	4611	4620
FAX7 INTRON 6	AAAAATTA	9	12025.4642 6286368	19.5946421 56534352	4735	4744
FAX7 INTRON 6	ATAACTAAA	9	12025.4642 6286368	23.7322919 39851848	4935	4944
FAX7 INTRON 6	AAAACTAAA	9	12025.4642 6286368	23.7770113 89571346	5052	5101
FAX7 INTRON 6	TAAAAAAAA	9	12025.4642 6286368	22.0481729 9458485	5104	5113
FAX7 INTRON 6	AAGAATAAA	9	12025.4642 6286368	21.3297510 59130928	5285	5294
FAX7 INTRON 6	ATAACAAAA	9	12025.4642 6286368	22.3632743 66030574	5582	5591
FAX7 INTRON 6	TAAATAAA	9	12025.4642 6286368	23.4171905 68406124	6269	6278
FAX7 INTRON 6	AAAAACAAA	9	12025.4642 6286368	22.4079938 16150068	6361	6370

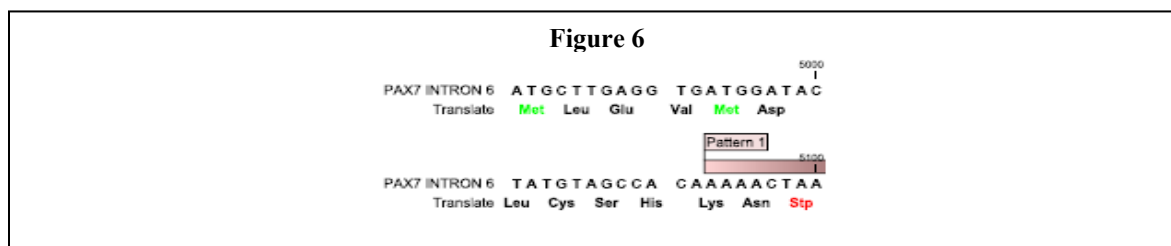


Figure 6: *Cis* regulatory region predicted by CLC Gene Workbench v. 1.0 on forward strand from 5000-5100bps; **Pattern found within this *cis* regulatory region.**

### PAX7 INTRON ANALYSIS: INTRON 7

PAX7 intron 7 patterns found by Softberry Pattern Search Software: Found 5 pattern(s)

- 1) *Pattern 1*, Length = 10, Power: 1, 1134bp – 1143bp CCCTCCCCCT
- 2) *Pattern 2*, Length = 10, Power: 1, 1133bp – 1142bp TCCCTCCCCC
- 3) *Pattern 3*, Length = 10, Power: 1, 870bp - 879bp CCCCCACTC
- 4) *Pattern 4*, Length = 10, Power: 1, 2157bp – 2166bp CCTCCCTCC
- 5) *Pattern 5*, Length = 10, Power: 1, 2156bp – 2165bp CCCTCCCTC

Proscan: Version 1.7 No promoter regions predicted.

Softberry TSSG: 2 promoter/enhancer(s) predicted

Promoter Pos: 1015 LDF: TATA box at 985bp TATAAGAT

Promoter Pos: 333 LDF: TATA box at 304bp TAAAATC

Promoter 2.0 Prediction Server:

Position	Score	Likelihood
600	0.670	Marginal prediction
1100	0.648	Marginal prediction

2000 0.661 Marginal prediction

Softberry programs:

Promoter Pos: 333 LDF: TATA box at 304bp TAAAAATC

CLC Gene Workbench v.1.0.1. Pattern Discovery Search (Table 7)

**Table 7:CLC Gene Workbench v.1.0.1. Pattern Discovery Search**

Sequence	Type	Pattern	Length	ModelScore	PatternScore	StartPos	EndPos
PAX7 INTRON 7	0	GTGCGTGC ATGAGTGT GTG	19	3097.358 06266126 06	38.12965 92222016 6	501	520
PAX7 INTRON 7	0	GTGAGTGC ATGAGTGT GTG	19	3097.358 06266126 06	38.29963 11277832 3	523	542
PAX7 INTRON 7	0	GTGAGTGA ATGAGTGT GTG	19	3097.358 06266126 06	36.92717 29807169 96	549	568
PAX7 INTRON 7	0	GTGTGTGC ATGAGTGT GTG	19	3097.358 06266126 06	37.45462 95379055 25	571	590
PAX7 INTRON 7	0	GTGAGTGA ATGAGTGT GTG	19	3097.358 06266126 06	36.92717 29807169 96	597	616
PAX7 INTRON 7	0	GTGTGTGC ATGAGTGT GTG	19	3097.358 06266126 06	37.45462 95379055 26	617	636
PAX7 INTRON 7	1	AAAAAAA A	9	3061.440 20397315 5	25.60557 39621374 73	730	739
PAX7 INTRON 7	1	AAAAAAA A	9	3061.440 20397315 5	25.60557 39621374 73	1359	1368
PAX7 INTRON 7	1	AAAAAAA A	9	3061.440 20397315 5	25.60557 39621374 73	1520	1529
PAX7 INTRON 7	1	AAAAAAGA T	9	3061.440 20397315 5	21.38725 10521093 77	1539	1548
PAX7 INTRON 7	1	AAAACAAA A	9	3061.440 20397315 5	22.42846 93302109 1	1926	1935
PAX7 INTRON 7	2	TGAGTGTG T	10	3034.940 20891377 3	17.33187 63899655 1	1	11
PAX7 INTRON 7	2	TGAGAGAG T	10	3034.940 20891377 3	20.74271 80997815 16	467	477
PAX7 INTRON 7	2	TGTGCGTG T	10	3034.940 20891377 3	20.24010 59152686 7	490	500
PAX7 INTRON 7	2	TGTGTGTG TA	10	3034.940 20891377 3	19.46281 99903847 65	646	656
PAX7 INTRON 7	2	TGAGTGGG T	10	3034.940 20891377 3	22.95006 44044530 5	1033	1043
PAX7 INTRON 7	2	TGTGTGAG TG	10	3034.940 20891377 3	22.06218 71065785 56	1805	1815
PAX7 INTRON 7	2	TGAGAGGG T	10	3034.940 20891377 3	21.17269 39414678 7	2143	2153

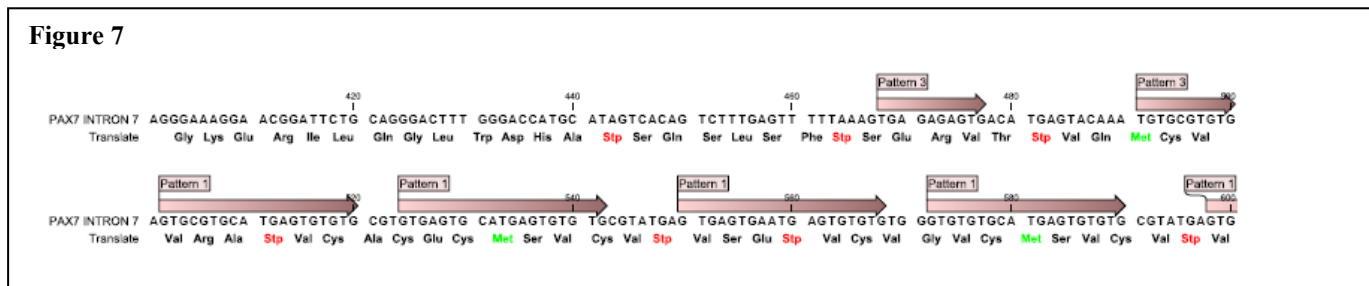


Figure 7: *Cis* regulatory region predicted by CLC Gene Workbench v. 1.0 on forward strand from 300 -600bps; **Patterns found within this *cis* regulatory region.**

**Table 8a:CLC Gene Workbench v.1.0.1. Pattern Discovery Search**

Sequence	Pattern	Length	ModeScore	PatternScore	StartPos	EndPos
PAX7 INTRON	CCCTGCC	8	44637.1815	24.6125917	519	527
PAX7 INTRON	CCCTGCC	8	44637.1815	23.2068722	815	823
PAX7 INTRON	CCCTGCC	8	44637.1815	23.1372743	1562	1570
PAX7 INTRON	CCCTGCC	8	44637.1815	21.2420949	2454	2462
PAX7 INTRON	CCCTGCC	8	44637.1815	20.9773635	2489	2497
PAX7 INTRON	CCCTGCC	8	44637.1815	20.9773635	2831	2839
PAX7 INTRON	CCCTGCC	8	44637.1815	20.9466311	2974	2982
PAX7 INTRON	CCCTGCC	8	44637.1815	20.9466311	3330	3338
PAX7 INTRON	CCCTGCC	8	44637.1815	20.9466311	3339	3347
PAX7 INTRON	CCCTGCC	8	44637.1815	20.9466311	4211	4219
PAX7 INTRON	CCCTGCC	8	44637.1815	20.9773635	4724	4732
PAX7 INTRON	CCCTGCC	8	44637.1815	22.4526808	4739	4747
PAX7 INTRON	CCCTGCC	8	44637.1815	22.4526808	4900	4908
PAX7 INTRON	CCCTGCC	8	44637.1815	22.4219485	5946	5954
PAX7 INTRON	CCCTGCC	8	44637.1815	25.1248958	7105	7113
PAX7 INTRON	CCCTGCC	8	44637.1815	23.6276659	7433	7441
PAX7 INTRON	CCCTGCC	8	44637.1815	25.0941635	7705	7713
PAX7 INTRON	CCCTGCC	8	44637.1815	24.8892358	7793	7801
PAX7 INTRON	CCCTGCC	8	44637.1815	22.2170208	8058	8106
PAX7 INTRON	CCCTGCC	8	44637.1815	25.0941635	8315	8323
PAX7 INTRON	CCCTGCC	8	44637.1815	25.1248958	8432	8440

**Table 8b: CLC Gene Workbench v.1.0.1. Pattern Discovery Search**

Sequence	Pattern	Length	ModeScore	PatternScore	StartPos	EndPos
PAX7 INTRON	CCCTGCC	8	44637.1815	23.2068722	8597	8595
PAX7 INTRON	CCCTGCC	8	44637.1815	25.1248958	8648	8656
PAX7 INTRON	CCCTGCC	8	44637.1815	27.2848057	9205	9214
PAX7 INTRON	CCCTGCC	8	44637.1815	22.2170208	9887	9895
PAX7 INTRON	CCCTGCC	8	44637.1815	22.2170208	11042	11050
PAX7 INTRON	CCCTGCC	8	44637.1815	22.2170208	11822	11830
PAX7 INTRON	CCCTGCC	8	44637.1815	21.2469814	11936	11908
PAX7 INTRON	CCCTGCC	8	44637.1815	20.9466311	12371	12379
PAX7 INTRON	CCCTGCC	8	44637.1815	25.0941635	12877	12885
PAX7 INTRON	CCCTGCC	8	44637.1815	25.1248958	13072	13080
PAX7 INTRON	CCCTGCC	8	44637.1815	24.6125917	13137	13145
PAX7 INTRON	CCCTGCC	8	44637.1815	22.9342527	13376	13384
PAX7 INTRON	CCCTGCC	8	44637.1815	25.0941635	13423	13431
PAX7 INTRON	CCCTGCC	8	44637.1815	20.9466311	13466	13464
PAX7 INTRON	CCCTGCC	8	44637.1815	21.2420949	13482	13490
PAX7 INTRON	CCCTGCC	8	44637.1815	22.8670294	13521	13529
PAX7 INTRON	CCCTGCC	8	44637.1815	25.1248958	13568	13576
PAX7 INTRON	CCCTGCC	8	44637.1815	27.2848057	13726	13734
PAX7 INTRON	CCCTGCC	8	44637.1815	25.1248958	14095	14103
PAX7 INTRON	CCCTGCC	8	44637.1815	23.1372743	14143	14151
PAX7 INTRON	CCCTGCC	8	44637.1815	23.6276659	14170	14178
PAX7 INTRON	CCCTGCC	8	44637.1815	27.2848057	14272	14280
PAX7 INTRON	CCCTGCC	8	44637.1815	22.2170208	14510	14518

**CLC Gene Workbench v.1.0.1. Pattern Discovery Search (Table 8a & 8b)**

**PAX7 INTRON ANALYSIS: INTRON 8**

PAX7 intron 8 patterns found by Softberry Pattern Search Software: No patterns found

From the other four software programs used, many *cis* elements predicted (32335 bps).

Proscan: Version 1.7: Promoter region predicted on forward strand in 2557 to 2807

TATA found at 2792, Est. TSS = 2822

**Table 8c:CLC Gene Workbench v.1.0.1. Pattern Discovery Search**

Sequence	Pattern	Length	ModeScore	PatternScore	StartPos	EndPos
PAX7 INTRON	CTCCAGCC	8	44637.1815	25.0941635	2105	22113
PAX7 INTRON	CCCTGCC	8	44637.1815	22.6626351	22114	22122
PAX7 INTRON	CTCCAGCC	8	44637.1815	25.0941635	22139	22147
PAX7 INTRON	CCCTGCC	8	44637.1815	23.1372743	22396	22404
PAX7 INTRON	CCCTGCC	8	44637.1815	21.4777550	22799	22807
PAX7 INTRON	CCCTGCC	8	44637.1815	22.9342527	22927	22935
PAX7 INTRON	CCCTGCC	8	44637.1815	21.6708080	23383	23391
PAX7 INTRON	CCCTGCC	8	44637.1815	25.1248958	23584	23592
PAX7 INTRON	CTCTGCC	8	44637.1815	20.9466311	26734	26742
PAX7 INTRON	CCCTGCC	8	44637.1815	25.1248958	27163	27161
PAX7 INTRON	CCCTGCC	8	44637.1815	25.1248958	27222	27230
PAX7 INTRON	CCCTGCC	8	44637.1815	25.1248958	27488	27496
PAX7 INTRON	CCCTGCC	8	44637.1815	24.8892358	27509	27517
PAX7 INTRON	CCCTGCC	8	44637.1815	24.8892358	28052	28050
PAX7 INTRON	CCCTGCC	8	44637.1815	27.2848057	28301	28309
PAX7 INTRON	CCCTGCC	8	44637.1815	22.1956352	28465	28463
PAX7 INTRON	CCCTGCC	8	44637.1815	24.6125917	28780	28788
PAX7 INTRON	CCCTGCC	8	44637.1815	27.2848057	29634	29642
PAX7 INTRON	CCCTGCC	8	44637.1815	22.1956352	29619	29627
PAX7 INTRON	CTCCAGCC	8	44637.1815	25.0941635	29848	29856
PAX7 INTRON	CCCTGCC	8	44637.1815	22.4526808	30079	30087
PAX7 INTRON	CTCCAGCC	8	44637.1815	22.4219485	30091	30099
PAX7 INTRON	CCCTGCC	8	44637.1815	25.1248958	30397	30405

**Table 8d:CLC Gene Workbench v.1.0.1. Pattern Discovery Search**

Sequence	Pattern	Length	ModeScore	PatternScore	StartPos	EndPos
PAX7 INTRON	CTCCAGCC	8	44637.1815	22.9342527	15106	15114
PAX7 INTRON	CCCTGCC	8	44637.1815	24.8892358	15245	15253
PAX7 INTRON	CCCTGCC	8	44637.1815	21.0915048	15431	15439
PAX7 INTRON	CTCCAGCC	8	44637.1815	22.4219485	15483	15481
PAX7 INTRON	CCCTGCC	8	44637.1815	27.2848057	15704	15712
PAX7 INTRON	CCCTGCC	8	44637.1815	24.6125917	16062	16070
PAX7 INTRON	CCCTGCC	8	44637.1815	23.1372743	16362	16370
PAX7 INTRON	CCCTGCC	8	44637.1815	23.2068722	16542	16550
PAX7 INTRON	CCCTGCC	8	44637.1815	25.0941635	16922	16930
PAX7 INTRON	CTCCAGCC	8	44637.1815	22.6589526	17814	17822
PAX7 INTRON	CCCTGCC	8	44637.1815	25.1248958	19029	19037
PAX7 INTRON	CTCCAGCC	8	44637.1815	25.0941635	19057	19065
PAX7 INTRON	CCCTGCC	8	44637.1815	24.8892358	18132	18140
PAX7 INTRON	CCCTGCC	8	44637.1815	22.8670294	18146	18154
PAX7 INTRON	CCCTGCC	8	44637.1815	23.6276659	18175	18183
PAX7 INTRON	CCCTGCC	8	44637.1815	23.1372743	18951	18959
PAX7 INTRON	CTCCAGCC	8	44637.1815	25.0941635	19055	19063
PAX7 INTRON	CTCCAGCC	8	44637.1815	22.6589526	19374	19382
PAX7 INTRON	CCCTGCC	8	44637.1815	22.8670294	19660	19668
PAX7 INTRON	CTCCAGCC	8	44637.1815	21.0162300	20605	20613
PAX7 INTRON	CCCTGCC	8	44637.1815	23.2068722	21527	21535
PAX7 INTRON	CCCTGCC	8	44637.1815	20.9254946	22007	22015

Softberry TSSG: *No promoter regions predicted*  
 Promoter 2.0 Prediction Server: 31 promoters predicted

CLC Gene Workbench v.1.0.1. Pattern Discovery Search (Table 8e)

**Table 8e:CLC Gene Workbench v.1.0.1. Pattern Discovery Search**

Sequence	Pattern	Length	ModelScore	PatternScore	StartPos	EndPos
PAX7 INTRON 8	CCCCACCT	8	44637.1815 51375776	21.4777550 3883967	30993	31001
PAX7 INTRON 8	CCTCTCCC	8	44637.1815 51375776	24.8892358 22012967	31090	31098
PAX7 INTRON 8	CCTCTCCC	8	44637.1815 51375776	24.8892358 22012967	31104	31112
PAX7 INTRON 8	CCTCTCCC	8	44637.1815 51375776	24.8892358 22012967	31159	31167
PAX7 INTRON 8	GCCCTCCC	8	44637.1815 51375776	23.2068722 6817531	31198	31206
PAX7 INTRON 8	CCACTCCC	8	44637.1815 51375776	21.8304835 83157623	31229	31237
PAX7 INTRON 8	CTTCTCCC	8	44637.1815 51375776	22.6985926 41211352	31260	31268
PAX7 INTRON 8	CACCTCCC	8	44637.1815 51375776	21.5708080 6456451	31302	31310
PAX7 INTRON 8	CCTCACCC	8	44637.1815 51375776	22.7293250 0239665	31420	31428
PAX7 INTRON 8	CCTCTCCC	8	44637.1815 51375776	24.8892358 22012967	31447	31455

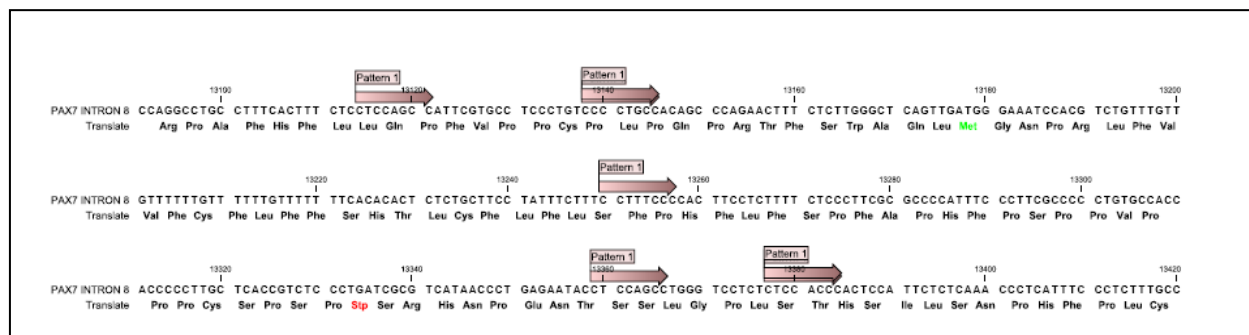


Figure 8: *Cis* regulatory region predicted by CLC Gene Workbench v. 1.0 on forward strand in 13487 to 13737bps; *Patterns found within this cis regulatory region.*

**Table 9. SUMMARY OF MOST LIKELY *CIS* REGULATORY SEQUENCES PREDICTED FOR EACH INTRON OF *PAX7*.**

<u>Intron number</u>	<u>Pattern (cis element?)</u>	<u>Length( bp)</u>	<u>Start Position in intron</u>	<u>End Position in intron</u>
PAX7 INTRON 1	GAGGAGAG	8	1284	1292
PAX7 INTRON 3	GGAAAGAA	8	190	198
PAX7 INTRON 4	GGAAAGAA	8	205	213
PAX7 INTRON 5	AGGGGGAGG	9	46054	46063
	GGGGATGGG	9	46164	46173
PAX7 INTRON 6	AAACTAAA	9	5092	5101

PAX7 INTRON 7	GTGAGTGCATGAGTGTG TG	19	523	542
PAX7 INTRON 8	CCCCACCC	8	13072	13080
	CCCCTGCC	8	13137	13145
	CTCCACCC	8	13376	13384
	CTCCTCCC	8	13423	13431

The results shown in table 9 are the predicted *cis*-regulatory elements for *PAX7* and were chosen from the results of computer scans and based on the four criteria listed above. Table 10 displays the transcription factors most likely to bind to these *cis*-elements with the exception of the *cis*-element in intron 5 for which no transcription factor was identified. Transcription factors were identified using the TRANSFAC database. The transcription factors previously identified as being associated with tumorigenesis are indicated in Table 10.

**Table 10. SUMMARY OF MOST LIKELY *CIS* REGULATORY SEQUENCES PREDICTED FOR EACH INTRON OF *PAX7* WITH CORRESPONDING TRANSCRIPTION FACTORS**

<u>Intron Number</u>	<u>Cis element</u>	<u>Binding Transcription factor from Transfactor</u> ***
PAX7 INTRON 1	GAGGAGAG	EBNA-1;RAR-gamma; R2; Zmhoxla
PAX7 INTRON 3	GGAAAGAA	NP-TCII; <b>NF-1</b> ; GT-IIA
PAX7 INTRON 4	GGAAAGAA	NP-TCII; <b>NF-1</b> ; GT-IIA
PAX7 INTRON 5	AGGGGGAGG	Six-3; DR1; <b>CACCC-BF</b> ; <b>CAC-BF</b> ; <b>Sp1</b> ; ADR1
PAX7 INTRON 5	GGGGATGGG	NONE
PAX7 INTRON 6	AAAACATAA	SRY; PHO2
PAX7 INTRON 7	GTGAGTGCATGAGTGTGTG	Zeste; GCN4; Zeste; MEP-1; MBF-I; Sp1; GHF-1; Pit-1a; RAP1/SBF-E/TUF; USF; TEF;TTF-1
PAX7 INTRON 8	**CCCCACCC	TEF2;MIG1; ACCC-BF; <b>AP-2</b> ; <b>CAC-BF</b> ; <b>Sp1</b>
PAX7 INTRON 8	*CCCCTGCC	<b>AP-2</b> ; <b>CAC-BF</b> ; Ttk;LVc
PAX7 INTRON 8	**CTCCACCC	<b>CACCC-BF</b> ; <b>CAC-BF</b> ; <b>Sp1</b>
PAX7 INTRON 8	*CTCCTCCC	<b>CAC-BF</b> ; ADR1; <b>Sp1</b>

\*Found in *NF1* & *PAX3*;

\*\* Found in *PAX3*

\*\*\*Transcription factors in blue are associated with tumorigenesis.

<http://www.mdcb Berlin.de/forschung/schwerpunkte/cancer/rosenbauer.htm>

## 2. Conservation of intron 8 region containing novel *cis* regulatory region indicating possible functional significance

To ascertain the possible functional significance of the putative *cis*-elements identified above, sequences surrounding these *cis*-elements were used to search for conservation of the regulatory region in other cancer related human genes, such as in human *PAX3*. Comparisons between DNA sequences of *PAX3* and *PAX7* can be used to determine the relationship between the gene sequences from which functional or regulatory regions can be ascertained which assist with identification of the functions of *PAX7* and its role in tumorigenesis.



Figure 9: Conserved sequence in intron 8 of *PAX7* also found in intron 23 of the human *NF1* gene (GenBank Accession Number for *NF-1* gene is AH005101). Conserved regions are shown by sequences coloured in blue. The novel *cis*-element identified in intron 8 of *PAX7* is also found in this conserved sequence in intron 10 of *PAX3* at nucleotide 71560 .

One *cis*-element identified in intron 8 was found to be located within a conserved sequence that is also present in alternative intron 10 of human *PAX3* as well as within intron 23 of *NF1* (sequence length ~100 bps.). The sequence, approximately 155 nucleotides in length is highly conserved between *PAX7* and *NF-1* (89% conserved) (Figure 9) and between *PAX3* and *NF1* (72% conserved) (Figure 10).

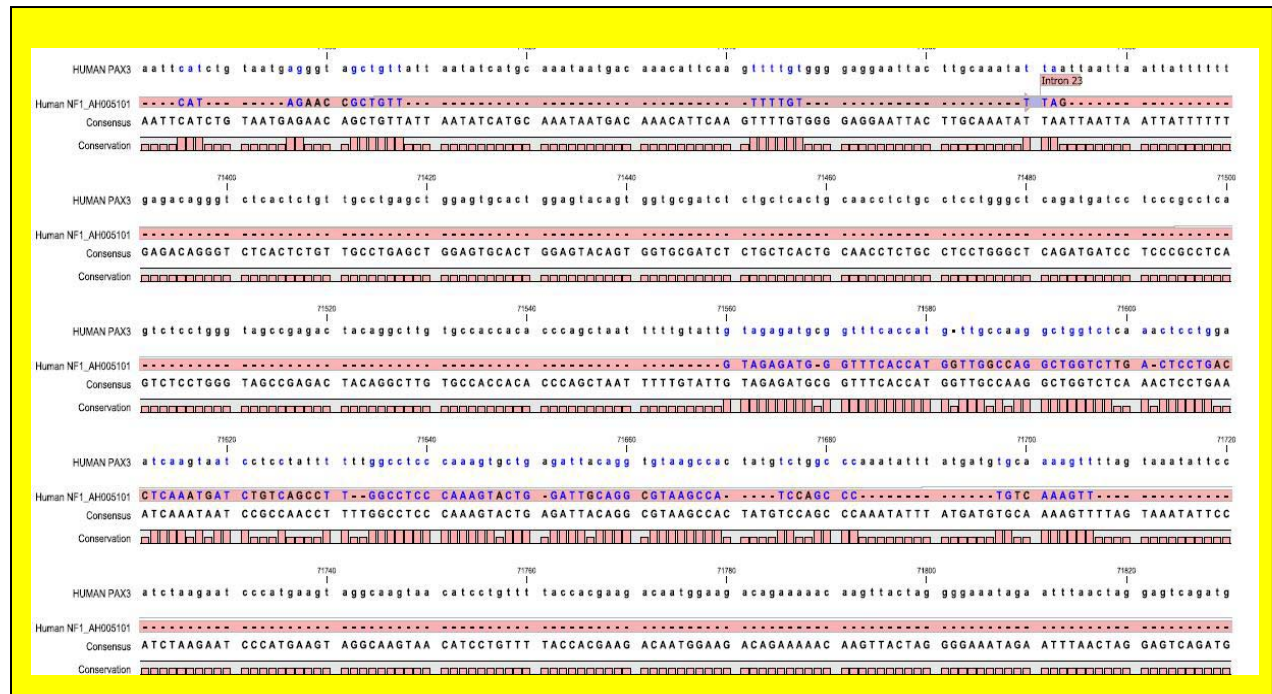


Figure10. Conserved sequence in intron 8 of *PAX7* and intron 23 of *NF-1* also found in alternative intron 10 of *PAX3* (GenBank Accession Number for *PAX3* gene is NM\_013942 ). Conserved regions are shown by sequences coloured in blue.

## DISCUSSION

In this paper we have identified novel *cis*-elements in intronic regions of human *PAX7*. We have also identified a conserved intronic region of *PAX7* that is present in introns of *PAX3* and *NF-1*. Moreover, the conserved region contains a newly identified *PAX7 cis*-element and the same *cis* element occurs in the conserved sequence in all three genes. These findings highlight the ability of *in silico* methodologies to uncover putative *cis* regulatory regions. In addition, the sequence alignments performed in this article confirm that patterns of conservation can be useful in identifying regulatory regions.

*Cis* elements are known to be important in upregulation of genes or in splicing of intronic regions (Pethe et al., 1999; Martin et al., 2004) and therefore crucial in the tumorigenic functions of a gene. The region we have identified in intron 8 of *PAX7*, also found in intron 23 of *NF-1* and alternative intron 10 of *PAX3* may contain regulatory functions common to all three genes and it seems probable that transcription factors and/or spliceosomes would act similarly on all three genes.

Recent experiments identify specific sequences in *NF-1* as being associated with increased tumorigenicity in the childhood cancer, alveolar rhabdomyosarcoma (Dei Tos, et al., 1997). Similarly, *PAX7* and *PAX3* are associated with alveolar rhabdomyosarcoma (Sorensen, et al, 2002). The intronic sequence common to all three genes may be implicated in their tumorigenic properties.

The conserved sequence containing the *cis* regulatory element identified in intron 8 of *PAX7*, intron 10 of *PAX3* and intron 23 of *NF-1* may have arisen by insertion of a regulatory element in all three gene regions or by homologous recombination between chromosome 1 (*PAX7*), chromosome 2 (*PAX3*) and/or chromosome 17 (*NF-1*). The significance of this finding is currently being investigated further by *in vitro* studies.

Only in recent literature has there been a spark to delve into the intronic regions of genomic sequences (Oguzkan, et al, 2006). Historically, introns have been viewed as non-coding, nonsense "place holders" between the exons of a given gene (Bennett et al., 2003; de Roos et al, 2005). It was not until the great race for decoding the human genome that researchers realized that introns constitute a large portion of the regulatory regions of the genome (Davies, 2001; Patrinos, 2001). This can only lead one to believe that the once overlooked introns may play a significant role in regulation of cell functions such as cell cycle control, apoptosis, or aberrant cell cycle control as in tumorigenesis. The research performed in this paper represents a cornerstone in *in silico* research of gene sequences as it points the way for future bench work

studies so that the findings can be verified and validated.

In conclusion, the results presented here may present significant findings that can be utilised ultimately for the development of therapeutics for the treatment of alveolar rhabdomyosarcoma and other cancers associated with *PAX7*. Furthermore, the methods and findings may have implications for other diseases and other genes. *In silico* biology is currently used by pharmaceutical companies to facilitate and hasten the development of new therapeutics for many diseases.

## Acknowledgment

We would like to thank the Memorial Sloan Kettering Institute DNA Sequencing Core Facility Lab manager and technician (Dr. Diane Tabarini & Ms. Donna Wong, respectively) and Memorial Sloan Kettering Cancer Center's Diagnostic Molecular Genetics Laboratory Director (Cindy Yee, PhD) and technologists (Mrs. Nilofer Kreonidis, Mr. Ruben Bacares and Ms. Nadia Shaukat) for their support and assistance for the clinical portions of this project. I would also like to extend my deepest gratitude to Mr. Geoffrey Jackson, of the Centers for Disease Control & Prevention (CDC) who provided the much needed equipment for this project.

## Correspondence to:

Maika G. Blackman-Mitchell  
Memorial Sloan Kettering Cancer Center  
Rockefeller Research Laboratories  
430 East 67<sup>th</sup> Street  
4<sup>th</sup> Floor, Room 453  
New York City, New York 10021, USA  
Email: [blackmam@mskcc.org](mailto:blackmam@mskcc.org)

## REFERENCES

1. Glaser, T., Jepeal, L., Edwards, J. G., Young, S. R., Favor, J., and Maas, R. L. (1994). "PAX6 gene dosage effect in a family with congenital cataracts, aniridia, anophthalmia and central nervous system defects." *Nat. Genet* 7:463-471.
2. Relaix, F., Rocancourt, D. et al. (2004). "Divergent functions of murine Pax3 and Pax7 in limb muscle development." *Genes Dev.* 18(9): 1088-1105.
3. Chi, N., Epstein J.A. (2002). "Getting your Pax straight: Pax proteins in development and disease." *Trends Genet.* 18(1): 41-7.
4. Barr, F. G., Fitzgerald, J. C. et al. (1999). "Predominant Expression of Alternative PAX3 and PAX7 Forms in Myogenic and Neural Tumor Cell Lines." *Cancer Res.* 59(21): 5443-5448.
5. Mercado, G. E., Barr, F.G. (2005). "Looking Downstream of Sarcoma-Associated Chimeric Transcription Factors: When is a Target Really a Target?" *Cancer Biol. Ther.* 4(4): 456-8.
6. Macina R. A., Barr F. G., Galili N., Riethman H. C. (1995). Genomic organization of the human *PAX3* gene: DNA sequence analysis of the region disrupted in alveolar rhabdomyosarcoma. *Genomics*, 26: 1-8.
7. Goulding M. D., Chalepakis G., Deutsch U., Erselius J. R., Gruss P. (1991) Pax-3, a novel murine DNA binding protein expressed during early neurogenesis. *EMBO J.*, 10: 1135-1147.



8. Bennicelli J. L., Guerry D. I. (1993). Production of multiple cytokines by cultured human melanomas. *Exp. Dermatol.*, 2: 186-190.
9. Schulte T. W., Toretsky J. A., Ress E., Helman L., Neckers L. M. (1997) Expression of PAX3 in Ewing's sarcoma family of tumors. *Biochem. Mol. Med.*, 60: 121-126.
10. Hadjistilianou T, Mastrangelo D, Gragnoli A, Capretti MC, De Francesco S, Galluzzi P. (2002) Letter to the editor: neurofibromatosis type 1 (NF 1) associated with embryonal rhabdomyosarcoma of the orbit. *Med Pediatr Oncol.* 38. 6:449.
11. Dei Tos AP, Dal Cin P. (1997) The role of cytogenetics in the classification of soft tissue tumours. *Virchows Arch.* 431(2):83-94.
12. Woodruff JM, Christensen WN. Glandular peripheral nerve sheath tumors. *Cancer.* (1993). 72. 12:3618-28
13. Oguzkan, et al., (2006) Two neurofibromatosis type 1 cases associated with Rhabdomyosarcoma of bladder, one with a large deletion in the NF1 gene., *Cancer Genetics and Cytogenetics* 164, 159–163
14. Park, Ben Ho and Vogelstein, Bert (2003) *Cancer Medicine* Volume 6. BC Decker Inc. Hamilton, London
15. Lewin, Benjamin *Genes VII.* (2000). Oxford University Press
16. Robson, Ewan J. D., He, Shu-Jie, (2006) A Panorama of PAX Genes in Cancer and Development., *Nat Rev Cancer.* 6(1):52-62
17. Frith, et al., (2004) Spouge3 and Zhiping Weng Finding functional sequence elements by multiple local alignment *Nucleic Acids Research*, Vol. 32, No. 1 189±200
18. Liu, J.S., Neuwald, A.F. and Lawrence, C.E. (1995) Bayesian models for multiple local sequence alignment and Gibbs sampling strategies. *J. Am. Stat. Assoc.*, 90, 1156±1170.
19. Chen, Jianjun, Sun, Miao, Rowley, Janet D, Hurst, Laurence D, (2005) The small introns of antisense genes are better explained by selection for rapid transcription than by 'genomic design', *Genetics*, 171(4):2151-5.
20. Martin, Natalia, Patel, Satyakam, Segre, Julia (2004) A. Long-range comparison of human and mouse Sprr loci to identify conserved noncoding sequences involved in coordinate regulation. *Genome Res.* 14: 2430-2438
21. Vaiju Pethe, and P. V. Malathy Shekhar (1999). Estrogen Inducibility of c-Ha-ras Transcription in Breast Cancer Cells. Identification of Functional Estrogen-Responsive Transcriptional Regulatory Elements in Exon 1/Intron 1 of the c-Ha-ras Gene. *J. Biol. Chem.* 274: 30969-30978.
22. Dei Tos AP, Dal Cin P. (1997). The role of cytogenetics in the classification of soft tissue tumours. *Virchows Arch.* Aug;431(2):83-94. Review
23. Sorensen, Poul H.B., Lynch, James C., Qualman, Stephen J., Tirabosco, Roberto, Lim, Jerian F., Maurer, Harold M., Bridge, Julia A., Crist, William M., Triche, Timothy J., Barr, Frederic G. (2002). PAX3-FKHR and PAX7-FKHR Gene Fusions Are Prognostic Indicators in Alveolar Rhabdomyosarcoma: A Report From the Children's Oncology Group *J Clin Oncol.* 20: 2672-2679
24. Albert D. G. de Roos. (2005) Origins of introns based on the definition of exon modules and their conserved interfaces *Bioinformatics Advance Access*, DOI 10.1093/bioinformatics/bth475. *Bioinformatics* 21: 2-9.
25. Bennett T. K. Lee, Tin Wee Tan, and Shoba Ranganathan (2003) MG AlignIt: a web service for the alignment of mRNA/EST and genomic sequences. *Nucleic Acids Res.*; 31(13): 3533–3536.
26. Ari Patrinos. (2001). Initial sequencing and analysis of the human genome. The Genome International Sequencing Consortium. "*Nature* 409, 860-921.
27. Kevin Davies., (2001) *Cracking The Genome: Inside The Race To Unlock Human DNA.* Free Press, A division of Simon & Schuster, Inc.

## Nobel Prizes from 1901

Ma Hongbao

East Lansing, Michigan, USA, Email: [hongbao@msu.edu](mailto:hongbao@msu.edu)

The Nobel Prizes were set up by the final will of Alfred Nobel, a Swedish chemist, industrialist, and the inventor of dynamite on November 27, 1895 at the Swedish-Norwegian Club in Paris, which are awarding to people and organizations who have done outstanding research, invented groundbreaking techniques or equipment, or made outstanding contributions to society. The Nobel Prizes are generally awarded annually in the categories as following:

1. **Chemistry**, decided by the Royal Swedish Academy of Sciences
2. **Economics**, decided by the Royal Swedish Academy of Sciences
3. **Literature**, decided by the Swedish Academy
4. **Peace**, decided by the Norwegian Nobel Committee, appointed by the Norwegian Parliament, Stortinget
5. **Physics**, decided by the Royal Swedish Academy of Sciences
6. **Physiology or Medicine**, decided by Karolinska Institutet

Nobel Prizes are widely regarded as the highest prize in the world today. As of November 2005, a total of 776 Nobel Prizes have been awarded, 758 to individuals and 18 to organizations. [Nature and Science. 2006;4(3):86-94].

### I. List of All Nobel Prize Winners (1901 – 2005):

- |  |  |
|--|--|
| 1. <b>1901</b> - Chemistry, Jacobus H. van 't Hoff | 31. Physics, Philipp Lenard                      |
| 2. Literature, Sully Prudhomme                     | 32. <b>1906</b> - Chemistry, Henri Moissan       |
| 3. Medicine, Emil von Behring                      | 33. Literature, Giosuè Carducci                  |
| 4. Peace, Henry Dunant                             | 34. Medicine, Camillo Golgi                      |
| 5. Peace, Frédéric Passy                           | 35. Medicine, Santiago Ramón y Cajal             |
| 6. Physics, Wilhelm Conrad Röntgen                 | 36. Peace, Theodore Roosevelt                    |
| 7. <b>1902</b> - Chemistry, Emil Fischer           | 37. Physics, J.J. Thomson                        |
| 8. Literature, Theodor Mommsen                     | 38. <b>1907</b> - Chemistry, Eduard Buchner      |
| 9. Medicine, Ronald Ross                           | 39. Literature, Rudyard Kipling                  |
| 10. Peace, Élie Ducommun                           | 40. Medicine, Alphonse Laveran                   |
| 11. Peace, Albert Gobat                            | 41. Peace, Ernesto Teodoro Moneta                |
| 12. Physics, Hendrik A. Lorentz                    | 42. Peace, Louis Renault                         |
| 13. Physics, Pieter Zeeman                         | 43. Physics, Albert A. Michelson                 |
| 14. <b>1903</b> - Chemistry, Svante Arrhenius      | 44. <b>1908</b> - Chemistry, Ernest Rutherford   |
| 15. Literature, Bjørnstjerne Bjørnson              | 45. Literature, Rudolf Eucken                    |
| 16. Medicine, Niels Ryberg Finsen                  | 46. Medicine, Paul Ehrlich                       |
| 17. Peace, Randal Cremer                           | 47. Medicine, Ilya Mechnikov                     |
| 18. Physics, Henri Becquerel                       | 48. Peace, Klas Pontus Arnoldson                 |
| 19. Physics, Pierre Curie                          | 49. Peace, Fredrik Bajer                         |
| 20. Physics, Marie Curie                           | 50. Physics, Gabriel Lippmann                    |
| 21. <b>1904</b> - Chemistry, Sir William Ramsay    | 51. <b>1909</b> - Chemistry, Wilhelm Ostwald     |
| 22. Literature, José Echegaray                     | 52. Literature, Selma Lagerlöf                   |
| 23. Literature, Frédéric Mistral                   | 53. Medicine, Theodor Kocher                     |
| 24. Medicine, Ivan Pavlov                          | 54. Peace, Auguste Beernaert                     |
| 25. Peace, Institute of International Law          | 55. Peace, Paul Henri d'Estournelles de Constant |
| 26. Physics, Lord Rayleigh                         | 56. Physics, Ferdinand Braun                     |
| 27. <b>1905</b> - Chemistry, Adolf von Baeyer      | 57. Physics, Guglielmo Marconi                   |
| 28. Literature, Henryk Sienkiewicz                 | 58. <b>1910</b> - Chemistry, Otto Wallach        |
| 29. Medicine, Robert Koch                          | 59. Literature, Paul Heyse                       |
| 30. Peace, Bertha von Suttner                      | 60. Medicine, Albrecht Kossel                    |

61.	Peace, Permanent International Peace Bureau	113.	Literature, Knut Hamsun
62.	Physics, Johannes Diderik van der Waals	114.	Medicine, August Krogh
63.	<b>1911</b> - Chemistry, Marie Curie	115.	Peace, Léon Bourgeois
64.	Literature, Maurice Maeterlinck	116.	Physics, Charles Edouard Guillaume
65.	Medicine, Allvar Gullstrand	117.	<b>1921</b> - Chemistry, Frederick Soddy
66.	Peace, Tobias Asser	118.	Literature, Anatole France
67.	Peace, Alfred Fried	119.	Medicine, No Prize was Awarded
68.	Physics, Wilhelm Wien	120.	Peace, Hjalmar Branting
69.	<b>1912</b> - Chemistry, Victor Grignard	121.	Peace, Christian Lange
70.	Chemistry, Paul Sabatier	122.	Physics, Albert Einstein
71.	Literature, Gerhart Hauptmann	123.	<b>1922</b> - Chemistry, Francis W. Aston
72.	Medicine, Alexis Carrel	124.	Literature, Jacinto Benavente
73.	Peace, Elihu Root	125.	Medicine, Archibald V. Hill
74.	Physics, Gustaf Dalén	126.	Medicine, Otto Meyerhof
75.	<b>1913</b> - Chemistry, Alfred Werner	127.	Peace, Fridtjof Nansen
76.	Literature, Rabindranath Tagore	128.	Physics, Niels Bohr
77.	Medicine, Charles Richet	129.	<b>1923</b> - Chemistry, Fritz Pregl
78.	Peace, Henri La Fontaine	130.	Literature, William Butler Yeats
79.	Physics, Heike Kamerlingh Onnes	131.	Medicine, Frederick G. Banting
80.	<b>1914</b> - Chemistry, Theodore W. Richards	132.	Medicine, John Macleod
81.	Literature, No Prize was Awarded	133.	Peace, No Prize was Awarded
82.	Medicine, Robert Bárány	134.	Physics, Robert A. Millikan
83.	Peace, No Prize was Awarded	135.	<b>1924</b> - Chemistry, No Prize was Awarded
84.	Physics, Max von Laue	136.	Literature, Wladyslaw Reymont
85.	<b>1915</b> - Chemistry, Richard Willstätter	137.	Medicine, Willem Einthoven
86.	Literature, Romain Rolland	138.	Peace, No Prize was Awarded
87.	Medicine, No Prize was Awarded	139.	Physics, Manne Siegbahn
88.	Peace, No Prize was Awarded	140.	<b>1925</b> - Chemistry, Richard Zsigmondy
89.	Physics, William Bragg	141.	Literature, George Bernard Shaw
90.	Physics, Lawrence Bragg	142.	Medicine, No Prize was Awarded
91.	<b>1916</b> - Chemistry, No Prize was Awarded	143.	Peace, Sir Austen Chamberlain
92.	Literature, Verner von Heidenstam	144.	Peace, Charles G. Dawes
93.	Medicine, No Prize was Awarded	145.	Physics, James Franck
94.	Peace, No Prize was Awarded	146.	Physics, Gustav Hertz
95.	Physics, No Prize was Awarded	147.	<b>1926</b> - Chemistry, The Svedberg
96.	<b>1917</b> - Chemistry, No Prize was Awarded	148.	Literature, Grazia Deledda
97.	Literature, Karl Gjellerup	149.	Medicine, Johannes Fibiger
98.	Literature, Henrik Pontoppidan	150.	Peace, Aristide Briand
99.	Medicine, No Prize was Awarded	151.	Peace, Gustav Stresemann
100.	Peace, International Committee of the Red Cross	152.	Physics, Jean Baptiste Perrin
101.	Physics, Charles Glover Barkla	153.	<b>1927</b> - Chemistry, Heinrich Wieland
102.	<b>1918</b> - Chemistry, Fritz Haber	154.	Literature, Henri Bergson
103.	Literature, No Prize was Awarded	155.	Medicine, Julius Wagner-Jauregg
104.	Medicine, No Prize was Awarded	156.	Peace, Ferdinand Buisson
105.	Peace, No Prize was Awarded	157.	Peace, Ludwig Quidde
106.	Physics, Max Planck	158.	Physics, Arthur H. Compton
107.	<b>1919</b> - Chemistry, No Prize was Awarded	159.	Physics, C.T.R. Wilson
108.	Literature, Carl Spitteler	160.	<b>1928</b> - Chemistry, Adolf Windaus
109.	Medicine, Jules Bordet	161.	Literature, Sigrid Undset
110.	Peace, Woodrow Wilson	162.	Medicine, Charles Nicolle
111.	Physics, Johannes Stark	163.	Peace, No Prize was Awarded
112.	<b>1920</b> - Chemistry, Walther Nernst	164.	Physics, Owen Willans Richardson
		165.	<b>1929</b> - Chemistry, Arthur Harden
		166.	Chemistry, Hans von Euler-Chelpin

167. Literature, Thomas Mann  
 168. Medicine, Christiaan Eijkman  
 169. Medicine, Sir Frederick Hopkins  
 170. Peace, Frank B. Kellogg  
 171. Physics, Louis de Broglie  
 172. **1930** - Chemistry, Hans Fischer  
 173. Literature, Sinclair Lewis  
 174. Medicine, Karl Landsteiner  
 175. Peace, Nathan Söderblom  
 176. Physics, Venkata Raman  
 177. **1931** - Chemistry, Friedrich Bergius  
 178. Chemistry, Carl Bosch  
 179. Literature, Erik Axel Karlfeldt  
 180. Medicine, Otto Warburg  
 181. Peace, Jane Addams  
 182. Peace, Nicholas Murray Butler  
 183. Physics, No Prize was Awarded  
 184. **1932** - Chemistry, Irving Langmuir  
 185. Literature, John Galsworthy  
 186. Medicine, Edgar Adrian  
 187. Medicine, Sir Charles Sherrington  
 188. Peace, No Prize was Awarded  
 189. Physics, Werner Heisenberg  
 190. **1933** - Chemistry, No Prize was Awarded  
 191. Literature, Ivan Bunin  
 192. Medicine, Thomas H. Morgan  
 193. Peace, Sir Norman Angell  
 194. Physics, Paul A.M. Dirac  
 195. Physics, Erwin Schrödinger  
 196. **1934** - Chemistry, Harold C. Urey  
 197. Literature, Luigi Pirandello  
 198. Medicine, George R. Minot  
 199. Medicine, William P. Murphy  
 200. Medicine, George H. Whipple  
 201. Peace, Arthur Henderson  
 202. Physics, No Prize was Awarded  
 203. **1935** - Chemistry, Frédéric Joliot  
 204. Chemistry, Irène Joliot-Curie  
 205. Literature, No Prize was Awarded  
 206. Medicine, Hans Spemann  
 207. Peace, Carl von Ossietzky  
 208. Physics, James Chadwick  
 209. **1936** - Chemistry, Peter Debye  
 210. Literature, Eugene O'Neill  
 211. Medicine, Sir Henry Dale  
 212. Medicine, Otto Loewi  
 213. Peace, Carlos Saavedra Lamas  
 214. Physics, Carl D. Anderson  
 215. Physics, Victor F. Hess  
 216. **1937** - Chemistry, Norman Haworth  
 217. Chemistry, Paul Karrer  
 218. Literature, Roger Martin du Gard  
 219. Medicine, Albert Szent-Györgyi  
 220. Peace, Robert Cecil  
 221. Physics, Clinton Davisson  
 222. Physics, George Paget Thomson  
 223. **1938** - Chemistry, Richard Kuhn  
 224. Literature, Pearl Buck  
 225. Medicine, Corneille Heymans  
 226. Peace, Nansen International Office for Refugees  
 227. Physics, Enrico Fermi  
 228. **1939** - Chemistry, Adolf Butenandt  
 229. Chemistry, Leopold Ruzicka  
 230. Literature, Frans Eemil Sillanpää  
 231. Medicine, Gerhard Domagk  
 232. Peace, No Prize was Awarded  
 233. Physics, Ernest Lawrence  
 234. **1940** - Chemistry, No Prize was Awarded  
 235. Literature, No Prize was Awarded  
 236. Medicine, No Prize was Awarded  
 237. Peace, No Prize was Awarded  
 238. Physics, No Prize was Awarded  
 239. **1941** - Chemistry, No Prize was Awarded  
 240. Literature, No Prize was Awarded  
 241. Medicine, No Prize was Awarded  
 242. Peace, No Prize was Awarded  
 243. Physics, No Prize was Awarded  
 244. **1942** - Chemistry, No Prize was Awarded  
 245. Literature, No Prize was Awarded  
 246. Medicine, No Prize was Awarded  
 247. Peace, No Prize was Awarded  
 248. Physics, No Prize was Awarded  
 249. **1943** - Chemistry, George de Hevesy  
 250. Literature, No Prize was Awarded  
 251. Medicine, Henrik Dam  
 252. Medicine, Edward A. Doisy  
 253. Peace, No Prize was Awarded  
 254. Physics, Otto Stern  
 255. **1944** - Chemistry, Otto Hahn  
 256. Literature, Johannes V. Jensen  
 257. Medicine, Joseph Erlanger  
 258. Medicine, Herbert S. Gasser  
 259. Peace, International Committee of the Red Cross  
 260. Physics, Isidor Isaac Rabi  
 261. **1945** - Chemistry, Artturi Virtanen  
 262. Literature, Gabriela Mistral  
 263. Medicine, Ernst B. Chain  
 264. Medicine, Sir Alexander Fleming  
 265. Medicine, Sir Howard Florey  
 266. Peace, Cordell Hull  
 267. Physics, Wolfgang Pauli  
 268. **1946** - Chemistry, John H. Northrop  
 269. Chemistry, Wendell M. Stanley  
 270. Chemistry, James B. Sumner  
 271. Literature, Hermann Hesse  
 272. Medicine, Hermann J. Muller

273.	Peace, Emily Greene Balch	326.	Medicine, Frederick C. Robbins
274.	Peace, John R. Mott	327.	Medicine, Thomas H. Weller
275.	Physics, Percy W. Bridgman	328.	Peace, Office of the United Nations High Commissioner for Refugees
276.	<b>1947</b> - Chemistry, Sir Robert Robinson	329.	Physics, Max Born
277.	Literature, André Gide	330.	Physics, Walther Bothe
278.	Medicine, Carl Cori	331.	<b>1955</b> - Chemistry, Vincent du Vigneaud
279.	Medicine, Gerty Cori	332.	Literature, Halldór Laxness
280.	Medicine, Bernardo Houssay	333.	Medicine, Hugo Theorell
281.	Peace, Friends Service Council	334.	Peace, No Prize was Awarded
282.	Peace, American Friends Service Committee	335.	Physics, Polykarp Kusch
283.	Physics, Edward V. Appleton	336.	Physics, Willis E. Lamb
284.	<b>1948</b> - Chemistry, Arne Tiselius	337.	<b>1956</b> - Chemistry, Sir Cyril Hinshelwood
285.	Literature, T.S. Eliot	338.	Chemistry, Nikolay Semenov
286.	Medicine, Paul Müller	339.	Literature, Juan Ramón Jiménez
287.	Peace, No Prize was Awarded	340.	Medicine, André F. Cournand
288.	Physics, Patrick M.S. Blackett	341.	Medicine, Werner Forssmann
289.	<b>1949</b> - Chemistry, William F. Giaouque	342.	Medicine, Dickinson W. Richards
290.	Literature, William Faulkner	343.	Peace, No Prize was Awarded
291.	Medicine, Walter Hess	344.	Physics, John Bardeen
292.	Medicine, Egon Moniz	345.	Physics, Walter H. Brattain
293.	Peace, Lord Boyd Orr	346.	Physics, William B. Shockley
294.	Physics, Hideki Yukawa	347.	<b>1957</b> - Chemistry, Lord Todd
295.	<b>1950</b> - Chemistry, Kurt Alder	348.	Literature, Albert Camus
296.	Chemistry, Otto Diels	349.	Medicine, Daniel Bovet
297.	Literature, Bertrand Russell	350.	Peace, Lester Bowles Pearson
298.	Medicine, Philip S. Hench	351.	Physics, Tsung-Dao Lee
299.	Medicine, Edward C. Kendall	352.	Physics, Chen Ning Yang
300.	Medicine, Tadeus Reichstein	353.	<b>1958</b> - Chemistry, Frederick Sanger
301.	Peace, Ralph Bunche	354.	Literature, Boris Pasternak
302.	Physics, Cecil Powell	355.	Medicine, George Beadle
303.	<b>1951</b> - Chemistry, Edwin M. McMillan	356.	Medicine, Joshua Lederberg
304.	Chemistry, Glenn T. Seaborg	357.	Medicine, Edward Tatum
305.	Literature, Pär Lagerkvist	358.	Peace, Georges Pire
306.	Medicine, Max Theiler	359.	Physics, Pavel A. Cherenkov
307.	Peace, Léon Jouhaux	360.	Physics, Il'ja M. Frank
308.	Physics, John Cockcroft	361.	Physics, Igor Y. Tamm
309.	Physics, Ernest T.S. Walton	362.	<b>1959</b> - Chemistry, Jaroslav Heyrovsky
310.	<b>1952</b> - Chemistry, Archer J.P. Martin	363.	Literature, Salvatore Quasimodo
311.	Chemistry, Richard L.M. Synge	364.	Medicine, Arthur Kornberg
312.	Literature, François Mauriac	365.	Medicine, Severo Ochoa
313.	Medicine, Selman A. Waksman	366.	Peace, Philip Noel-Baker
314.	Peace, Albert Schweitzer	367.	Physics, Owen Chamberlain
315.	Physics, Felix Bloch	368.	Physics, Emilio Segrè
316.	Physics, E. M. Purcell	369.	<b>1960</b> - Chemistry, Willard F. Libby
317.	<b>1953</b> - Chemistry, Hermann Staudinger	370.	Literature, Saint-John Perse
318.	Literature, Winston Churchill	371.	Medicine, Sir Frank Macfarlane Burnet
319.	Medicine, Hans Krebs	372.	Medicine, Peter Medawar
320.	Medicine, Fritz Lipmann	373.	Peace, Albert Lutuli
321.	Peace, George C. Marshall	374.	Physics, Donald A. Glaser
322.	Physics, Frits Zernike	375.	<b>1961</b> - Chemistry, Melvin Calvin
323.	<b>1954</b> - Chemistry, Linus Pauling	376.	Literature, Ivo Andrić
324.	Literature, Ernest Hemingway	377.	Medicine, Georg von Békésy
325.	Medicine, John F. Enders	378.	Peace, Dag Hammarskjöld

379. Physics, Robert Hofstadter  
380. Physics, Rudolf Mössbauer  
381. **1962** - Chemistry, John C. Kendrew  
382. Chemistry, Max F. Perutz  
383. Literature, John Steinbeck  
384. Medicine, Francis Crick  
385. Medicine, James Watson  
386. Medicine, Maurice Wilkins  
387. Peace, Linus Pauling  
388. Physics, Lev Landau  
389. **1963** - Chemistry, Giulio Natta  
390. Chemistry, Karl Ziegler  
391. Literature, Giorgos Seferis  
392. Medicine, Sir John Eccles  
393. Medicine, Alan L. Hodgkin  
394. Medicine, Andrew F. Huxley  
395. Peace, International Committee of the Red Cross  
396. Peace, League of Red Cross Societies  
397. Physics, Maria Goeppert-Mayer  
398. Physics, J. Hans D. Jensen  
399. Physics, Eugene Wigner  
400. **1964** - Chemistry, Dorothy Crowfoot Hodgkin  
401. Literature, Jean-Paul Sartre  
402. Medicine, Konrad Bloch  
403. Medicine, Feodor Lynen  
404. Peace, Martin Luther King  
405. Physics, Nicolay G. Basov  
406. Physics, Aleksandr M. Prokhorov  
407. Physics, Charles H. Townes  
408. **1965** - Chemistry, Robert B. Woodward  
409. Literature, Mikhail Sholokhov  
410. Medicine, François Jacob  
411. Medicine, André Lwoff  
412. Medicine, Jacques Monod  
413. Peace, United Nations Children's Fund  
414. Physics, Richard P. Feynman  
415. Physics, Julian Schwinger  
416. Physics, Sin-Itiro Tomonaga  
417. **1966** - Chemistry, Robert S. Mulliken  
418. Literature, Samuel Agnon  
419. Literature, Nelly Sachs  
420. Medicine, Charles B. Huggins  
421. Medicine, Peyton Rous  
422. Peace, No Prize was Awarded  
423. Physics, Alfred Kastler  
424. **1967** - Chemistry, Manfred Eigen  
425. Chemistry, Ronald G.W. Norrish  
426. Chemistry, George Porter  
427. Literature, Miguel Angel Asturias  
428. Medicine, Ragnar Granit  
429. Medicine, Haldan K. Hartline  
430. Medicine, George Wald  
431. Peace, No Prize was Awarded  
432. Physics, Hans Bethe  
433. **1968** - Chemistry, Lars Onsager  
434. Literature, Yasunari Kawabata  
435. Medicine, Robert W. Holley  
436. Medicine, H. Gobind Khorana  
437. Medicine, Marshall W. Nirenberg  
438. Peace, René Cassin  
439. Physics, Luis Alvarez  
440. **1969** - Chemistry, Derek Barton  
441. Chemistry, Odd Hassel  
442. Economics, Ragnar Frisch  
443. Economics, Jan Tinbergen  
444. Literature, Samuel Beckett  
445. Medicine, Max Delbrück  
446. Medicine, Alfred D. Hershey  
447. Medicine, Salvador E. Luria  
448. Peace, International Labour Organization  
449. Physics, Murray Gell-Mann  
450. **1970** - Chemistry, Luis Leloir  
451. Economics, Paul A. Samuelson  
452. Literature, Alexandr Solzhenitsyn  
453. Medicine, Julius Axelrod  
454. Medicine, Sir Bernard Katz  
455. Medicine, Ulf von Euler  
456. Peace, Norman Borlaug  
457. Physics, Hannes Alfvén  
458. Physics, Louis Néel  
459. **1971** - Chemistry, Gerhard Herzberg  
460. Economics, Simon Kuznets  
461. Literature, Pablo Neruda  
462. Medicine, Earl W. Sutherland, Jr.  
463. Peace, Willy Brandt  
464. Physics, Dennis Gabor  
465. **1972** - Chemistry, Christian Anfinsen  
466. Chemistry, Stanford Moore  
467. Chemistry, William H. Stein  
468. Economics, Kenneth J. Arrow  
469. Economics, John R. Hicks  
470. Literature, Heinrich Böll  
471. Medicine, Gerald M. Edelman  
472. Medicine, Rodney R. Porter  
473. Peace, No Prize was Awarded  
474. Physics, John Bardeen  
475. Physics, Leon N. Cooper  
476. Physics, Robert Schrieffer  
477. **1973** - Chemistry, Ernst Otto Fischer  
478. Chemistry, Geoffrey Wilkinson  
479. Economics, Wassily Leontief  
480. Literature, Patrick White  
481. Medicine, Konrad Lorenz  
482. Medicine, Nikolaas Tinbergen  
483. Medicine, Karl von Frisch  
484. Peace, Le Duc Tho  
485. Peace, Henry Kissinger

486. Physics, Leo Esaki  
 487. Physics, Ivar Giaever  
 488. Physics, Brian D. Josephson  
 489. **1974** - Chemistry, Paul J. Flory  
 490. Economics, Gunnar Myrdal  
 491. Economics, Friedrich August von Hayek  
 492. Literature, Eyvind Johnson  
 493. Literature, Harry Martinson  
 494. Medicine, Albert Claude  
 495. Medicine, Christian de Duve  
 496. Medicine, George E. Palade  
 497. Peace, Seán MacBride  
 498. Peace, Eisaku Sato  
 499. Physics, Antony Hewish  
 500. Physics, Martin Ryle  
 501. **1975** - Chemistry, John Cornforth  
 502. Chemistry, Vladimir Prelog  
 503. Economics, Leonid Vitaliyevich Kantorovich  
 504. Economics, Tjalling C. Koopmans  
 505. Literature, Eugenio Montale  
 506. Medicine, David Baltimore  
 507. Medicine, Renato Dulbecco  
 508. Medicine, Howard M. Temin  
 509. Peace, Andrei Sakharov  
 510. Physics, Aage N. Bohr  
 511. Physics, Ben R. Mottelson  
 512. Physics, James Rainwater  
 513. **1976** - Chemistry, William Lipscomb  
 514. Economics, Milton Friedman  
 515. Literature, Saul Bellow  
 516. Medicine, Baruch S. Blumberg  
 517. Medicine, D. Carleton Gajdusek  
 518. Peace, Mairead Corrigan  
 519. Peace, Betty Williams  
 520. Physics, Burton Richter  
 521. Physics, Samuel C.C. Ting  
 522. **1977** - Chemistry, Ilya Prigogine  
 523. Economics, James E. Meade  
 524. Economics, Bertil Ohlin  
 525. Literature, Vicente Aleixandre  
 526. Medicine, Roger Guillemin  
 527. Medicine, Andrew V. Schally  
 528. Medicine, Rosalyn Yalow  
 529. Peace, Amnesty International  
 530. Physics, Philip W. Anderson  
 531. Physics, Sir Nevill F. Mott  
 532. Physics, John H. van Vleck  
 533. **1978** - Chemistry, Peter Mitchell  
 534. Economics, Herbert A. Simon  
 535. Literature, Isaac Bashevis Singer  
 536. Medicine, Werner Arber  
 537. Medicine, Daniel Nathans  
 538. Medicine, Hamilton O. Smith  
 539. Peace, Anwar al-Sadat  
 540. Peace, Menachem Begin  
 541. Physics, Pyotr Kapitsa  
 542. Physics, Arno Penzias  
 543. Physics, Robert Woodrow Wilson  
 544. **1979** - Chemistry, Herbert C. Brown  
 545. Chemistry, Georg Wittig  
 546. Economics, Sir Arthur Lewis  
 547. Economics, Theodore W. Schultz  
 548. Literature, Odysseus Elytis  
 549. Medicine, Allan M. Cormack  
 550. Medicine, Godfrey N. Hounsfield  
 551. Peace, Mother Teresa  
 552. Physics, Sheldon Glashow  
 553. Physics, Abdus Salam  
 554. Physics, Steven Weinberg  
 555. **1980** - Chemistry, Paul Berg  
 556. Chemistry, Walter Gilbert  
 557. Chemistry, Frederick Sanger  
 558. Economics, Lawrence R. Klein  
 559. Literature, Czeslaw Milosz  
 560. Medicine, Baruj Benacerraf  
 561. Medicine, Jean Dausset  
 562. Medicine, George D. Snell  
 563. Peace, Adolfo Pérez Esquivel  
 564. Physics, James Cronin  
 565. Physics, Val Fitch  
 566. **1981** - Chemistry, Kenichi Fukui  
 567. Chemistry, Roald Hoffmann  
 568. Economics, James Tobin  
 569. Literature, Elias Canetti  
 570. Medicine, David H. Hubel  
 571. Medicine, Roger W. Sperry  
 572. Medicine, Torsten N. Wiesel  
 573. Peace, Office of the United Nations High Commissioner for Refugees  
 574. Physics, Nicolaas Bloembergen  
 575. Physics, Arthur L. Schawlow  
 576. Physics, Kai M. Siegbahn  
 577. **1982** - Chemistry, Aaron Klug  
 578. Economics, George J. Stigler  
 579. Literature, Gabriel García Márquez  
 580. Medicine, Sune K. Bergström  
 581. Medicine, Bengt I. Samuelsson  
 582. Medicine, John R. Vane  
 583. Peace, Alfonso García Robles  
 584. Peace, Alva Myrdal  
 585. Physics, Kenneth G. Wilson  
 586. **1983** - Chemistry, Henry Taube  
 587. Economics, Gerard Debreu  
 588. Literature, William Golding  
 589. Medicine, Barbara McClintock  
 590. Peace, Lech Walesa  
 591. Physics, Subramanyan Chandrasekhar

592. Physics, William A. Fowler  
 593. **1984** - Chemistry, Bruce Merrifield  
 594. Economics, Richard Stone  
 595. Literature, Jaroslav Seifert  
 596. Medicine, Niels K. Jerne  
 597. Medicine, Georges J.F. Köhler  
 598. Medicine, César Milstein  
 599. Peace, Desmond Tutu  
 600. Physics, Carlo Rubbia  
 601. Physics, Simon van der Meer  
 602. **1985** - Chemistry, Herbert A. Hauptman  
 603. Chemistry, Jerome Karle  
 604. Economics, Franco Modigliani  
 605. Literature, Claude Simon  
 606. Medicine, Michael S. Brown  
 607. Medicine, Joseph L. Goldstein  
 608. Peace, International Physicians for the Prevention of Nuclear War  
 609. Physics, Klaus von Klitzing  
 610. **1986** - Chemistry, Dudley R. Herschbach  
 611. Chemistry, Yuan T. Lee  
 612. Chemistry, John C. Polanyi  
 613. Economics, James M. Buchanan Jr.  
 614. Literature, Wole Soyinka  
 615. Medicine, Stanley Cohen  
 616. Medicine, Rita Levi-Montalcini  
 617. Peace, Elie Wiesel  
 618. Physics, Gerd Binnig  
 619. Physics, Heinrich Rohrer  
 620. Physics, Ernst Ruska  
 621. **1987** - Chemistry, Donald J. Cram  
 622. Chemistry, Jean-Marie Lehn  
 623. Chemistry, Charles J. Pedersen  
 624. Economics, Robert M. Solow  
 625. Literature, Joseph Brodsky  
 626. Medicine, Susumu Tonegawa  
 627. Peace, Oscar Arias Sánchez  
 628. Physics, J. Georg Bednorz  
 629. Physics, K. Alex Müller  
 630. **1988** - Chemistry, Johann Deisenhofer  
 631. Chemistry, Robert Huber  
 632. Chemistry, Hartmut Michel  
 633. Economics, Maurice Allais  
 634. Literature, Naguib Mahfouz  
 635. Medicine, Sir James W. Black  
 636. Medicine, Gertrude B. Elion  
 637. Medicine, George H. Hitchings  
 638. Peace, United Nations Peacekeeping Forces  
 639. Physics, Leon M. Lederman  
 640. Physics, Melvin Schwartz  
 641. Physics, Jack Steinberger  
 642. **1989** - Chemistry, Sidney Altman  
 643. Chemistry, Thomas R. Cech  
 644. Economics, Trygve Haavelmo  
 645. Literature, Camilo José Cela  
 646. Medicine, J. Michael Bishop  
 647. Medicine, Harold E. Varmus  
 648. Peace, The 14th Dalai Lama  
 649. Physics, Hans G. Dehmelt  
 650. Physics, Wolfgang Paul  
 651. Physics, Norman F. Ramsey  
 652. **1990** - Chemistry, Elias James Corey  
 653. Economics, Harry M. Markowitz  
 654. Economics, Merton H. Miller  
 655. Economics, William F. Sharpe  
 656. Literature, Octavio Paz  
 657. Medicine, Joseph E. Murray  
 658. Medicine, E. Donnall Thomas  
 659. Peace, Mikhail Gorbachev  
 660. Physics, Jerome I. Friedman  
 661. Physics, Henry W. Kendall  
 662. Physics, Richard E. Taylor  
 663. **1991** - Chemistry, Richard R. Ernst  
 664. Economics, Ronald H. Coase  
 665. Literature, Nadine Gordimer  
 666. Medicine, Erwin Neher  
 667. Medicine, Bert Sakmann  
 668. Peace, Aung San Suu Kyi  
 669. Physics, Pierre-Gilles de Gennes  
 670. **1992** - Chemistry, Rudolph A. Marcus  
 671. Economics, Gary S. Becker  
 672. Literature, Derek Walcott  
 673. Medicine, Edmond H. Fischer  
 674. Medicine, Edwin G. Krebs  
 675. Peace, Rigoberta Menchú Tum  
 676. Physics, Georges Charpak  
 677. **1993** - Chemistry, Kary B. Mullis  
 678. Chemistry, Michael Smith  
 679. Economics, Robert W. Fogel  
 680. Economics, Douglass C. North  
 681. Literature, Toni Morrison  
 682. Medicine, Richard J. Roberts  
 683. Medicine, Phillip A. Sharp  
 684. Peace, F.W. de Klerk  
 685. Peace, Nelson Mandela  
 686. Physics, Russell A. Hulse  
 687. Physics, Joseph H. Taylor Jr.  
 688. **1994** - Chemistry, George A. Olah  
 689. Economics, John C. Harsanyi  
 690. Economics, John F. Nash Jr.  
 691. Economics, Reinhard Selten  
 692. Literature, Kenzaburo Oe  
 693. Medicine, Alfred G. Gilman  
 694. Medicine, Martin Rodbell  
 695. Peace, Yasser Arafat  
 696. Peace, Shimon Peres  
 697. Peace, Yitzhak Rabin  
 698. Physics, Bertram N. Brockhouse



699. Physics, Clifford G. Shull  
 700. **1995** - Chemistry, Paul J. Crutzen  
 701. Chemistry, Mario J. Molina  
 702. Chemistry, F. Sherwood Rowland  
 703. Economics, Robert E. Lucas Jr.  
 704. Literature, Seamus Heaney  
 705. Medicine, Edward B. Lewis  
 706. Medicine, Christiane Nüsslein-Volhard  
 707. Medicine, Eric F. Wieschaus  
 708. Peace, Pugwash Conferences on Science and World Affairs  
 709. Peace, Joseph Rotblat  
 710. Physics, Martin L. Perl  
 711. Physics, Frederick Reines  
 712. **1996** - Chemistry, Robert F. Curl Jr.  
 713. Chemistry, Sir Harold Kroto  
 714. Chemistry, Richard E. Smalley  
 715. Economics, James A. Mirrlees  
 716. Economics, William Vickrey  
 717. Literature, Wislawa Szymborska  
 718. Medicine, Peter C. Doherty  
 719. Medicine, Rolf M. Zinkernagel  
 720. Peace, Carlos Filipe Ximenes Belo  
 721. Peace, José Ramos-Horta  
 722. Physics, David M. Lee  
 723. Physics, Douglas D. Osheroff  
 724. Physics, Robert C. Richardson  
 725. **1997** - Chemistry, Paul D. Boyer  
 726. Chemistry, Jens C. Skou  
 727. Chemistry, John E. Walker  
 728. Economics, Robert C. Merton  
 729. Economics, Myron S. Scholes  
 730. Literature, Dario Fo  
 731. Medicine, Stanley B. Prusiner  
 732. Peace, International Campaign to Ban Landmines  
 733. Peace, Jody Williams  
 734. Physics, Steven Chu  
 735. Physics, Claude Cohen-Tannoudji  
 736. Physics, William D. Phillips  
 737. **1998** - Chemistry, Walter Kohn  
 738. Chemistry, John Pople  
 739. Economics, Amartya Sen  
 740. Literature, José Saramago  
 741. Medicine, Robert F. Furchgott  
 742. Medicine, Louis J. Ignarro  
 743. Medicine, Ferid Murad  
 744. Peace, John Hume  
 745. Peace, David Trimble  
 746. Physics, Robert B. Laughlin  
 747. Physics, Horst L. Störmer  
 748. Physics, Daniel C. Tsui  
 749. **1999** - Chemistry, Ahmed Zewail  
 750. Economics, Robert A. Mundell  
 751. Literature, Günter Grass  
 752. Medicine, Günter Blobel  
 753. Peace, Médecins Sans Frontières  
 754. Physics, Gerardus 't Hooft  
 755. Physics, Martinus J.G. Veltman  
 756. **2000** - Chemistry, Alan Heeger  
 757. Chemistry, Alan G. MacDiarmid  
 758. Chemistry, Hideki Shirakawa  
 759. Economics, James J. Heckman  
 760. Economics, Daniel L. McFadden  
 761. Literature, Gao Xingjian  
 762. Medicine, Arvid Carlsson  
 763. Medicine, Paul Greengard  
 764. Medicine, Eric R. Kandel  
 765. Peace, Kim Dae-jung  
 766. Physics, Zhores I. Alferov  
 767. Physics, Jack S. Kilby  
 768. Physics, Herbert Kroemer  
 769. **2001** - Chemistry, William S. Knowles  
 770. Chemistry, Ryoji Noyori  
 771. Chemistry, K. Barry Sharpless  
 772. Economics, George A. Akerlof  
 773. Economics, A. Michael Spence  
 774. Economics, Joseph E. Stiglitz  
 775. Literature, V.S. Naipaul  
 776. Medicine, Leland H. Hartwell  
 777. Medicine, Tim Hunt  
 778. Medicine, Sir Paul Nurse  
 779. Peace, United Nations  
 780. Peace, Kofi Annan  
 781. Physics, Eric A. Cornell  
 782. Physics, Wolfgang Ketterle  
 783. Physics, Carl E. Wieman  
 784. **2002** - Chemistry, John B. Fenn  
 785. Chemistry, Koichi Tanaka  
 786. Chemistry, Kurt Wüthrich  
 787. Economics, Daniel Kahneman  
 788. Economics, Vernon L. Smith  
 789. Literature, Imre Kertész  
 790. Medicine, Sydney Brenner  
 791. Medicine, H. Robert Horvitz  
 792. Medicine, John E. Sulston  
 793. Peace, Jimmy Carter  
 794. Physics, Raymond Davis Jr.  
 795. Physics, Riccardo Giacconi  
 796. Physics, Masatoshi Koshiha  
 797. **2003** - Chemistry, Peter Agre  
 798. Chemistry, Roderick MacKinnon  
 799. Economics, Robert F. Engle III  
 800. Economics, Clive W.J. Granger  
 801. Literature, J.M. Coetzee  
 802. Medicine, Paul C. Lauterbur  
 803. Medicine, Sir Peter Mansfield  
 804. Peace, Shirin Ebadi  
 805. Physics, Alexei A. Abrikosov

806. Physics, Vitaly L. Ginzburg  
 807. Physics, Anthony J. Leggett  
 808. **2004** - Chemistry, Aaron Ciechanover  
 809. Chemistry, Avram Hershko  
 810. Chemistry, Irwin Rose  
 811. Economics, Finn E. Kydland  
 812. Economics, Edward C. Prescott  
 813. Literature, Elfriede Jelinek  
 814. Medicine, Richard Axel  
 815. Medicine, Linda B. Buck  
 816. Peace, Wangari Maathai  
 817. Physics, David J. Gross  
 818. Physics, H. David Politzer  
 819. Physics, Frank Wilczek  
 820. **2005** - Chemistry, Yves Chauvin  
 821. Chemistry, Robert H. Grubbs  
 822. Chemistry, Richard R. Schrock  
 823. Economics, Robert J. Aumann  
 824. Economics, Thomas C. Schelling  
 825. Literature, Harold Pinter  
 826. Medicine, Barry J. Marshall  
 827. Medicine, J. Robin Warren  
 828. Peace, International Atomic Energy Agency  
 829. Peace, Mohamed ElBaradei  
 830. Physics, Roy J. Glauber  
 831. Physics, John L. Hall  
 832. Physics, Theodor W. Hänsch

## II. Prize Awarded Organizations (All are Peace Prizes)

1. 1904 - Institute of International Law
2. 1910 - Permanent International Peace Bureau
3. 1917 - International Committee of the Red Cross
4. 1938 - Nansen International Office for Refugees
5. 1944 - International Committee of the Red Cross
6. 1947 - Friends Service Council
7. 1947 - American Friends Service Committee
8. 1954 - Office of the United Nations High Commissioner for Refugees
9. 1963 - International Committee of the Red Cross
10. 1963 - League of Red Cross Societies
11. 1965 - United Nations Children's Fund
12. 1969 - International Labour Organization
13. 1977 - Amnesty International
14. 1981 - Office of the United Nations High Commissioner for Refugees
15. 1985 - International Physicians for the Prevention of Nuclear War
16. 1988 - United Nations Peacekeeping Forces

17. 1995 - Pugwash Conferences on Science and World Affairs
18. 1997 - International Campaign to Ban Landmines
19. 1999 - Médecins Sans Frontières
20. 2001 - United Nations
21. 2005 - International Atomic Energy Agency

## III. Women Prize Winners

### Chemistry

1. 1911 - Marie Curie
2. 1935 - Irène Joliot-Curie
3. 1964 - Dorothy Crowfoot Hodgkin

### Literature

1. 1909 - Selma Lagerlöf
2. 1926 - Grazia Deledda
3. 1928 - Sigrid Undset
4. 1938 - Pearl Buck
5. 1945 - Gabriela Mistral
6. 1966 - Nelly Sachs
7. 1991 - Nadine Gordimer
8. 1993 - Toni Morrison
9. 1996 - Wislawa Szymborska
10. 2004 - Elfriede Jelinek

### Peace


1. 1905 - Bertha von Suttner
2. 1931 - Jane Addams
3. 1946 - Emily Greene Balch
4. 1976 - Betty Williams
5. 1976 - Mairead Corrigan
6. 1979 - Mother Teresa
7. 1982 - Alva Myrdal
8. 1991 - Aung San Suu Kyi
9. 1992 - Rigoberta Menchú Tum
10. 1997 - Jody Williams
11. 2003 - Shirin Ebadi
12. 2004 - Wangari Maathai

### Physics

1. 1903 - Marie Curie
2. 1963 - Maria Goeppert-Mayer

### Physiology or Medicine

1. 1947 - Gerty Cori
2. 1977 - Rosalyn Yalow
3. 1983 - Barbara McClintock
4. 1986 - Rita Levi-Montalcini
5. 1988 - Gertrude B. Elion
6. 1995 - Christiane Nüsslein-Volhard
7. 2004 - Linda B. Buck




**SIDNEY KIMMEL  
CANCER CENTER**  
Conference on

**New Targets and Delivery Systems  
in Cancer Diagnosis and Treatment**

*Chairs: A. Deisseroth, J. Schnitzer, R. Weichselbaum, N. Habib*

**March 5-7, 2007**



**HOTEL DEL CORONADO**  
San Diego, CA

---


TOPICS INCLUDE

- New Targets in Cancer Cells
- New Targets in Tumor Microenvironment & Vasculature
- Imaging Through Nanoparticles, Vectors & Recombinant Biologics
- Tumor Inflammation and Cell Homing
- Molecular Targeting
- Nanomedicine
- Cellular and Molecular Delivery Systems
- Emerging Strategies for Cancer Diagnosis & Treatment

*Reduced Registration fees for Postdoctoral Fellows*

Visit the Conference Web Site for Updates on:  
Call for Abstracts, Program, Registration  
Website: <http://www.skcc.org>

E-mail: [skcc@pcmisandiego.com](mailto:skcc@pcmisandiego.com)




**SIDNEY KIMMEL  
CANCER CENTER**  
Conference on

**New Targets and Delivery Systems  
in Cancer Diagnosis and Treatment**

*Chairs: A. Deisseroth, J. Schnitzer, R. Weichselbaum, N. Habib*

**March 5-7, 2007**



**HOTEL DEL CORONADO**  
San Diego, CA

---


TOPICS INCLUDE

- New Targets in Cancer Cells
- New Targets in Tumor Microenvironment & Vasculature
- Imaging Through Nanoparticles, Vectors & Recombinant Biologics
- Tumor Inflammation and Cell Homing
- Molecular Targeting
- Nanomedicine
- Cellular and Molecular Delivery Systems
- Emerging Strategies for Cancer Diagnosis & Treatment

*Reduced Registration fees for Postdoctoral Fellows*

Visit the Conference Web Site for Updates on:  
Call for Abstracts, Program, Registration  
Website: <http://www.skcc.org>

E-mail: [skcc@pcmisandiego.com](mailto:skcc@pcmisandiego.com)




**SIDNEY KIMMEL  
CANCER CENTER**  
Conference on

**New Targets and Delivery Systems  
in Cancer Diagnosis and Treatment**

*Chairs: A. Deisseroth, J. Schnitzer, R. Weichselbaum, N. Habib*

**March 5-7, 2007**



**HOTEL DEL CORONADO**  
San Diego, CA

---


TOPICS INCLUDE

- New Targets in Cancer Cells
- New Targets in Tumor Microenvironment & Vasculature
- Imaging Through Nanoparticles, Vectors & Recombinant Biologics
- Tumor Inflammation and Cell Homing
- Molecular Targeting
- Nanomedicine
- Cellular and Molecular Delivery Systems
- Emerging Strategies for Cancer Diagnosis & Treatment

*Reduced Registration fees for Postdoctoral Fellows*

Visit the Conference Web Site for Updates on:  
Call for Abstracts, Program, Registration  
Website: <http://www.skcc.org>

E-mail: [skcc@pcmisandiego.com](mailto:skcc@pcmisandiego.com)




**SIDNEY KIMMEL  
CANCER CENTER**  
Conference on

**New Targets and Delivery Systems  
in Cancer Diagnosis and Treatment**

*Chairs: A. Deisseroth, J. Schnitzer, R. Weichselbaum, N. Habib*

**March 5-7, 2007**



**HOTEL DEL CORONADO**  
San Diego, CA

---

TOPICS INCLUDE

- New Targets in Cancer Cells
- New Targets in Tumor Microenvironment & Vasculature
- Imaging Through Nanoparticles, Vectors & Recombinant Biologics
- Tumor Inflammation and Cell Homing
- Molecular Targeting
- Nanomedicine
- Cellular and Molecular Delivery Systems
- Emerging Strategies for Cancer Diagnosis & Treatment

*Reduced Registration fees for Postdoctoral Fellows*

Visit the Conference Web Site for Updates on:  
Call for Abstracts, Program, Registration  
Website: <http://www.skcc.org>

E-mail: [skcc@pcmisandiego.com](mailto:skcc@pcmisandiego.com)

# *Nature and Science*

ISSN 1545-0740

The *Nature and Science* is an international journal with a purpose to enhance our natural and scientific knowledge dissemination in the world under the free publication principle. Any valuable papers that describe natural phenomena and existence or any reports that convey scientific research and pursuit are welcome, including both natural and social sciences. Papers submitted could be reviews, objective descriptions, research reports, opinions/debates, news, letters, and other types of writings that are nature and science related.

## 1. General Information

(1) **Goals:** As an international journal published both in print and on internet, *Nature and Science* is dedicated to the dissemination of fundamental knowledge in all areas of nature and science. The main purpose of *Nature and Science* is to enhance our knowledge spreading in the world under the free publication principle. It publishes full-length papers (original contributions), reviews, rapid communications, and any debates and opinions in all the fields of nature and science.

(2) **What to Do:** *Nature and Science* provides a place for discussion of scientific news, research, theory, philosophy, profession and technology - that will drive scientific progress. Research reports and regular manuscripts that contain new and significant information of general interest are welcome.

(3) **Who:** All people are welcome to submit manuscripts in any fields of nature and science.

(4) **Distributions:** Web version of the journal is freely opened to the world, without any payment or registration. The journal will be distributed to the selected libraries and institutions for free. For the subscription of other readers please contact with: [editor@americanscience.org](mailto:editor@americanscience.org) or [americansciencej@gmail.com](mailto:americansciencej@gmail.com) or [editor@sciencepub.net](mailto:editor@sciencepub.net).

(5) **Advertisements:** The price will be calculated as US\$400/page, i.e. US\$200/a half page, US\$100/a quarter page, etc. Any size of the advertisement is welcome.

## 2. Manuscripts Submission

(1) **Submission Methods:** Electronic submission through email is encouraged and hard copies plus an IBM formatted computer diskette would also be accepted.

(2) **Software:** The Microsoft Word file will be preferred.

(3) **Font:** Normal, Times New Roman, 10 pt, single space.

(5) **Manuscript:** Don't use "Footnote" or "Header and Footer".

(6) **Cover Page:** Put detail information of authors and a short title in the cover page.

(7) **Title:** Use Title Case in the title and subtitles, e.g. "**Debt and Agency Costs**".

(8) **Figures and Tables:** Use full word of figure and table, e.g. "**Figure 1. Annual Income of Different Groups**", **Table 1. Annual Increase of Investment**".

(9) **References:** Cite references by "last name, year", e.g. "(Smith, 2003)". References should include all the authors' last names and initials, title, journal, year, volume, issue, and pages etc.

### Reference Examples:

**Journal Article:** Hacker J, Hentschel U, Dobrindt U. Prokaryotic chromosomes and disease. *Science* 2003;301(34):790-3.

**Book:** Berkowitz BA, Katzung BG. Basic and clinical evaluation of new drugs. In: Katzung BG, ed. Basic and clinical pharmacology. Appleton & Lance Publisher. Norwalk, Connecticut, USA. 1995:60-9.

(10) **Submission Address:** [editor@sciencepub.net](mailto:editor@sciencepub.net), Marsland Company, P.O. Box 21126, Lansing, Michigan 48909, The United States.

(11) **Reviewers:** Authors are encouraged to suggest 2-8 competent reviewers with their name and email.

## 2. Manuscript Preparation

Each manuscript is suggested to include the following components but authors can do their own ways:

(1) **Title page:** including the complete article title; each author's full name; institution(s) with which each author is affiliated, with city, state/province, zip code, and country; and the name, complete mailing address, telephone number, facsimile number (if available), and e-mail address for all correspondence.

(2) **Abstract:** including Background, Materials and Methods, Results, and Discussions.

(3) **Keywords.**

(4) **Introduction.**

(5) **Materials and Methods.**

(6) **Results.**

(7) **Discussions.**

(8) **Acknowledgments.**

(9) **References.**

### Journal Address:

Marsland Company  
P.O. Box 21126  
Lansing, Michigan 48909  
The United States  
Telephone:(517) 303-3990  
E-mail: [editor@sciencepub.net](mailto:editor@sciencepub.net);  
[naturesciencej@gmail.com](mailto:naturesciencej@gmail.com)  
Websites: <http://www.sciencepub.org>

ISSN 1545-0740

